

Defining Memory B-cell Responses to Human Rhinovirus Infection

Jacob David Eccles

Corvallis, Oregon

B.A. Swarthmore College, 2007

M.S. University of Virginia, 2019

A Dissertation presented to the Graduate Faculty  
of the University of Virginia in Candidacy for the Degree of  
Doctor of Philosophy

Department of Microbiology, Immunology, and Cancer Biology

University of Virginia

May, 2019

## Abstract

Rhinoviruses, which account for the majority of cases of common cold, arguably cause more frequent illness in humans than any other pathogen. Despite this, relatively little is known about B-cell and humoral responses to this ubiquitous virus, and in particular, about the failure of infection to induce durable immunity to multiple rhinovirus strains. Here, we aimed to rigorously elucidate these processes, and in doing so we revealed a novel B-cell subset endowed with a unique advantage in viral clearance. Specifically, we found that IgG-restricted B-cells that lack the chemokine receptor CXCR5 express a molecular signature consistent with effector memory, and secrete antibodies that cross-react with different rhinovirus strains, whereas lymphotropic memory cells that express CXCR5 typically target only a single strain. High-dimensional phenotyping by mass cytometry identified a novel dual-specific B-cell “effector memory” subset that expressed the transcription factor T-bet, consistent with an “age-associated” signature. These cells were able to secrete cross-reactive IgG more rapidly compared with their mono-specific counterparts, expanded *in vivo* in the blood of infected humans after acute infection, and their phenotype mirrored cell bodies and secreted antibodies detected in the acutely infected nose. The kinetics and quality of serum antibody profiles coupled with cellular fluxes during infection also implied a link between serum antibody responses that lack cross-reactive activity and mono-specific memory B-cells. Our results suggest that B-cell recall responses to rhinovirus efficiently clear infection, but fail to

provide long-term protection against heterotypic strains, based on the dogma that long-lived plasma cells derive from conventional CXCR5<sup>+</sup> memory. These findings query the respective lineages of B-cells that resemble central memory and effector memory phenotypes, and how they acquire and recognize antigen. We propose that harnessing the attributes of cross-reactive memory B-cells might provide an opportunity for inducing durable cross-protective immunity against this troublesome virus.

## Table of Contents

<b>ABSTRACT.....</b>	<b>I</b>
<b>LIST OF FIGURES .....</b>	<b>VII</b>
<b>LIST OF TABLES .....</b>	<b>X</b>
<b>LIST OF ABBREVIATIONS .....</b>	<b>XI</b>
<b>ACKNOWLEDGMENTS.....</b>	<b>XV</b>
<b>INTRODUCTION .....</b>	<b>1</b>
RHINOVIRUS HEALTH IMPACT .....	1
THE ROLE OF B-CELLS IN IMMUNITY .....	2
GENERATION OF IMMUNOGLOBULIN DIVERSITY .....	4
B-CELL ACTIVATION.....	6
CLASS SWITCH RECOMBINATION .....	8
SOMATIC HYPERMUTATION .....	10
T-CELL HELP .....	11
DEFINING THE T-FOLLICULAR HELPER LINEAGE .....	13
T-FOLLICULAR HELPER INDUCTION.....	14
IDENTIFYING T-FOLLICULAR HELPER CELLS IN PERIPHERAL BLOOD .....	15
B-CELL DIFFERENTIATION .....	16
PLASMA CELL PHENOTYPE AND FUNCTION .....	17
MEMORY B-CELL PHENOTYPE AND FUNCTION .....	19
AGE-ASSOCIATED B-CELLS.....	20

ROLE OF THE TRANSCRIPTION FACTOR T-BET IN THE ADAPTIVE RESPONSE .....	22
EFFECTOR MEMORY: ANALOGIES BETWEEN B- AND T-CELLS .....	23
RHINOVIRUS VIROLOGY AND B-CELL IMMUNITY .....	25
NEUTRALIZING ANTIBODIES .....	26
POTENTIAL DEFECTS IN THE HUMORAL IMMUNE RESPONSE TO RHINOVIRUS.....	28
<b>THESIS RATIONALE AND PROPOSAL.....</b>	<b>36</b>
<b>MATERIALS AND METHODS .....</b>	<b>39</b>
DEVELOPMENT OF NEW TOOLS APPLIED TO AN EXISTING HUMAN INFECTION MODEL.....	39
STUDY SUBJECTS AND EXPERIMENTAL INFECTION MODEL.....	41
DETERMINATION OF INFECTION STATUS.....	42
PREPARATION OF VIRUS FOR MULTIPLEX SEROLOGY ASSAYS AND LABELING B-CELLS .....	42
MULTIPLEX SEROLOGY ASSAY .....	43
MULTI-COLOR FLOW CYTOMETRY .....	44
MASS CYTOMETRY.....	44
PLASMABLAST DIFFERENTIATION CULTURE.....	45
SINGLE-CELL MRNA SEQUENCING.....	46
FLUORESCENCE MICROSCOPY .....	47
<b>TISSUE HOMING MEMORY B CELLS RAPIDLY INDUCE LOCAL CROSS REACTIVE IGG</b>	
<b>UPON HUMAN RHINOVIRUS INFECTION .....</b>	<b>54</b>
INTRODUCTION .....	54
RESULTS.....	56
<i>Whole Virus Detects Multiple RV-specific Isotypes.....</i>	<i>56</i>

<i>Dual-specific B-cells are Expanded in the Blood and Lack CXCR5 .....</i>	<i>58</i>
<i>Dual-specific B-cells Rapidly Secrete Cross-Reactive IgG, but not IgA or IgM.....</i>	<i>60</i>
<i>Dual-specific B-cells Display "Effector Memory" by High Dimensional Analysis.....</i>	<i>96</i>
<i>Dual-specific B-cells Expand After RV Infection .....</i>	<i>98</i>
<i>Early Antibody Responses to RV in the Nose are Cross-reactive, Limited to IgG, and Coincide with B-Cell Infiltrates.....</i>	<i>123</i>
<i>Dual-specific B-cells are Clonally Distinct from Their Mono-specific Counterparts.....</i>	<i>124</i>
DISCUSSION .....	146
<b>CONCLUSIONS AND FUTURE DIRECTIONS .....</b>	<b>157</b>
EFFECTOR MEMORY AND SYMMETRY IN LYMPHOCYTES.....	158
THEORETICAL BENEFITS OF B-EFFECTOR MEMORY .....	159
EVALUATING THE PRACTICAL ROLE OF B-EFFECTOR MEMORY .....	161
ASSOCIATION OF SPECIFICITY AND PHENOTYPE.....	163
ASSOCIATION OF SPECIFICITY AND ISOTYPE.....	167
T-HELPER SKEWING APPLIED TO B-EFFECTOR MEMORY.....	169
INDUCTION OF B-EFFECTOR MEMORY.....	171
B-EFFECTOR MEMORY IN TISSUE AND BEYOND.....	173
HARNESSING B-EFFECTOR MEMORY.....	175
HUMORAL IMMUNITY TO RHINOVIRUS .....	177
B-EFFECTOR MEMORY AND RHINOVIRUS.....	180
RHINOVIRUS, B-CELLS, AND ASTHMA .....	182
SUMMARY.....	183

**REFERENCES .....191**

## List of Figures

Figure 1: The B-cell Response to Infection or Vaccination.....	30
Figure 2: Immunoglobulin Gene Recombination and Hypermutation .....	32
Figure 3: RV Capsid Pentamer Crystal Structure at High Resolution .....	34
Figure 4: Cell Purity Obtained by Flow Cytometry Sorting .....	52
Figure 5: Purified Whole Virus is Stable and Structurally Uniform .....	62
Figure 6: Experimental RV Strains are Genomically and Structurally Distinct ....	64
Figure 7: Whole Virus is Isolated to High Purity .....	66
Figure 8: Model of Experimental RV Infection in Humans.....	68
Figure 9: Whole Virus Detects Multiple RV-specific Isotypes.....	70
Figure 10: Serum Antibodies Remain Unchanged in Uninfected Subjects .....	72
Figure 11: VP1 Capsid Subunit Does Not Detect RV-specific Antibodies.....	74
Figure 12: RV-specific B-cells are Enriched in the CXCR5-neg Memory.....	76
Figure 13: Dual-specific B-cells are Expanded in Blood and Lack CXCR5.....	78
Figure 14: Dual-specific B-cells are Highly Enriched in CXCR5- Memory .....	80
Figure 15: Dual-specific B-cells are Predominantly CXCR5- Memory .....	82
Figure 16: B-cell Binding of RV is Independent of ICAM-1.....	84
Figure 17: CXCR5- B-cell Memory is Distinct from CXCR5+ Memory .....	86
Figure 18: Dual-specific B-cells Rapidly Secrete Cross-Reactive IgG .....	88
Figure 19: Dual-specific B-cells Do Not Rapidly Secrete Cross-Reactive IgA ....	90
Figure 20: Dual-specific B-cells Do Not Rapidly Secrete Cross-Reactive IgM....	92

Figure 21: CXCR5- Memory B-cells Transition Rapidly Under Plasma Cell Differentiating Conditions .....	94
Figure 22: B-cells Analyzed by Mass Cytometry in Experimental Infection.....	101
Figure 23: Visual Representation by t-SNE of B-cell Phenotypes Identified by FlowSOM.....	103
Figure 24: Dual-specific B-cells Display "Effector Memory" Phenotype by High Dimensional Analysis .....	105
Figure 25: RV-specific CXCR5+ Memory B-cells Primarily Target a Single Strain .....	107
Figure 26: Dual-specific B-cells are T-bet+ .....	109
Figure 27: Discrete Circulating B-cell Clusters Fluctuate in Response to Infection.....	111
Figure 28: Change in Frequency of Selected Clusters During Infection.....	113
Figure 29: Overlay of B-cell Clusters Related to RV Infection on t-SNE Maps .	115
Figure 30: Expansion of Circulating Extrafollicular Plasmablasts Coincides with a Decrease in a CXCR5+ Memory B-cell Cluster .....	117
Figure 31: Change in the Signature of Dual-specific B-cells (Cluster #19) During RV Infection .....	119
Figure 32: Change in Percentages of CXCR5+ and CXCR5- Mono-specific and Dual-specific Memory B-cells during RV Infection .....	121
Figure 33: Uninfected Nasal Biopsies Stain Sparsely for B-cells and T-cells....	126
Figure 34: Infected Inferior Turbinate Stains Densely for B-cells and T-cells....	128

Figure 35: Infected Middle Turbinate Stains Densely for B-cells and T-cells ....	130
Figure 36: Infected Nasopharynx Stains Densely for B-cells and T-cells .....	132
Figure 37: Infected Nasal Tissue Demonstrates Dense Lymphocytic Infiltrates .....	134
Figure 38: Immunofluorescence Analysis of CD20 in Nasal Biopsy Specimens from RV-Infected Subjects.....	136
Figure 39: Early Antibody Responses to RV in the Nose are Cross-reactive and Limited to IgG .....	138
Figure 40: Weak IgG Responses to Rhinovirus are Present in the Nose of Uninfected Subjects After RV Challenge.....	140
Figure 41: Dual-specific and CXCR5- B-cells are Hypermutated at Similar Levels as their Mono-specific and CXCR5+ Counterparts .....	142
Figure 42: Dual-specific B-cells are Clonally Distinct from Their Mono-specific Counterparts .....	144
Figure 43: T-bet and CXCR5 Expression in IgD+ and IgD- B-cells .....	153
Figure 44: Immunofluorescence Analysis of T-bet+ B-cells in Spleen .....	155
Figure 45: Schematic of B-cell Memory Subsets Responding Acutely to RV....	185
Figure 46: CD11c is Expressed by Infiltrating non-B-cells .....	187
Figure 47: RV-Infected Asthmatic Subjects Produce Serum IgE Against RV ...	189

## List of Tables

Table 1: Rhinovirus RT-PCR Primers.....	49
Table 2: 70X Barcoding Scheme for Mass Cytometry.....	50
Table 3: Mass Cytometry Antibody Panel .....	51

## List of Abbreviations

A	Adenosine
ABC	Age-associated B-cell
AID	Activation-induced cytidine deaminase
APC	Antigen-presenting cell
ASC	Antibody-secreting cell
Bcm	B-cell central memory
BCR	B-cell receptor
Bem	B-cell effector memory
Beff	B-cell effector (plasma cell)
BSA	Bovine serum albumin
C	Cytidine
CD	Cluster of differentiation
CDHR	Cadherin-related family member
CSR	Class-switch recombination
D	Diversity immunoglobulin gene segment
DAMP	Damage-associated molecular pattern
DAPI	4',6-diamidino-2-phenylindole
DC	Dendritic cell
DMSO	Dimethyl sulfoxide
DNA	Deoxyribonucleic acid
ER	Endoplasmic reticulum

FACS	Fluorescence activated cell sorting
Fab	Immunoglobulin region: Fragment, antigen binding
Fc	Immunoglobulin region: Fragment, crystallizable (constant)
FCS	Fetal calf serum
G	Guanosine
GC	Germinal center
HEPES	4-(2-hydroxyethyl)-1-piperazineethanesulfonic acid
HEV	High endothelial venule
ICAM	Intracellular adhesion molecule
ICOS	Inducible T-cell costimulator
ICP-MS	Inductively-coupled plasma mass spectrometry
IFN	Interferon
Ig	Immunoglobulin
IL	Interleukin
J	Joining immunoglobulin gene segment
L	Ligand
LDL	Low-density lipoprotein
LLPC	Long-lived Plasma Cell
LN	Lymph node
MACS	Magnetically activated cell sorting
MAP	Mitogen-activated protein
MHCI	Major histocompatibility complex, class I

MHCII	Major histocompatibility complex, class II
NHS	N-hydroxysuccinimide
NK	Natural Killer
PAGE	Polyacrylamide gel electrophoresis
PAMP	Pathogen-associated molecular pattern
PB	Plasmablast (pre-plasma cell)
PC	Plasma cell (B-cell effector)
PBS	Phosphate buffered saline
PD-1	Programmed death 1
PLC	Phospholipase C
PNAd	Peripheral node addressin (CD62L)
RAG	Recombinase activating gene
RNA	Ribonucleic acid
RV	Rhinovirus
S1P	Sphingosine-1-phosphate
SDS	Sodium dodecyl sulfate
SHM	Somatic hypermutation
STAT	Signal transducer and activator of transcription proteins
T	Thymidine
Tcm	T-cell central memory
TCR	T-cell receptor
Tem	T-cell effector memory

Teff	T-cell effector
Tfh	T-follicular helper cell
TGF	Transforming growth factor
Th	T-helper cell
TLR	Toll-like receptor
U	Uracil
μg	Microgram
μL	Microliter
V	Variable immunoglobulin gene segment
V(D)J	Variable, (diversity), and joining gene segment combination

## Acknowledgments

Above all, I would like to thank my mentor, Dr. Judith Woodfolk, for her guidance and support, both scientific and professional, over the past five years. I came to the lab under complicated circumstances, and she entrusted me with a unique project of immense potential at a time when I would have settled for much less. The work was expensive and often extended beyond the historical expertise of the lab, and I appreciate the financial and intellectual investments she was willing to make on my behalf to ensure our progress. I would also like to thank my co-mentor, Dr. Loren Erickson, for the optimism and validation he brought to the project, as well as the thoughtful input of the additional members my committee: Dr. Young Hahn, Dr. Thomas Braciale, and chairman, Dr. Timothy Bender. This project required the coordination of all Woodfolk lab personnel, including Nicole Kirk, Paul Wright, Dr. Liesbeth Paul, Marcia Ripley, and especially Dr. Lyndsey Muehling, whose work formed the basis for the study that my research was built upon. Given our human-based model, experimental samples were often in limited supply, and collective success depended upon sharing resources equitably. For this spirit of collegiality I am grateful to our lab, as well as our collaborators: Dr. Ronald Turner, Dr. Peter Heymann, Dr. Larry Borish, and Dr. John Steinke.

Though it has been several years since our brief work together in the lab of Dr. Victor Engelhard, it is important that I thank Dr. Sherin Rouhani for the training she provided in experimental methods in immunology. This constituted the foundation of the technical skills documented herein, without which I might

not have successfully initiated study under Dr. Woodfolk. I should also thank Dr. Thomas Platts-Mills for keeping me company many weekends in lab, for sharing his encyclopedic knowledge, scientific and otherwise, and for establishing a welcoming community in the allergy division at UVA. I am also forever indebted to Dr. Gary Owens, Dr. Dean Kedes, Dorothy Williams, and Ashley Woodward at the MSTP for giving me the opportunity to pursue this career and for supporting me as I made my way to the Woodfolk lab and thereafter.

Lastly, I thank my friends and family for their efforts to maintain our relationships while I spent so much time away and while the scope of my daily experience grew vanishingly narrow. I particularly want to thank my mother for raising me in the forest and for exemplifying a life of service to others, thus setting me on the course toward humanistic naturalism that I continue to pursue to this day, with this document as evidence. I also appreciate my aunt Wendy and uncle Lee for providing a connection to family in Virginia, far from my home, and for the food, conversation, and protest marches we shared. I recognize my friend and classmate, Carolyn, for visiting so frequently since moving away for medical residency, even as I was largely unable to repay her visits. And in closing, I thank my girlfriend, Jennifer, for supporting me throughout this entire process, and for continuing her medical training at UVA, allowing us to be together as much as possible. Given the time and attention this work has required, I have rarely met the standards I set for myself as a partner, and I hope in the future to prove myself worthy of her love and patience.

## Introduction

The overarching objective of this thesis was to explore B-cell responses to rhinovirus, the major cause of common cold. This chapter discusses fundamental aspects related to B-cell biology, including their development and differentiation, subcategorization, known functions and role in immunity, and interactions with other immune cell-types. Current knowledge of the immune response to rhinovirus, and major knowledge gaps, are also highlighted.

### **Rhinovirus Health Impact**

Rhinovirus (RV) is the cause of the majority of cases of the common cold in the general population where it represents an enormous economic burden (1). Recent estimates within the U.S. suggest that 3 in 4 people experience infection annually with an average of 2.5 infections per capita-year. The annual consequences of this high infection rate include 96 million work-days and 93 million school-days lost, 100 million physician visits, and 41 million prescriptions written for unwarranted antibiotics (2). The approximated aggregate costs exceed \$40 billion per year, while needless antibiotic use contributes to the development of drug-resistant bacterial pathogens. Meanwhile, RV frequently provokes life-threatening exacerbations in patients living with asthma and chronic pulmonary disease (3–10). Furthermore, it can cause fatal pneumonia in the immunocompromised and elderly, severe bronchiolitis in infants, and has been implicated as an initial cause of lifelong asthma in children, which now affects

roughly one in ten people in industrialized countries (11,12). Despite these substantial health liabilities, no effective therapy or vaccine has yet been developed (1).

### **The Role of B-cells in Immunity**

B-cells are lymphocytes that play a key role in the adaptive immune response by secreting antibodies, which form the basis of protection following immunization (13,14). Such immunization can occur via natural infection or through artificial intervention, termed vaccination, in reference to the phenomenon by which cowpox (vaccinia) exposure prevents future infection with the deadly smallpox virus (15). B-cells derive their name from their maturation in the bone marrow, but these cells and the antibodies they secrete are capable of traveling to and impacting any tissue. Antibodies are dynamic molecules that bind pathogens, labeling them for destruction or inhibiting their mechanisms of virulence (16,17). B-cells are capable, on an ongoing basis, of producing antibodies against virtually any target antigen, regardless of structure or elemental/molecular composition (18). This process, termed adaptive immunity, does not require the presence of a given antigen on an evolutionary timescale. Rather than natural selection promoting survival of a subset of the population through inborn resistance, instead mammalian B-cells generate immunity at the level of the individual by synthesizing and continuously optimizing immunoglobulin (antibody) genes in real time to address their target (19,20). This allows the immune system to protect against infectious or toxic agents, which are

themselves rapidly evolving. B-cells circulate through lymphatics and blood, but generally reside in lymph node (LN) follicles, where they await antigen draining from peripheral tissue (21,22). B-cells compete for this antigen on the basis of their ability to bind it through B-cell receptors (BCR), cell-surface transmembrane immunoglobulin molecules, which vary in structure and binding specificity from cell to cell (23). Antigen is internalized, proteolytically processed, and presented in the context of major histocompatibility complex II (MHCII) (24). Those B-cells bearing sufficient cognate peptide to engage pre-activated “helper” CD4+ T-cells are given the signal to divide and differentiate (25,26). The culmination of the differentiation process is a plasma cell (PC), which converts its membrane-immunoglobulin to the soluble isoform (27,28). Such antibody-secreting cells exit the lymphatic system and home to various sites, often mucosa or bone marrow, where they manifest humoral immunity for the remainder of their lifespan, which can be a considerable duration (**Figure 1**). Marrow resident PCs have been known to persist over months to decades (29). The resulting antibodies, binding with specific affinity through their N-terminal variable Fab regions, subsequently coat invading pathogens (30). This labeling process, termed opsonization, enables target immunogens to be seized, engulfed, and degraded by immune cells specialized for this function. Most prominently, neutrophils, macrophages, and other such myeloid lineage phagocytes accomplish this by their expression of surface Fc-receptors, which bind to antibody C-terminal constant regions (31–33). Captured pathogens are

digested in phagolysosomes by exposure to acidic pH and reactive oxidative species, such as peroxide and hypochlorite (colloquially, chlorine bleach) (34,35).

### **Generation of Immunoglobulin Diversity**

Soon after lymphoid progenitor cells commit to the B-cell lineage, they begin to develop their respective antigen specificities, and remain in the bone marrow unlike nascent T-cells, which must travel to the thymus for further differentiation (36). Specificity is initially established by selection of variable (V), diversity (D), and joining (J) gene segments at the immunoglobulin heavy chain locus, and solely V and J gene segments at the light chain locus (**Figure 2**) (37,38). These loci contain a variety of each segment type (29-46 in V, 23 in D, and 4-6 in J) and selection occurs as intervening segments are excised from the germline DNA by RAG1 and RAG2 enzymes to render two segments adjacent that were once distant from one another (39,40). The number of possible VDJ combinations is vast, but the overall diversity becomes almost infinite given that the joining process involves the insertion of a random sequence of nucleotides of varying length between adjoined segments (termed N-nucleotides), which is flanked by palindromic sequences of varying lengths derived from the termini of the adjoining segments (termed P-nucleotides) (41,42). Thus a VDJ combination may more aptly be represented as VXDYJ, where V, D, and J are germline sequences, but X and Y are entirely novel. As may be expected, such a stochastic process frequently gives rise to nonviable gene products by incurring premature stop codons, frame-shifting the downstream constant region, or simply

giving rise to a full-length protein that cannot fold (43). In these cases, further V, D, and J segments are excised and germline DNA is rejoined until an appropriate sequence is achieved, or the cell undergoes apoptosis (44). When successful immunoglobulin construction occurs with a homodimer of heavy and light chain heterodimers, functionality is established once products arrive at their proper cellular location at the plasma membrane. At this point, kinase enzymes associated with the intracellular C-termini of the transmembrane BCR complex indicate that it has formed a conduit to the extracellular environment (45,46). This positively-selecting signal results from a weak “crosslinking” (localized clustering) of BCR molecules as their N-termini exhibit slight affinity for one another. This brings intracellular C-termini into close proximity with one another, allowing accompanying kinases, bound through Ig $\alpha$  and Ig $\beta$ , to mutually phosphorylate their neighbors. In contrast, a strong crosslinking event will induce further VDJ recombination or apoptosis, roughly equivalent to the outcome of a nonfunctional immunoglobulin, as above (47,48). This effective deletion of autoreactive BCRs greatly limits the production of B-cells that could cause autoimmune pathology. B-cells assembling functionally appropriate BCRs reach maturity and downregulate the chemokine receptor CXCR4, which had previously maintained their bone marrow localization via migration toward CXCL12, secreted by marrow stroma (49). These cells then begin to circulate in blood. At this point, B-cells begin to express L-selectin (CD62L), and chemokine receptors CCR7 and CXCR5 (50,25). In concert, these initiate a trafficking pattern out of blood,

through high endothelial venules (HEV) expressing peripheral node addressin (PNAd), via L-selectin, and into LNs via CCR7 (for CCL19/21), and then into the B-cell zone, or follicle via CXCR5 (for CXCL13). Lymph homing cells meander within the node and gradually migrate through lymphatic endothelial vessels from node to node along an increasing gradient of sphingosine-1-phosphate (S1P) until they eventually exit lymphatic ducts back into circulating blood at the superior vena cava (51–53). In this manner, mature B-cells are continually dispersed and recirculated throughout the body.

### **B-cell Activation**

B-cells traverse the circuit of blood and lymph until they encounter cognate antigen with sufficient affinity for their BCR (21,22). Affinity results from energetically favorable interfacing between BCR and antigen surfaces, respectively, as dictated by electrostatic attraction, hydrogen bonding, van der Waals forces, and hydrophobic interaction. This interaction can have several productive outcomes, in the absence of which, the B-cell will continue circulating and eventually undergo apoptosis. The first, called T-independent type I, occurs without T-cell help and requires only weak antigen affinity (54). Here the primary signal is delivered through an innate pathogen-associated molecular pattern (PAMP) or damage-associated molecular pattern (DAMP) receptor, such as a toll-like receptor (TLR), and antigen binding the BCR plays a secondary and indeterminate role, though it is required. A cascade of phosphorylation ensues from the TLR via MyD88/TRIF and the BCR via Syk, Btk, and PLC to initiate the

MAP kinase pathway and calcium flux, culminating with transcriptional activity mediated by NF $\kappa$ B, NFAT, and other factors downstream of ERK (55–57). The second type of activation, called T-independent type II, occurs when the bound antigen is highly repetitive and a single molecule simultaneously binds many BCRs (58,59). These BCRs and their associated signaling molecules (CD19, CD21, and CD79) are thus drawn together such that they are massively crosslinked, initiating signaling cascade, as in type I above (60). The third type is T-dependent and occurs when an activated T-cell is present that recognizes a peptide from the antigen bound by the BCR (61,26). In this scenario, bound antigen is endocytosed and processed for MHCII presentation. The greater the affinity, the more antigen bound, the more peptide-MHCII presented on the surface, the stronger and more enduring the synapse with the T-cell (23). A previously activated T-cell is crucial because it will provide CD40L to a synapsing B-cell, which generates an analogous signal to the PAMP/DAMP in T-independent type I above (62,63). This latter T-dependent pathway is by far the most efficient, however, B-cells activated via any of these mechanisms may respond by proliferating and differentiating their phenotype toward immunoglobulin secretion, thus contributing toward immunity (27,28). As will be discussed in the next section, antibodies can be secreted in several distinct physical formats with divergent functional traits. Thus, antigen-specific humoral responses can be further tailored to effect clearance, depending on the class of pathogen targeted and its route of virulence.

## Class Switch Recombination

Prior to initial cognate antigen exposure and activation of all types, functionally mature B-cells simultaneously express two BCR isoforms, which, in the context of immunoglobulins, are known as isotypes. These are IgD and IgM, defined by the C-terminal constant region of the BCR heavy chain (64). Both sequences are encoded in DNA and transcribed, but the distinction in translated protein is established via mRNA processing and splicing (65). Apart from these two isotypes, however, the constant region contains additional exons encoding further isotypes, which are inaccessible to naïve B-cells (66). The complete sequence of all human exons is as follows: IgM, IgD, IgG3, IgG1, IgA1, IgG2, IgG4, IgE, and IgA2 (67). Through the process of class switch recombination (CSR), which is coupled to cellular activation, the supplementary isotypes can be transcribed in lieu of IgD and IgM (**Figure 2**). B-cells experiencing activation of all types will begin to express activation-induced cytidine deaminase (AID) under the control of NFκB, however IL-21 secreted by LN-resident CD4<sup>+</sup> T-cells specialized for B-cell help, called T-follicular helpers (Tfh), appears to exert the strongest effect on CSR (68,69). Through a mechanism that is only partially understood, this enzyme is targeted to the immunoglobulin heavy chain DNA locus where it converts cytidine to uracil at particular sites, creating a base pair mismatch (70,71). DNA repair enzymes respond with base excision repair, which creates nicks in the double strand (72). Similar to the process of VDJ recombination, stretches of DNA intervening between nicks can be excised before the nicks are

repaired, with the resulting broken strand mended by non-homologous end joining. As before, this places exon segments adjacent to one another that were once distant in the germline DNA. In this manner, the IgM and IgD constant regions can be removed to yield a B-cell expressing any downstream isotype (73). In fact, any isotype can convert to any other isotype downstream, but never upstream as excised DNA is lost permanently (67,74). The immunoglobulin isotype of a given B-cell is determined by whichever constant region exon lies directly downstream of the VDJ variable region, with the exception of naïve cells which can produce IgD, despite the intervening IgM constant region, which, as stated above, is spliced out on a portion of transcripts. The value of these isotypes becomes apparent once they are secreted and bind pathogens. The default format, IgM is secreted as a pentamer, increasing its overall avidity for repetitive structures (75,76). It has the unique property of efficiently inducing further opsonization via the complement system, the ultimate outcome of which is assembly of the membrane attack complex, which can directly lyse bacteria (32,77,78). B-cells activated in the context of infection by intracellular pathogens, such as viruses, are induced to switch to IgG (particularly IgG1) by gamma interferon (IFN- $\gamma$ ) signaling (79–81). IgG-opsonized pathogens are bound by high-affinity Fc-receptors on phagocytes and destroyed in phagolysosomes (32,33). Furthermore, infected host cells expressing pathogen-derived antigen on their surface may be killed off by cytotoxic lymphocytes, also binding through high-affinity Fc-receptors. Large parasites doing mechanical damage to tissues

or defying phagocytosis by virtue of their size give rise to IL-33 and PGE<sub>2</sub>, respectively, which drive class-switch to IgE through IL-4 and IL-13 (82,83). Mast cells, basophils, and eosinophils, binding parasites through IgE, release irritants to damage such organisms or drive them out (84–86). Finally, mucosal flora is continuously surveyed by the immune system under homeostatic conditions, whereupon TGF- $\beta$  drives switch to IgA. This isotype is specialized for secretion across mucosal epithelial barriers (87,88). It is also divalent to increase complex formation, and generally serves to maintain flora, commensal and pathogenic alike, appropriately within the anatomical lumen (89–91).

### **Somatic Hypermutation**

Another consequence of activation is somatic hypermutation (SHM), wherein AID mutates nucleotides within the VDJ-containing variable regions of both the immunoglobulin light and heavy chains (92). Again, this process is much more efficient when facilitated by T-cell help, and occurs by essentially the same mechanism described above for CSR, though rather than entire segments of DNA being deleted, mismatch repair by base excision runs to completion, but without preserving the original pairing (93,25,94). Thus G:C becomes G:U,  $\_$ :U, A:U, with uracil ultimately excised and replaced with thymine. In some cases A:T can also become G:C, though this is less well understood (20). Given the mechanistic parity with CSR, these two phenomena are linked and correlated, with increasing SHM rates according to IgD < IgM < IgG < IgA (95). The process is imperfect and frequently nonsense mutations are incurred or long stretches of

DNA are removed that render the B-cell without a functional BCR, dooming it to apoptosis. Like RAG-dependent lymphopoiesis, attrition rates are high and the overall process is extremely inefficient from the standpoint of energy and resources consumed. However, what it permits is both affinity maturation (increasing per exposure for a given antigen) and another layer of real-time adaptation to pathogen mutation (19,96,97). As humans, we may lament our relatively slow evolution when compared with microbial species, and yet SHM in B-cells precisely represents an equivalent capability that can keep pace with microbes. Thus initial recombination events allow for at least marginal affinity for literally any antigen, while SHM hones that affinity and tracks with that antigen should it mutate toward a reduction in affinity (98,23).

### **T-cell Help**

While CSR and SHM can occur following any of the three types of B-cell activation, they are much more robust and consistent with T-cell help (68,69). The classical context for this phenomenon is a germinal center (GC) in the B-cell follicle of a LN, where it proceeds with the participation of the specialized CD4+ Tfh-cell (**Figure 1**) (99,25). Early in an immune response, when B-cells and Tfh-cell are beginning to gather in follicles, T/B collaboration is more common at the margin of the T-cell zone, but this activity ultimately migrates deeper into the follicle as the Tfh phenotype develops fully in CD4+ T-cells with appropriate specificity (21,22). Initial “extrafollicular” synapses tend to produce short-lived IgM+ PCs, given the lack of mature Tfh, but these early effectors likely play an

important role in constraining the growth of infectious pathogens (100,94). B-cells receiving Tfh stimulus begin proliferating, and the resulting mass of mitotic cells constitutes a GC. The B-cell-helping effector functions exhibited by Tfh-cells result, at least in part, from downregulating T-cell zone-homing receptor CCR7, upregulating follicle-homing receptor CXCR5, sufficient affinity to maintain synapse between B-cell peptide-MHCII and T-cell receptor (TCR), and the ability to provide B-cell stimulating factors such as IL-21, IL-4, and CD40-L (68,69,101,102). As antigen drains through afferent lymphatic vessels into nodes, B-cells with inherent BCR affinity for antigen are selected to enter the GC by virtue of Tfh-cell synapse via peptide-MHCII antigen presentation to TCR, the affinity and multiplicity of which determine whether overall avidity is sufficient to maintain contact (23,103,104). This process is competitive, and B-cells with greater BCR affinity for antigen are enabled, through endocytosis, to present higher levels of peptide-MHCII and create higher avidity contacts with Tfh-cells. The limiting factor in this process is generally Tfh-cell quantity, and only the B-cells creating high-avidity interactions are allowed to maintain synapse without being crowded out (105). Those sustaining contact receive stimulus to clonally expand and undergo CSR and SHM (25,96). B-cells must separate from Tfh-cells while undergoing these processes, migrating from the follicular “light zone” to the “dark zone” over a CXCL12 gradient via CXCR4, and resultant B-cell progeny must then gather further antigen and attempt Tfh-synapse again (104,106). Through many iterations of this cycle, affinity is “matured” and high-affinity clones

are selected for expansion into memory B-cells and plasmablast (PB, pre-PC) effector cells, while less competitive clones are lost to apoptosis (26,103,104). B-cell interclonal competition and Tfh-cell availability, thus, must both exist within certain bounds to engender an efficient response (107–109). An overly-competitive environment will limit the robustness of the humoral response, while a weakly competitive environment will limit affinity maturation.

### **Defining the T-Follicular Helper Lineage**

There is consensus that the Tfh cell-type is required for the generation of long-lived plasma cell (LLPC) effectors, providing steady-state humoral immunity, however some controversy surrounds the phenotypic durability of Tfh-cells. Tfh-cells may be defined as those CD4<sup>+</sup> T-cells that provide help to B-cells and facilitate GC reactions and affinity maturation, but, outside of that functional context, their identity becomes less certain (99,110–112). Theories range from this phenotype simply being an effector activity that all CD4<sup>+</sup> helper T-cells are capable of, should they happen to establish synapse with a B-cell, to Tfh being a durable lineage of its own, akin to Th1, Th2, or Th17 (113–115). The truth is likely somewhere in between, given that CD4<sup>+</sup> T-cells exhibit a spectrum of B-cell-helping potential and competent B-cell helpers tend to demonstrate some degree of cytokine-secretion skewing toward the alternative lineages noted above. In fact, Tfh-cells with such skewing induce B-cell class-switching toward analogous isotype secretion, with Th1-like cells inducing IgG via IFN- $\gamma$  to opsonize or neutralize unicellular and viral pathogens, Th2-like inducing IgE with

IL-4 in response to larger tissue parasites, and Th17 inducing IgA by IL-17 to prevent pathologic colonization of the gut by bacteria (116–119). Thus, given such overlap, Tfh is not mutually exclusive from other T-helper programs. At the current state of the field, no CD4<sup>+</sup> T-cell can be categorically discounted from Tfh potential, and helper T-cell lineage commitment toward Th1, Th2, Th17, or otherwise, may serve to skew B-cell isotypes in the GC, thereby complementing Tfh-cell effector activity.

### **T-Follicular Helper Induction**

Functional Tfh-cells in the GC express chemokine-homing marker CXCR5, as B-cells do, allowing their accumulation adjacent to follicular dendritic cells (DC), which secrete the receptor's ligand, CXCL13, to organize B-cell zones within LNs (101,99,102). In this context, Tfh-cells also express ICOS and PD-1, both of which are engaged by corresponding receptors on B-cells. While ICOS signaling has been demonstrated to be crucial for Tfh-cell induction and maintenance, the role of PD-1 is more subtle, contributing, at least in mice, to the longevity of PCs released from the GC (104,120–123). Tfh-cells receiving sufficient TCR and ICOS signaling from a B-cell in synapse will reciprocate by supplying growth-inducing CD40-L and IL-21, the latter of which acts analogously in B-cells as IL-2 in T-cells, with both receptors integrating the common gamma chain (69,26,104,124). These signals stimulate B-cell clonal expansion, and AID-mediated SHM and CSR. Finally, Tfh-cell function is considered to be governed by transcription factor Bcl-6, although Ascl-2, c-Maf, FOXO-1, and Klf-2

have also been demonstrated to be instrumental in generating the phenotype (125–130). The wealth of markers enumerated herein would suggest that Tfh-cells ought to be easily identified. Certainly this is true of active Tfh-cells in the GC, however, upon resolution of the immune response, without antigen to drive Tfh-B-cell synapse, these markers are uniformly lost.

### **Identifying T-Follicular Helper Cells in Peripheral Blood**

Given that human lymphatic tissue can rarely be harvested for study of GC Tfh-cells during experimental immunization, much effort has been invested in the collection of Tfh-cells from blood. Initial attempts to identify resting human Tfh-cells in peripheral blood relied upon CXCR5. Due to residual expression, this marker was useful at time points soon after resolution of infection or withdrawal of antigen stimulus, and sorted cells demonstrated B-cell helping capacity *in vitro*, while measured circulating frequencies correlated with GC activity and humoral immunity (102,114,131–133). However, progressive loss of the receptor from memory Tfh-cells, coupled with its transient non-specific upregulation on recently-activated CD4<sup>+</sup> T-cells, has limited its use. PD-1 exhibits still more rapid kinetics in Tfh-cells, and even the putative master-transcription factor of Tfh-cells, Bcl-6, is often undetectable in blood CD4<sup>+</sup> T-cells under homeostatic conditions. Various attempts have been made to use other chemokine receptors to mark human CD4<sup>+</sup> T-cells with Tfh capacity. Most notably, these have included CXCR3, CCR4, and CCR6, but no consensus could be reached in the field, and results were highly dependent upon experimental design (102,106,131,134). To

date, the most reliable readout of the Tfh phenotype is expression of ICOS upon stimulation (134). It is not yet clear whether this characteristic informs the history of the cell, whether it was previously a GC Tfh-cell that since retired to peripheral circulation. However, this marker does accurately predict subsequent B-cell-helping activity. Tfh-cell function is also known to depend partially upon the GC cytokine milieu, and, until recently, *in vitro* conditions reflected those established by murine models. A combination of IL-6, IL-12, and IL-21 were thought to provide appropriate support for Tfh-cell function, until it was discovered that human cells had a unique requirement for TGF- $\beta$  (135–137). Exhaustive work testing dozens of cytokine combinations established that STAT-3 (via IL-6 or IL-10) and STAT-4 (via IL-12 or IL-23) alone poorly facilitated *in vitro* Tfh-induced B-cell expansion and differentiation, but that addition of TGF- $\beta$  had a profound impact on the simulated GC. This effect was absent in murine cell culture, and addition of TGF- $\beta$  almost completely abrogated the Tfh phenotype. Going forward, the field is prepared for human GC modeling *in vitro*. Tfh-cells can be selected by ICOS-upregulation upon stimulation, and a combination of STAT-3, STAT-4, and TGF- $\beta$  signaling promotes an environment conducive to B-cell-helping activity.

### **B-cell Differentiation**

Many B-cells fail to receive adequate growth stimulus and die in GCs, but those surviving are thought to pursue two distinct paths. These include the memory B-cell, and the terminally-differentiated PC, also known as the B-effector

(Beff) or antibody-secreting cell (ASC). This latter term, however, can be applied more broadly to rare phenotypes defying the categorizations discussed so far, which nonetheless produce soluble immunoglobulin, such as innate-like B1-cells (25,28). The factors determining these outcomes are somewhat unclear, as are those determining the longevity of these phenotypes, although memory tends to be created earlier in the GC and with lower affinity for antigen than PCs (138,139). In general, memory cells, as their name would suggest, are longer-lived, more proliferative, and express more markers of “stemness” and genes repressing apoptosis, such as Bcl-2 and Bcl-x<sub>L</sub> (140,141). As is the pattern of the immune system broadly, such durability comes at the cost of immediate functionality, although memory B-cells require less robust signals for activation and differentiation than naïve cells do (142). PCs are extremely efficient producers of immunoglobulin and manage their highly anabolic state by maintaining an endoplasmic reticulum (ER) stress response, aiding protein folding and directed by transcription factor, XBP1 (143). PCs also reduce their expression of the plasma membrane-anchored BCR isoform of immunoglobulin (144,27). BCR is essentially absent on IgG<sup>+</sup> PCs, and is maintained slightly on IgA<sup>+</sup> and IgM<sup>+</sup> cells (145). Thus PCs are poorly dependent on external signals and carry out their task of antibody secretion for the term of their existence.

### **Plasma Cell Phenotype and Function**

When a human PC is created in a GC, it downregulates CD19 (somewhat) and CD20 (completely), and increases expression of CD27 and CD38 (146).

Expression of the T-cell co-stimulatory molecules CD80 and CD86 also increases, which suggests further occasion for T-cell synapse (via CD28) however whether this occurs to a meaningful extent is unclear (147). Once PC differentiation is engaged, cells effect their exit from the lymphatic system by downregulating CCR7 and CXCR5, and upregulating S1P-receptor (27,28). Depending on the signals received from the particular Tfh-cell that induced its differentiation, a given PC will instead begin to express homing receptors directing it to one of a variety of possible locations (**Figure 1**). Many PCs contribute antibodies to serum from niches in bone marrow, which they are chemoattracted to via CXCR4 (for CXCL12) (51,21). This is the classical home of the LLPC, where such longevity is encouraged through growth factors (particularly APRIL) secreted by bone marrow stroma, and low oxidative stress in the hypoxic environment (29,148–150). Other PCs home to sites of inflammation via CXCR3 (for CXCL9/10/11), respiratory mucosa via integrin  $\alpha 4\beta 1$  and CCR10 (receptors for VCAM-1 and CCL28, respectively), or intestinal mucosa via integrin  $\alpha 4\beta 7$  and CCR9 (receptors for MadCAM-1 and CCL25, respectively) (151,152). CD138 is a late marker of human PCs, which can rarely be seen on cells en route to their ultimate destinations, but which becomes clearly evident once they have arrived (146,153). Expression of markers CD38 and CD138 are essentially reversed in the timing of their upregulation in mice, as compared with humans (154).

## Memory B-cell Phenotype and Function

A memory B-cell is defined by its continued persistence post-activation, which can occur through any of the mechanisms discussed above: T-independent type I (PAMP/DAMP ligation), T-independent type II (BCR cross-linking), or T-dependent (TCR + peptide-MHCII immunological synapse and CD40 stimulation) (54,58,99). Not all memory cells are created equal, however, and the latter pathway tends to imbue cells with improved longevity, as a result of higher expression of anti-apoptotic factors (155). Similarly, all three pathways, but again particularly the latter, can result in a CSR event that ceases the expression of IgD, however this is not always the case, and thus an absolute definition of memory remains elusive (79). In practice, IgD-negativity is used as a proxy for memory. Also, as will be discussed later, CD27-positivity is commonly used as a memory marker in conjunction with IgD (140). Unfortunately, this is likely even more problematic than using IgD alone, as a CD27-IgD- memory population will figure prominently in the work presented herein. To a first approximation, however, “naïve” B-cells are CD27-IgD+, activated naïve cells or “unswitched” (perhaps transitioning toward CSR) memory are CD27+IgD+, canonical “switched” memory cells are CD27+IgD-, and “double-negatives” are a minor population of CD27-IgD- cells, which have historically been largely ignored by most B-cell immunologists (156,157). Apart from prior CSR and SHM, memory B-cells behave and traffic much as naïve cells do (LN homing from blood via CD62L, CCR7, and CXCR5, and draining back in to blood via

S1P-receptor), though they have fewer requirements for subsequent activation, including the negligibility of STAT3 phosphorylation through IL-21 signaling (142). In general, memory B-cells have significantly less need for T-cell help, and may function normally, expanding upon antigen exposure and giving rise to PCs without Tfh-cell involvement (158). However further CSR and SHM occurring in memory B-cells are still thought to come about via GC-restricted T-cell help, upon secondary antigen stimulus. Also, importantly, T-cells constitute a major restraint on B-cell immunity, given their role as gatekeepers for naïve cells transitioning to long-lived memory or PC differentiation (25).

### **Age-Associated B-cells**

This title refers to the CD27-IgD<sup>-</sup> cells mentioned above that have received little attention until recently. The first report to provide substantial analysis of their phenotype noted their expression of the inhibitory Ig receptor FcRH4 and of tissue homing chemokine receptors CCR1 and CCR5 (159). It was also noted that these cells were morphologically larger than other memory cells, poised to produce antibody, and poorly mitotic with stimulation. The next account of this phenotype demonstrated its expansion in chronic HIV infection, where it was also found to lack the BCR co-receptor molecule CD21, explaining the previous observation of a declining proportion of CD21<sup>+</sup> B-cells in that patient population (160). These authors argued that these cells were exhausted and not only lacked proliferative capacity, but were also dysfunctional. In other work, the presence of tissue homing receptors prompted the term “tissue-like” to describe

the phenotype, which was extended further with the appreciation of another corresponding homing receptor, CXCR3, expressed by these cells, as well as the absence of CCR7 and CXCR5. Prior to these observations, the Th1-directing transcription factor, T-bet, had been knocked out in mice, demonstrating its role in CSR to IgG, and subsequently had been shown to be induced in B-cells by TLR9 ligand CpG (161,162). T-bet<sup>+</sup> B-cells also expressed the myeloid DC-associated marker CD11c, which had been previously noted on tissue-like cells. Thus T-bet, CD11c, and IgG were integrated into the phenotype. Further T-bet knockout studies in mice demonstrated the importance of this B-cell subtype in viral clearance (80,81). Meanwhile, in humans these cells were found to be expanded in autoimmune disease and in the elderly, hence their designation as age-associated B-cells (ABC) (163–167). Further reports confirmed that the tissue-like T-bet<sup>+</sup> cells expanded in chronic HIV were, in fact, possessed of BCRs specific to HIV antigen, and another demonstrated a differentiation status intermediate between memory and PC (168,169). Over time the “exhausted” narrative began to change, due to the accumulating evidence of alternative activation, particularly via viral-sensing TLRs 7 and 9 (162,80,164,167,170). Still, it remained unclear how to assess and categorize ABCs, and how they might simultaneously relate to acute and chronic viral infection, autoimmunity, and aging.

### **Role of the Transcription Factor T-bet in the Adaptive Response**

The immune system responds to different kinds of pathogens with distinct effector activities. The type of response is largely dictated by the cytokines secreted by the CD4<sup>+</sup> T-cells recruited (on the basis of their specificity for peptide-MHCII), and thus responses are named for the T-cell subtypes that drive them (171). Intracellular pathogens (and cancer, approximated by the immune system as viral infection) induce Th1 responses, which are orchestrated by CD4<sup>+</sup> T-cells secreting IFN- $\gamma$  (172,173). Given the sheltering of pathogens within cells, the most important effector activities are carried out by cytotoxic CD8<sup>+</sup> T-cells and natural killer (NK) cells, which detect foreign antigen presented as peptide-MHCI or detect the lack of appropriate antigen presentation, respectively (174). As above, this type of response also engenders IgG<sup>+</sup> PCs, whose secreted antibodies opsonize or neutralize extracellular pathogen to prevent intercellular transmission of infectious particles (80,161). The CD4<sup>+</sup> T-cells (Th1), CD8<sup>+</sup> T-cells, NK-cells, and GC B-cells and Tfh-cells involved all express the common transcription factor, T-bet, which seems to have evolved as a master regulator of immunity to intracellular pathogens (175,176). In all cell types it drives expression of CXCR3 and CCR5, which facilitates homing toward Th1 inflammation (177,178). This both enables circulating cells to locate sites of infection where they can exert their effector functions, and additionally aids Tfh- and memory B-cells of relevant specificity to find cognate GCs, which secrete corresponding chemokines within secondary lymphoid organs (179). The

effects of T-bet are not uniform across cell types, however, which is unsurprising given the inherent diversity of immune compartments encompassed. For example, in CD4<sup>+</sup> T-cells, increasing T-bet reinforces Th1 skewing and IFN- $\gamma$  secretion, while in CD8<sup>+</sup> T-cells, it drives terminal differentiation towards an effector phenotype (176). In B-cells, T-bet is expressed transiently in the GC (with the exception of ABCs, above), where it drives IgG<sup>+</sup> PC effector differentiation and CXCR3 expression (180). This effect is maintained even after T-bet downregulation, and comes at the cost of memory B-cells. Lastly, T-bet is required for NK-cell development and longevity, and expression is also necessary in dendritic cells (DCs) conferring a Th1-skewed phenotype when priming naïve CD4<sup>+</sup> T-cells (176).

### **Effector Memory: Analogies Between B- and T-cells**

The specifics of ABC trafficking have not been discussed in the literature to date, but the term “tissue-like” proposes a hypothesis. Despite chemokine receptor expression indicating that ABCs might be tissue-homing cells, B-cell dogma describes a single canonical memory phenotype, which is explicitly lymphoid-homing. Memory T-cells, however, are further subdivided into two circulating types: lymphoid-homing central memory (T<sub>cm</sub>) and tissue-homing effector memory (T<sub>em</sub>) (181). T<sub>cm</sub> is highly analogous to memory B-cells in that it is lymph node-tropic (via L-selectin and CCR7 for PNA<sup>d</sup> and CCL19/21, respectively), and in that it is proliferative and stem-like, but upon stimulation requires a substantial delay before differentiating toward effector function

(cytotoxicity or cytokine-secretion, in the case of T-cells) (51,182). Likewise, effector T-cells (Teff) parallel PBs given their tissue homing potential (via a variety of chemokine receptors, varying by target tissue) and capacity for immediate effector function (183,184). As with PBs above, these are predominantly short-lived cells, but, like LLPCs, some Teff persist in their tissue niches for long periods without recirculating in blood, and these have been termed “resident memory” (185–187). Effector memory, however, refers to a mixed phenotype sharing features of Tcm and Teff, but does not merely represent memory cells actively-transitioning toward effector differentiation; rather it is a stable subset of its own that currently applies solely to T-cells. Tem are long-lived circulating cells that lack the lymphoid-homing receptors of Tcm, and follow chemokine gradients into inflamed tissues where they rapidly differentiate toward effector activity upon TCR activation via cognate peptide presentation (188). This feature allows the adaptive immune system to deliver anamnestic effector activity to an infectious insult anywhere in the body, immediately after it has triggered innate immunity signaling through PAMP and DAMP receptors, rather than waiting a week or more for Teff to develop in the draining LNs. Curiously, Tem, like ABCs, express lower levels of activation markers (including CD27) than their Tcm counterparts, and have been shown to expand with age and chronic infection (189,190). Further similarities between Tem and ABCs are a primary concern of the work herein, and are explored in the context of rhinovirus infection, a universal and recurrent human pathogen.

## Rhinovirus Virology and B-cell Immunity

Even by viral standards, RV is small (30nm). It has a non-enveloped capsid and a positive-sense RNA genome (7,200bp), and is classified within the picornavirus family and enterovirus genus, closely related to polio, hepatitis A, Coxsackie, and enterovirus species (1,191). Like other picornaviruses, the genome is initially expressed as a single polyprotein, which is proteolytically processed by several enzymatic domains within its own structure to release four pre-folded capsid subunits, the RNA-dependent RNA polymerase, and other nonstructural components. For select RV strains, the capsid structure has been solved by X-ray crystallography to 2.15Å resolution, demonstrating that the four subunits together form a roughly triangular structure, of which five complexes form a pentamer, of which twelve form the icosahedral capsid, thus incorporating 60 copies of each subunit (**Figure 3**) (192). There are over 100 documented RV strains with distinct capsid structures, most using ICAM-1, others LDL-receptor family members, and still others cadherin-related family member 3 (CDHR3), as the cellular receptor for infection (193,194). Epithelial cells are the primary targets, although any cell bearing the widely-expressed receptors above is theoretically susceptible (195). Infection is spread by direct contact between hosts or via aerosolized particles, and begins in the upper airways, moving down to the lower airways, and causing an inflammatory response with kinin-release correlating closely with symptoms (1). Given that RV-infection does not inherently cause epithelial cytopathology, the symptoms are thought to be entirely due to

the host inflammatory response (4,196–198). RV does, however, induce loss of tight-junctional integrity, perhaps contributing to bacterial superinfection. In immunocompetent individuals, RV infection is self-limiting and involves an average incubation period of 2 days followed by 7-14 days of symptoms including runny nose, congestion, sore throat, cough, headache, and occasional fever. There is evidence to suggest that ensuing Th1 immunity is protective post-infection and correlates with reduced viral shedding and milder symptoms upon reinfection up to 16 weeks later; however, humoral immunity is required for viral clearance (199,200). Neutralizing antibodies specific to the inducing strain develop in the serum 1-2 weeks after infection and can persist for a year (201). These serum responses, in general, are not cross-protective, though murine monoclonal antibodies neutralizing a wide variety of strains have been successfully developed, indicating that the diversity of viral epitopes does not preclude cross-reactivity (202). Additionally, CD4+ helper T-cells in humans have been demonstrated to respond to viral peptides with broadly conserved sequences (203). Thus, no simple explanation currently accounts for human susceptibility to repeated RV infections and lack of durable and broadly-neutralizing humoral immunity.

### **Neutralizing Antibodies**

The neutralizing capacity of an antibody is a function of the pathogenic role of the epitope to which it binds as well as the affinity of that interaction (204–208). In the case of toxigenic bacteria, vaccines are often able to make selective

use of secreted toxin molecules to induce immunity to the most hazardous bacterial components, rather than distract the adaptive response with additional antigens (209–211). However, this single molecule/motif approach is complicated in viruses, which rely on intact virions to gain cell entry and exert their pathogenicity. Though immunity should ideally be directed against epitopes binding cellular entry-receptors, separating the implicated viral proteins from their native context frequently alters their conformation. Antibodies directed against individual protein components will likely bind with low affinity, if at all, to native pathogen in an infectious setting (212–214). This limitation is of particular relevance to non-enveloped viruses like RV where the host-cell binding epitope is composed of multiple capsid proteins. Thus, replication-defective or attenuated live virus is commonly used in corresponding vaccines. This rules out pre-selection of immunizing epitopes, and, accordingly, the primary goal of most viral vaccines is to induce high-affinity antibody responses to any exposed and available epitopes. In fairness to this approach, well-opsonized viruses are almost universally rendered non-infectious, even if antibodies are not directed against epitopes binding entry-receptors, and “high-affinity” can in most cases be considered synonymous with “neutralizing” (204–208). However, antibodies directed against viral surface epitopes not directly involved in infection are liable to lose affinity over time, as their targets are more prone to mutation than epitopes constrained by requirements of infection to bind host-cell entry-receptors. Errors in viral genome replication alter these non-conserved

epitopes, diminishing the neutralizing capacity of antibodies targeting them. For ICAM-1-dependent RV strains, antibodies against ICAM-1 binding domains have much greater potential to be cross-protective because of these constraints. Given that cross-protective humoral immunity to RV does not develop in humans, despite numerous infections, it seems likely that serum antibodies predominantly target non-conserved epitopes likely excluding ICAM-1-binding motifs.

### **Potential Defects in the Humoral Immune Response to Rhinovirus**

As we consider putative mechanisms undermining the B-cell response to RV, one intriguing observation is that RV has been documented to principally promote humoral responses against an epitope at the N-terminus of the capsid subunit protein VP1 (215,216). This 20-peptide sequence, buried at the virion's core, is highly conserved, though ostensibly not for its role in binding a host-cell entry-receptor. Rather, its impressive humoral immunogenicity suggests that it may serve an evolved function to distract B-cell responses, thus diluting neutralizing contributions. Its status as a "decoy" epitope is unconfirmed, however the neutralizing potential of antibodies directed against epitopes unavailable on viable virus (i.e. internal), must at the very least be held in doubt, if not ruled out completely. Another possible explanation for our chronic susceptibility to RV is that when the immune system is stimulated with an antigen that closely resembles another to which it has established immunity, it tends to employ the same T- and B-memory cells that were expanded previously, rather than induce naïve lymphocytes to respond (217). This rule holds even in cases

where the memory response is ineffective against a new pathogen, under a phenomenon termed “original antigenic sin” (218,219). This effect is largely unexplained. One mechanism proposed to contribute is the cross-linking of inhibitory Fc-receptors on naïve B-cells by circulating IgG, but under normal physiological circumstances this signaling cannot completely abrogate naïve responses (157,220,221). Original antigenic sin is well-appreciated in immunity to viruses that readily mutate, such as influenza or HIV, but is perhaps most notable in Dengue fever where initial infection by one of the four extant strains is fairly benign, but subsequent infection with another is deadly (222–224). This is seemingly due to cross-reactive, but non-neutralizing antibodies dominating the heterotypic recall response, and obstructing the outgrowth naïve neutralizing B-cell clones. Although the pathogeneses of RV and Dengue have little in common, the manner in which the memory response to previous exposure negligibly (or negatively) impacts subsequent protection to heterotypic strains may be analogous. In further support of this notion, a similar effect to that described above in Dengue has been demonstrated in mice infected with Coxsackievirus B, which is closely related to RV (219).

**Figure 1: The B-cell Response to Infection or Vaccination**

Naïve and memory B-cells circulate continuously, but periodically linger within lymph node follicles. In this location they may come into contact with cognate antigen derived from pathogens, draining through afferent lymphatic vessels from peripheral tissues. B-cell receptor-bound antigen is internalized and presented to specialized T-helper cells. B-cells engaging in this process are stimulated to divide and differentiate into antibody-secreting plasma cells. Plasma cells exit lymph nodes through efferent lymphatic vessels, and home to various sites including bone marrow, as well as sites of infection and inflammation. Thereafter, plasma cells secrete antibodies into blood, mucosa, or other tissues to control the inciting pathogen, and to preclude future susceptibility.

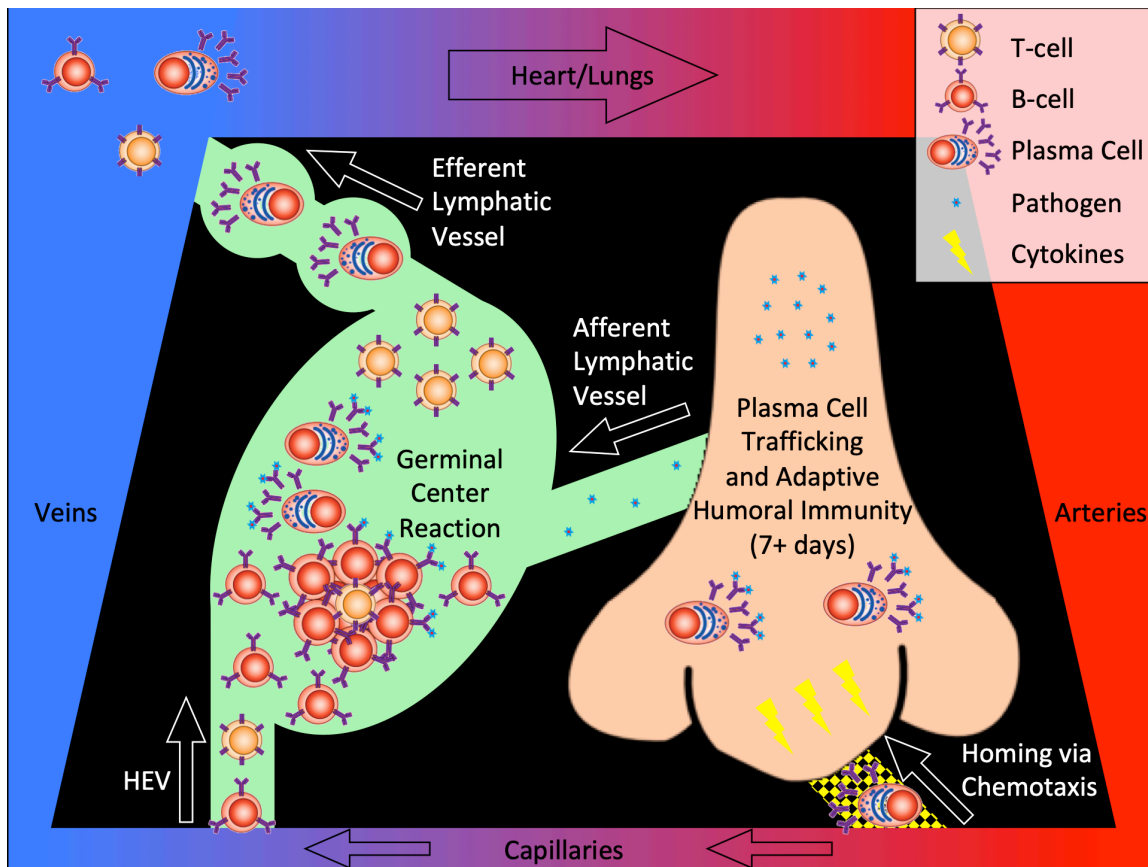
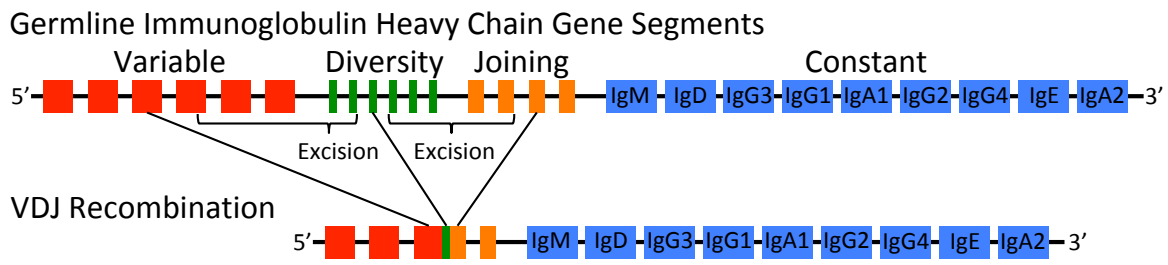


**Figure 2: Immunoglobulin Gene Recombination and Hypermutation**

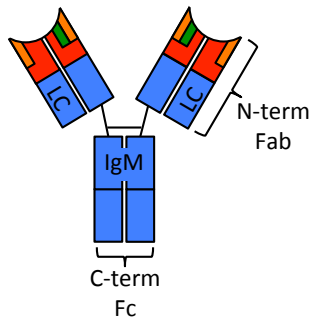
Developing B-cells excise V, D, and J DNA segments at the immunoglobulin heavy chain locus to assemble discrete VDJ combinations. An equivalent process occurs at the light chain (LC) locus, though it only contains V and J segments. Initially, functional BCRs are expressed with an IgM constant region. However, following specialized stimulus in germinal centers, AID enzyme activity is induced, leading to isotype switch through further excision of constant region segments, as well as VDJ hypermutation (indicated by yellow stars). The latter mechanism primarily incurs CG to UA missense base-pair substitutions to increase antibody affinity for antigen.



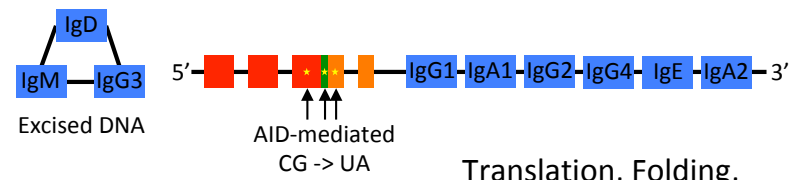
Transcription and mRNA Processing



Translation, Folding, and Assembly



Class Switch Recombination and Somatic Hypermutation



Transcription and mRNA Processing



Translation, Folding, and Assembly

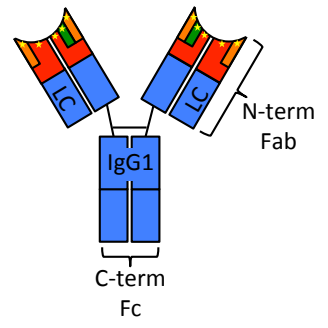
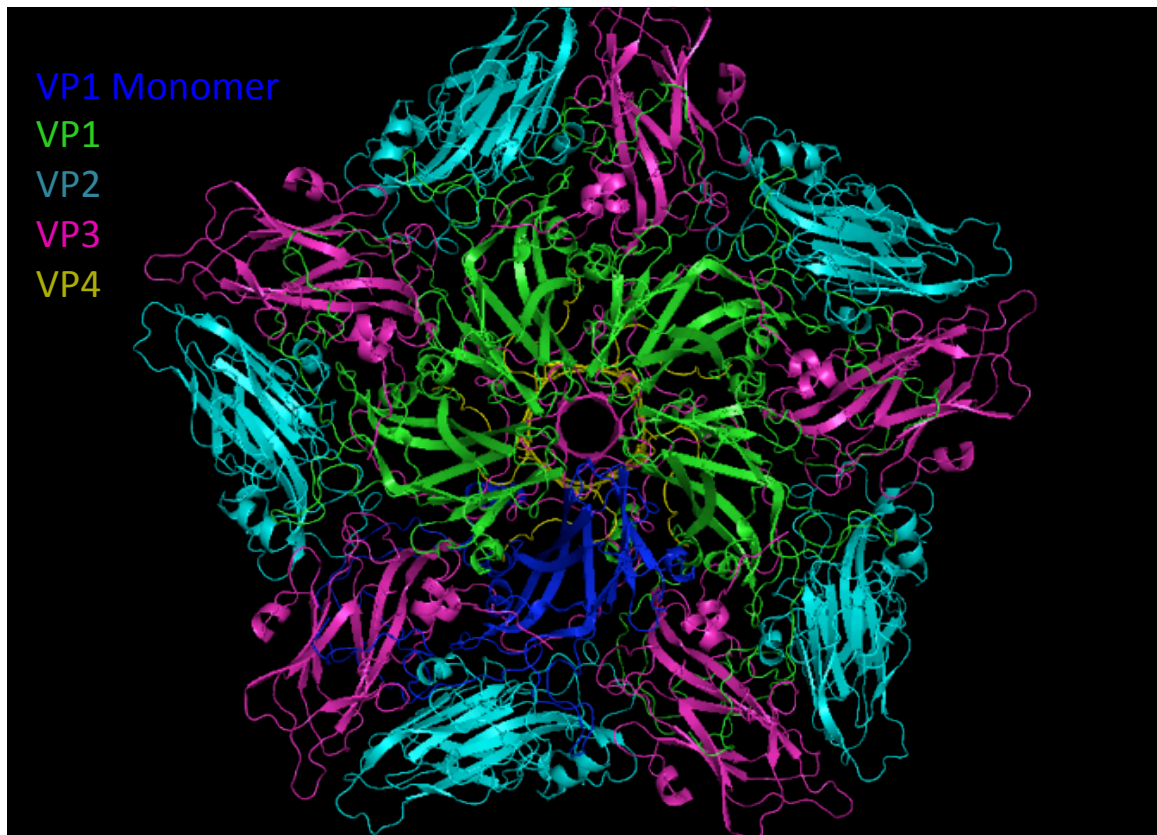


**Figure 3: RV Capsid Pentamer Crystal Structure at High Resolution**

The RV-A16 pentamer, composed of five discrete complexes of capsid subunit proteins VP1-4, is shown from its outward face at 2.15Å resolution. Twelve pentamers form the enclosed capsid and VP4 is entirely internal. One of five VP1 subunits is shown in blue to demonstrate its position and extent relative to neighboring VP1 molecules.



## Thesis Rationale and Proposal

RV is estimated to account for at least half of the billion cases of the common cold per year within the US, and triggers severe disease exacerbations in patients with comorbid respiratory or cardiovascular conditions. Attempts at vaccine development have routinely failed to provide immunity to the considerable diversity of RV strains, and systemic cross-protective adaptive responses generally are not engendered by infection with individual strains. Still, highly-conserved protein sequences can be found spanning many strains, suggesting that cross-protective T-cell and B-cell epitopes exist. Prior to the completion of this work, our lab had borne out cross-reactivity in CD4+ T-cells, but the presence of this phenomenon in the B-cell compartment remained purely hypothetical. Although humoral responses have been described in some detail, the approaches taken historically have a variety of weaknesses, and the cellular aspects of immunoglobulin generation against RV have never been rigorously examined in a human context. Moreover, while the finding that cross-reactive CD4+ T-cells recognizing conserved epitopes and responding to a variety of RV strains is encouraging when considering the possibility of a vaccine, on its own it is insufficient. The development of a neutralizing antibody response is additionally required for viral clearance, and this does not occur in a lasting, broadly protective manner.

To address the question of a potential defect in humoral immunity to RV and to elucidate the cellular mechanisms involved, we elected to track B-cell

responses in the blood of seronegative healthy human volunteers who were experimentally infected with one of two human RV strains (RV-A16 or RV-A39). B-cell specificity for the infecting strain, as well as the heterotypic strain, were analyzed in parallel. To this end, we employed conventional flow cytometry, as well as mass cytometry, incorporating fluorophore- and heavy metal-labeled virions, respectively, to identify B-cells specific for either a single RV strain or both strains. All RV-specific B-cells were phenotyped to determine the representation of subsets, including T-bet<sup>+</sup> ABCs (or tissue-like memory), and the various specificities were compared for their fluxes in total numbers and relative ratios upon acute infection and at convalescence. The contributions toward RV immunity of these diverse B-cell subsets, defined by phenotype and target epitope, were assessed by temporal analysis alongside measurements of secreted antibodies of all isotypes within serum and nasal washes.

We hypothesized both that B-cell immunity to RV is undermined, but also that cross-reactive B-cells nonetheless exist with specificity for multiple RV strains. The first theory was addressed by infecting human subjects with an RV strain to which they were naïve, and analyzing single-strain RV specificity within responding B-cells. Here we sought to explain the high frequency of RV infections to which humans are subject by illuminating a novel manifestation of original antigenic sin. Evidence for this would come in the form of a heterotypic response (against a previously cleared strain) poorly targeting the infecting strain. Our latter hypothesis was investigated by evaluating for the presence or

absence of B-cells with dual-strain specificity. Even if such cells are vanishingly rare, they would nevertheless validate the potential for broadly protective humoral responses. Overall, the results of this study take strides toward elucidating the role and value of specific B-cell subsets in RV clearance, and toward informing vaccine strategies to favor those subsets most crucial to immunity. In addition to what we learn about how RV-specific immunity functions and is constrained, we expect our human-based challenge model will help to address outstanding questions concerning more dangerous human pathogens, viral or otherwise.

## Materials and Methods

### **Development of New Tools Applied to an Existing Human Infection Model**

Though human RV challenge itself is relatively novel and employed by only a few groups worldwide, this work required several substantial innovations beyond the previously established model. Most importantly, it replaces recombinant viral capsid subunit proteins with intact virions as antigen for specific labeling/capturing of immunoglobulin, both in the context of assessing secreted antibodies and identifying RV-specific B-cells via surface BCR. This has one obvious initial advantage in that it preserves native viral epitopes comprised by multiple subunits in the quaternary capsid structure, which would be unavailable on purified monomer proteins. In further support of this strategy, we present data in this thesis that questions the validity of monomers as a physiologically-relevant antigen. Thus, by switching to whole virus, we can precisely quantify multiple antibody isotypes to RV for the first time, something other ongoing challenge models have not yet demonstrated. However, given the relative inefficiency of producing whole virus, compared with expressing recombinant capsid subunits, another innovation was required to make more economical use of purified antigen. Here we opted to develop a cytometric bead-based immunoassay, rather than apply the standard ELISA. For the equivalent readout, coating beads requires several orders of magnitude less antigen than coating a plate. Moreover, by multiplexing beads with four different antigens, and multiplexing readout with

four different antibody isotypes, we managed to spare serum and nasal wash specimens that were in limited supply. Ultimately, 0.2uL serum could generate 16 discrete pieces of data.

Perhaps the most illuminating benefit of querying our system with intact capsid became apparent when we succeeded in labeling RV-specific B-cells via BCR. This capability has been widely pursued in the field for several years, and we are the first to accomplish it. This advance enabled us to identify circulating human B-cells responding to RV infection for the first time, and to appreciate fluxes in their frequency and phenotype *in vivo*. It also allowed us to sort these cells for *in vitro* analysis, opening up further avenues of study. Importantly, it permitted us to address our hypotheses concerning the predominance of homotypic versus heterotypic responses, and the existence of cross-reactive B-cells specific for multiple viral strains. Finally, our cellular work was enhanced by implementing mass cytometry, which provided an expanded phenotyping panel. Given certain foibles of this technology, which remain poorly understood, samples must be barcoded and multiplexed prior to staining, to avoid batch-to-batch artifacts that subvert biologic findings. Our model included three time points with sample sizes of >20 each, necessitating 60+ discrete barcodes. Meanwhile, the largest published multiplexed mass cytometry experiment to date totaled a mere 20 samples (225). By incorporating antibody-labeling with two osmium isotopes, it was feasible to expand the batch size to 70 samples. This required oxidizing and dissolving metallic osmium in aqua regia for preparation

as a chloride salt. As a “noble metal” osmium is poorly amenable to this process (226). However, for our purposes we found it to be sufficiently soluble, albeit poorly and incompletely so, as quantified by inductively-coupled plasma mass spectrometry (ICP-MS). Notably, this application of OsCl could just as easily enable further expansion of a phenotyping panel, as it does a barcoding panel.

### **Study Subjects and Experimental Infection Model**

Healthy uninfected adults (ages 18-45 years) who were non-allergic based on clinical history or total IgE levels <150 IU/ml and who tested seronegative for the RV challenge strain (serum neutralizing antibody titer  $\leq 1:4$  for RV-A16 or RV-A39) were nasally inoculated with RV-A16 (300TCID<sub>50</sub>, 14 subjects, 4 male, 10 female, 22 years  $\pm$  1.9 years SD) or RV-A39 (100 TCID<sub>50</sub>, 16 subjects, 4 male, 12 female, 21 years  $\pm$  3.7 years SD) (Clinical trials.gov ID NCT02111772 and NCT01669603 respectively) (4,227,9,228,229). Blood was drawn for isolation of PBMCs immediately before virus inoculation (baseline, day 0), during the acute infection phase (day 4 or 5), and at convalescence (day 21). Cells were cryopreserved until sample collection was complete. Nasal washes were performed on days 0-5, 7, 14, and 21, and serum was collected at days 0, 4/5, 7 (RV-A16 challenge only), and 21. Nasal biopsy specimens were obtained on day 4 from healthy adults who received RV-A16 challenge (Clinical trials.gov ID NCT02910401). Additional uninfected subjects not undergoing RV challenge were recruited through the University of Virginia. Informed consent was obtained from all study participants and subjects were compensated for participation. The

research was approved by the Institutional Review Board for Health Sciences Research at the University of Virginia, the Food and Drug Administration, and the National Institute of Allergy and Infectious Diseases Safety Committee. All studies were conducted in compliance with Good Clinical Practices and in accordance with the Declaration of Helsinki.

### **Determination of Infection Status**

Neutralizing serum antibodies were evaluated using a standard microtiter assay (230), and nasal wash specimens collected on days 1-5 were cultured for virus by standard methods (231). Subjects who had at least a 4-fold increase in serum neutralizing antibody to RV-A16 or RV-A39, or virus isolated from at least one post-inoculation specimen (by culture or qPCR), were considered infected with the study virus (227).

### **Preparation of Virus for Multiplex Serology Assays and Labeling B-cells**

Cryovials of RV-A16 and RV-A39 were thawed and used to infect HeLa cell monolayers in serum-free minimal essential media, and supplemented with 10% fetal bovine serum after 4 hours (ThermoFisher). After 2 days, virus was released by serial freeze/thawing, cell debris was pelleted and lysates were used for virus purification. Virus was isolated by sucrose cushion (30%), followed by sucrose-gradient (15-45%), then buffer exchanged into PBS, concentrated, UV-irradiated, and maintained at 4<sup>0</sup>C (232). Capsid integrity was confirmed by electron microscopy, virus purity was assessed by SDS-PAGE analysis with

silver staining (Pharmacia PhastSystem), and the virus yield measured by BCA assay (Pierce Chemical Company). RV strain identity was confirmed by RT-PCR specific for the VP1 capsid subunit region of the RNA genome (**Table 1**). Concentrated virus was diluted to 0.5 $\mu$ g/ $\mu$ L in 200 $\mu$ L stock volumes and cryopreserved prior to use. To label RV-specific B-cells for detection by multi-color flow cytometry and mass cytometry, virus was tagged at lysine residue terminal amines with Alexa Fluor 488 NHS Ester and Alexa Fluor 568 NHS Ester (ThermoFisher), and isotopically enriched cisplatin 194 and 198 (Fluidigm), respectively (233). For serology assays, virus was biotinylated with NHS-LC-Biotin (ThermoFisher). Excess label was desalted on Zeba spin columns to exclude molecular weights below 40kD (ThermoFisher).

### **Multiplex Serology Assay**

Streptavidin-coated polystyrene beads (Spherotech) were first labeled with Alexa Fluor 405 (ThermoFisher) and/or Fixable Viability Stain 510 (Becton Dickinson) to create four different fluorescent signatures. Beads were then coated with biotinylated virus (RV-A16 or RV-A39), tetanus toxoid c-terminal fragment (positive control), or mouse IgG (negative control), respectively. Beads were washed and combined, and incubated with serum diluted 250x, nasal washes diluted 10x, or culture supernatants diluted 10x. After washing, antibody binding was detected using anti-human IgG (Becton Dickinson), IgM (BioLegend), IgA (Miltenyi), and IgE (BioLegend) isotypes. Beads were read on an Invitrogen Attune cytometer.

### **Multi-color Flow Cytometry**

PBMCs from eight uninfected subjects (3 male, 5 female, 43 years  $\pm$  18 years SD) were simultaneously Fc-blocked with mouse IgG (Lampire) and ICAM-1-blocked (BioLegend). After 30 minutes at 4<sup>0</sup>C, B-cells were stained with fluorescently tagged virus (Alexa Fluor 488-RV-A39 and Alexa Fluor 568-RV-A16), fluorescent antibodies against CD3 (BioLegend), CD19 (BioLegend), CD20 (BioLegend), CD27 (ThermoFisher), CD38 (Becton Dickinson), CCR5 (ThermoFisher), CXCR3 (BioLegend), CXCR5 (BioLegend), IgD (ThermoFisher), IgM (BioLegend), IgG (Becton Dickinson), IgA (Miltenyi), and viability dye Live/Dead Aqua (ThermoFisher), and incubated for 30 minutes at 4<sup>0</sup>C. Cells were then fixed and permeabilized (FoxP3 fix/perm kit, ThermoFisher) before staining for intracellular IgM (BioLegend), IgG (Becton Dickinson), IgA (Miltenyi), IgE (BioLegend), and T-bet (BioLegend). Cells were analyzed on an LSR Fortessa Cytometer (Becton Dickinson) using FlowJo version 10.5.3 (TreeStar).

### **Mass Cytometry**

PBMC were thawed in CTL buffer (Immunospot) with benzonase (Millipore), and acid-stripped of Fc-receptor-bound immunoglobulin. Cells were then barcoded using a 70-fold panel according to an 8 choose 4 scheme (**Table 2**) with combined anti-CD45 and anti-MHCI antibodies (BioLegend) bearing 102Pd, 104Pd, 105Pd, 106Pd, 108Pd, 110Pd, 190Os, and/or 192Os (Buylsotope) (234,235,225). Simultaneously with barcoding, cells were stained

with magnetic bead-conjugated antibodies against CD3, CD14, CD16, CD123, and CD235a (Miltenyi), labeled for viability using a 103Rh DNA intercalator (Fluidigm), Fc-blocked with mouse IgG (Lampire), and ICAM-1-blocked (BioLegend). After a 30-minute incubation at 4<sup>0</sup>C, samples were combined and sorted for the negative fraction on an autoMACSpro (Miltenyi). Magnetically enriched B-cells (30 to 50% CD19+) were then stained extracellularly for mass cytometry. After 30 minutes at 4<sup>0</sup>C, intracellular staining was carried out using FoxP3 fix/perm kit (eBioscience). The complete panel (**Table 3**) comprised an additional 45 markers, beyond barcoding and viability. Antibodies not purchased pre-conjugated through Fluidigm were tagged with the indicated metal isotope using Fluidigm conjugation kits. Multiplexed samples were read on a CyTOF2 (Fluidigm) and deconvoluted (computationally separated) prior to analysis. Fluctuations in B-cell populations were monitored over time in an unbiased manner using t-SNE dimensionality reduction analysis (236) and a clustering workflow (237) combining FlowSOM self-organizing maps and ConsensusClusterPlus (238–240). By this method, similarity to 100 phenotype vectors was scored to generate map coordinates, and cells were clustered into nodes on the basis of density across the map.

### **Plasmablast Differentiation Culture**

Freshly isolated PBMCs were prepared for flow cytometry (as above) from six human subjects (2 male, 4 female, 45 years  $\pm$  20 years SD), but were additionally labeled with magnetic bead-conjugated antibodies against CD3,

CD14, CD16, CD123, and CD235a (Miltenyi) during the initial blocking step. Samples were then enriched for B-cells by negative fractionation on an autoMACSpro (Miltenyi). Enriched B-cells (30 to 50% CD19+) were then stained using an abbreviated panel of CD3, CD19, CD20, IgD, CXCR5, RV-A16, and RVA39, omitting fix/perm steps. RV16-specific, RV39-specific, dual-specific, non-specific naïve (IgD+), non-specific CXCR5+ memory (IgD-), and non-specific CXCR5- memory (IgD-) B-cells (CD19+ CD20+ CD3-) were purified on an Influx Cell Sorter (Becton Dickinson) to >90% purity (**Figure 4**). Following isolation, 3-5,000 cells (RV-specific subsets) or 10,000 cells (other B-cell subsets) were plated and cultured for 10 days in IMDM supplemented with 10% FBS, non-essential amino acids, insulin/transferrin/selenium,  $\beta$ -mercaptoethanol, anti-CD40 (BioLegend), IL-2 (Miltenyi), IL-10 (Miltenyi), IL-21 (Miltenyi), and CpG DNA (Miltenyi) (241). Supernatants were collected every two days, and tested for secreted antibodies by bead-based multiplex assay.

### **Single-Cell mRNA Sequencing**

RV-specific B-cells (CD19+CD20+) isolated from a healthy uninfected subject (male, 33 years) were identified by multi-color flow cytometry, and sorted based on differential expression of CXCR5, and whether or not they were mono- or dual-specific. Sorted cells were immediately processed for single-cell V(D)J mRNA profiling by barcoding on a Chromium Controller, amplifying pooled cDNA and targeting enrichment for full-length V(D)J segments using primers specific to Ig constant regions (10xGenomics). Next-generation sequencing was

performed by MiSeq (Illumina). Reads were mapped to a human reference using Cellranger software (10xGenomics) and analyzed for somatic hypermutation and VDJ segment usage on vLoupe browser (10xGenomics). Mutations were compared for RV-specific subsets that were categorized based on antibody isotypes expressed.

### **Fluorescence Microscopy**

Five human subjects (5 male, 0 female, age  $22 \pm 2.8$  SD) were nasally inoculated with HRV-A16 and biopsies were collected at 4 days post-infection. Samples were collected from the inferior nasal turbinate, the middle turbinate, and the posterior nasopharynx. Deidentified healthy splenic tissue was procured from a cadaveric sample in a bio-tissue repository. All tissue was fixed in formalin, paraffin embedded, and sectioned. Prior to staining, sections were deparaffinized in xylenes, washed in 100% ethanol, and gradually transitioned to water. Epitope retrieval was conducted in citrate pH6 buffer (Abcam) at  $100.5^{\circ}\text{C}$  for 20 minutes. Slides were then blocked with 10% donkey serum (Southern Biotech), labeled with primary antibodies against CD3 (rabbit, ThermoFisher), CD11c (rabbit, Abcam), CD19 (rat, ThermoFisher), CD20 (mouse, BioPrime), RV-A16 VP2 (mouse, QED Bioscience), and/or T-bet (mouse, BioLegend) (or mouse, rat, and rabbit isotype controls from ThermoFisher) at 5 $\mu\text{g}/\text{mL}$ , reblocked, and stained with donkey anti-mouse, donkey anti-rat, and donkey anti-rabbit (ThermoFisher Scientific) at 5 $\mu\text{g}/\text{mL}$  tagged with Alexa Fluor 488 NHS Ester (ThermoFisher), tetramethylrhodamine NHS Ester (ThermoFisher), or Alexa Fluor

647 NHS Ester (ThermoFisher). Counterstaining was provided by DAPI at 1ug/mL (PromoKine). Imaging was performed on a Zeiss Axioimager with Apotome attachment using Zeiss optical filter numbers 49 (DAPI), 38HE (Alexa Fluor 488), 43HE (tetramethylrhodamine), and 50 (Alexa Fluor 647).

### **Statistical Analysis**

Paired analysis involving matched subject-data employed the Wilcoxon matched pairs signed-rank test to analyze serum antibodies and the percentage/MFI of different B-cell subsets, and employed the Friedman multiple comparisons test to analyze antibody secretion in plasmablast differentiation culture supernatants. Mann-Whitney ranked-sum test was used to analyze cell counts in nasal biopsies from different subjects and mutations in different immunoglobulin isotypes. Spearman correlation was used to test the relationship between the change in percentages for discrete B-cell subsets. Significant changes in B-cell clusters detected by mass cytometry were designated at a level of  $p < 0.01$  for stringency. A  $p$ -value  $< 0.05$  was considered significant for all other parameters tested.

**Table 1: Rhinovirus RT-PCR Primers**

<b>Strain</b>	<b>Direction</b>	<b>Sequence</b>
RV-A16	Forward	CATGAATCAGTGTTGGATATTGTGGAC
RV-A16	Reverse	AATGTGACCATCTTTGGCTGCTAC
RV-A39	Forward	CACATTTCCACAATTACTATGAAGAAGGAG
RV-A39	Reverse	ATCTTCACCTCTTCCAGCTATGCA

Table 2: 70X Barcoding Scheme for Mass Cytometry

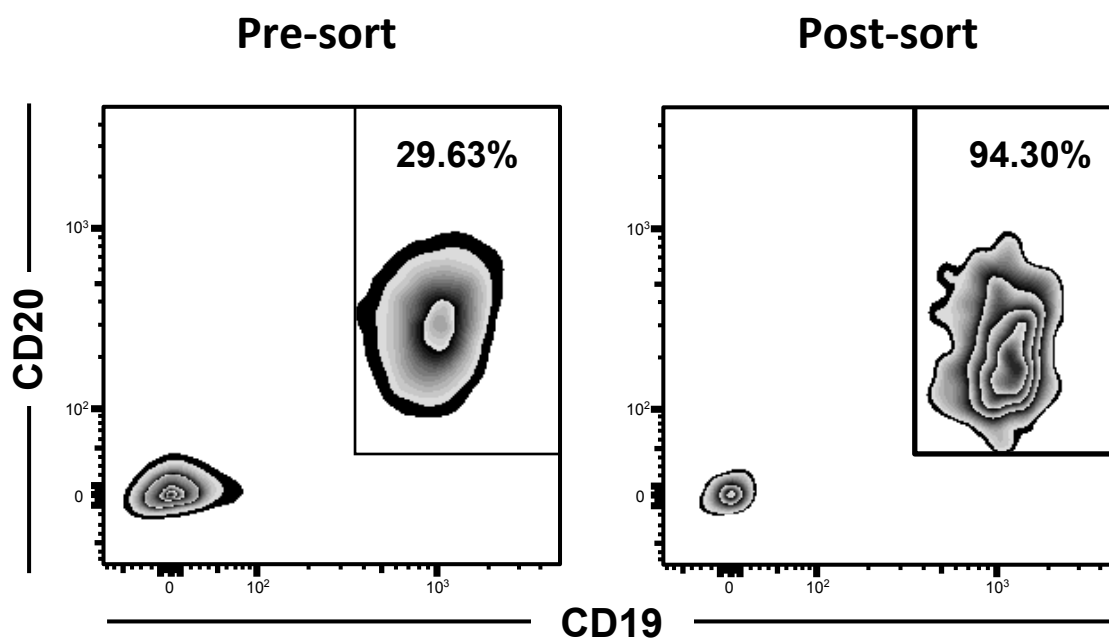
Barcode	102	104	105	106	108	110	190	192	Total
1	1	1	1	1	0	0	0	0	4
2	1	1	1	0	1	0	0	0	4
3	1	1	1	0	0	1	0	0	4
4	1	1	1	0	0	0	1	0	4
5	1	1	1	0	0	0	0	1	4
6	1	1	0	1	1	0	0	0	4
7	1	1	0	1	0	1	0	0	4
8	1	1	0	1	0	0	1	0	4
9	1	1	0	1	0	0	0	1	4
10	1	1	0	0	1	1	0	0	4
11	1	1	0	0	1	0	1	0	4
12	1	1	0	0	1	0	0	1	4
13	1	1	0	0	0	1	1	0	4
14	1	1	0	0	0	1	0	1	4
15	1	1	0	0	0	0	1	1	4
16	1	0	1	1	1	0	0	0	4
17	1	0	1	1	0	1	0	0	4
18	1	0	1	1	0	0	1	0	4
19	1	0	1	1	0	0	0	1	4
20	1	0	1	0	1	1	0	0	4
21	1	0	1	0	1	0	1	0	4
22	1	0	1	0	1	0	0	1	4
23	1	0	1	0	0	1	1	0	4
24	1	0	1	0	0	1	0	1	4
25	1	0	1	0	0	0	1	1	4
26	1	0	0	1	1	1	0	0	4
27	1	0	0	1	1	0	1	0	4
28	1	0	0	1	1	0	0	1	4
29	1	0	0	1	0	1	1	0	4
30	1	0	0	1	0	1	0	1	4
31	1	0	0	1	0	0	1	1	4
32	1	0	0	0	1	1	1	0	4
33	1	0	0	0	1	1	0	1	4
34	1	0	0	0	1	0	1	1	4
35	1	0	0	0	0	1	1	1	4
36	0	1	1	1	1	0	0	0	4
37	0	1	1	1	0	1	0	0	4
38	0	1	1	1	0	0	1	0	4
39	0	1	1	1	0	0	0	1	4
40	0	1	1	0	1	1	0	0	4
41	0	1	1	0	1	0	1	0	4
42	0	1	1	0	1	0	0	1	4
43	0	1	1	0	0	1	1	0	4
44	0	1	1	0	0	1	0	1	4
45	0	1	1	0	0	0	1	1	4
46	0	1	0	1	1	1	0	0	4
47	0	1	0	1	1	0	1	0	4
48	0	1	0	1	1	0	0	1	4
49	0	1	0	1	0	1	1	0	4
50	0	1	0	1	0	1	0	1	4
51	0	1	0	1	0	0	1	1	4
52	0	1	0	0	1	1	1	0	4
53	0	1	0	0	1	1	0	1	4
54	0	1	0	0	1	0	1	1	4
55	0	1	0	0	0	1	1	1	4
56	0	0	1	1	1	1	0	0	4
57	0	0	1	1	1	0	1	0	4
58	0	0	1	1	1	0	0	1	4
59	0	0	1	1	0	1	1	0	4
60	0	0	1	1	0	1	0	1	4
61	0	0	1	1	0	0	1	1	4
62	0	0	1	0	1	1	1	0	4
63	0	0	1	0	1	1	0	1	4
64	0	0	1	0	1	0	1	1	4
65	0	0	1	0	0	1	1	1	4
66	0	0	0	1	1	1	1	0	4
67	0	0	0	1	1	1	0	1	4
68	0	0	0	1	1	0	1	1	4
69	0	0	0	1	0	1	1	1	4
70	0	0	0	0	1	1	1	1	4

**Table 3: Mass Cytometry Antibody Panel**

<b>Metal</b>	<b>Isotope</b>	<b>Reagent</b>	<b>Source</b>
Pd	102	$\alpha$ CD45+MHCI	BioLegend
Rh	103	DNA Intercalator	Fluidigm
Pd	104	$\alpha$ CD45+MHCI	BioLegend
Pd	105	$\alpha$ CD45+MHCI	BioLegend
Pd	106	$\alpha$ CD45+MHCI	BioLegend
Pd	108	$\alpha$ CD45+MHCI	BioLegend
Pd	110	$\alpha$ CD45+MHCI	BioLegend
Pr	141	$\alpha$ T-bet	BioLegend
Nd	142	$\alpha$ CD19	Fluidigm
Nd	143	$\alpha$ CXCR4	BioLegend
Nd	144	$\alpha$ CCR5	Fluidigm
Nd	145	$\alpha$ CD40	BioLegend
Nd	146	$\alpha$ CCR6	BioLegend
Sm	147	$\alpha$ Bcl-2	BioLegend
Nd	148	$\alpha$ CD38	BioLegend
Sm	149	$\alpha$ CXCR3	BioLegend
Nd	150	$\alpha$ CD23	BioLegend
Eu	151	$\alpha$ CD71	BioLegend
Sm	152	$\alpha$ CD21	Fluidigm
Eu	153	$\alpha$ CD11c	BioLegend
Sm	154	$\alpha$ CD86	BioLegend
Gd	155	$\alpha$ CD22	BioLegend
Gd	156	$\alpha$ CLA	BioLegend
Gd	158	$\alpha$ CD27	BioLegend
Tb	159	$\alpha$ CCR7	Fluidigm
Gd	160	$\alpha$ tg $\beta$ 1	BioLegend
Dy	161	$\alpha$ CD95	BioLegend
Dy	162	$\alpha$ CD43	BioLegend
Dy	163	$\alpha$ CD24	BioLegend
Dy	164	$\alpha$ CD20	BioLegend
Ho	165	$\alpha$ Ki-67	BioLegend
Er	166	$\alpha$ tg $\beta$ 7	BioLegend
Er	167	$\alpha$ CXCR5	BioLegend
Er	168	$\alpha$ CD73	Fluidigm
Tm	169	$\alpha$ MHCII	BioLegend
Er	170	$\alpha$ CD3	Fluidigm
Er	170	$\alpha$ CD14	BioLegend
Er	170	$\alpha$ CD16	BioLegend
Er	170	$\alpha$ CD123	BioLegend
Er	170	$\alpha$ CD235a	BioLegend
Er	170	$\alpha$ Fc $\epsilon$ R1	BioLegend
Yb	171	$\alpha$ lgG4 (membrane)	T. Rispens
Yb	171	$\alpha$ lgG4 (secreted)	Becton Dickinson
Yb	172	$\alpha$ lgM	Fluidigm
Yb	173	$\alpha$ lgG	Becton Dickinson
Yb	174	$\alpha$ lgA	Miltenyi
Lu	175	$\alpha$ lgD	BioLegend
Yb	176	$\alpha$ lgE	BioLegend
Os	190	$\alpha$ CD45+MHCI	BioLegend
Os	192	$\alpha$ CD45+MHCI	BioLegend
Ir	193	DNA Intercalator	Fluidigm
Pt	194	RV-A39	In House
Pt	198	RV-A16	In House
Bi	209	$\alpha$ CD11b	Fluidigm

**Figure 4: Cell Purity Obtained by Flow Cytometry Sorting**

Contour plots from one sort experiment to isolate naïve B-cells (representative of 6 separate experiments). All samples for subsets specified in Figures 18-21, and 41-42 yielded >90% purity post-sorting.



## Tissue Homing Memory B cells Rapidly Induce Local Cross Reactive IgG Upon Human Rhinovirus Infection

### **Introduction**

Rhinovirus (RV) is a major cause of the common cold. This disease enacts an enormous health and economic burden based on the high infection rates in the general population, and its exacerbation of chronic respiratory disorders in infected patients (1,3,5). It has long been known that infection induces the production of neutralizing antibodies; however, these antibodies wane after several months, and do not appear to cross-protect against different RV strains (199,201). This latter feature has been attributed, at least in part, to the antigenic variability across the more than 160 serotypes of RV, which are responsible for an estimated 6-10 infections per year in children (11,7). Despite more than four decades of study on antibody responses to RV in infected humans, nothing is known about the nature of RV-specific B-cells in humans. Thus, advancing knowledge in this area could yield new insight into the humoral response to RV, and more specifically, the attributes of B-cell memory to one of the most ubiquitous viral pathogens in man.

Recent work has implicated human B-cells that express T-bet, in anti-viral responses (80,180). Although originally defined as a lineage-specifying transcription factor for Th1 cells, T-bet regulates anti-viral B-cell responses in

mouse models, and is pivotal to B-cell differentiation and CSR, as well as expression of IFN- $\gamma$  and the chemokine receptor CXCR3 in B-cells (176,178). T-bet<sup>+</sup> B-cells, which represent 0.1% to 2% of total B-cells, accumulate over the lives of humans and mice, and accordingly have been termed “age-associated B-cells” (ABCs) (164,166). These cells are also elevated in the circulation of patients with chronic viral infections and autoimmune diseases, consistent with their antigen-driven expansion (163,242,167). T-bet<sup>+</sup> B-cells express the myeloid marker CD11c, and predominantly express IgG, whereas expression of memory B-cell markers such as CD21 and CD27, is not prominent (243,165). Although their specificity remains largely unknown, this phenotype was recently found to comprise the majority of B-cells specific for gp140 in chronically-infected HIV-positive individuals (168). Consistent with the notion of a primary role in anti-viral immunity, selective knockout of T-bet in B-cells results in severe immune deficiency in a viral infection model (81).

We theorized that the high number of infections with RV in humans might favor outgrowth of virus-specific B-cells with attributes similar to T-bet<sup>+</sup> B-cells, but which lacked cross-reactive function. To address this, we performed the first comprehensive longitudinal analysis of human RV-specific B-cells in parallel with anti-viral antibody isotypes, both in steady state, and during experimental infection, using 2 different RV-A strains. Virus-specific B-cells were detected using whole virus, in conjunction with a high-dimensional method, that enabled the detection of subtle variations in rare B-cell types. By this approach,

virus-specific memory B-cells were found to display two distinct signatures consistent with LN homing (CXCR5+) and tissue homing (CXCR5-). Surprisingly, CXCR5- memory B-cells were dual-specific based on their labeling with both RV-A strains tested, expressed T-bet, and rapidly secreted cross-reactive IgG, but not IgA or IgM. Moreover, these cells expanded after infection, and sampling of the nose during acute infection revealed tissue-infiltrating B-cells, concomitant with rapid secretion of cross-reactive IgG. By contrast, CXCR5+ virus-specific B-cells were mono-specific, and secreted strain-specific isotypes that matched those antibody profiles found later in the nose and serum.

Our findings demonstrate a pivotal role for cross-reactive T-bet+ memory B-cells in the response to different RV-A strains, and establish distinct spatial and temporal effector functions for discrete virus-specific B-cell types that enable efficient clearance of different rhinoviruses during the acute phase, but narrow protection and continued susceptibility after infection. The findings also have broader implications for understanding the ontogeny and dichotomous functions of tissue homing and LN homing memory B-cells.

## **Results**

### *Whole Virus Detects Multiple RV-specific Isotypes*

High levels of antibodies to capsid protein subunits of RV have been reported in serum, regardless of infection status (202,215,244). Thus, the biological relevance of such antibodies is unclear. We posited that whole virus is

best suited to label RV-specific antibodies and identify virus-specific B-cells, since it contains native epitopes formed by the four capsid proteins integral to the icosahedral capsid structure. To this end, two distantly related strains of the RV-A species, RV-A16 and RV-A39 (76% genome identity, 80% capsid protein identity), were propagated in culture. Their structure and durability were verified by electron microscopy (**Figure 5**), identity was confirmed by RT-PCR (**Figure 6**) and purity assessed by SDS-PAGE analysis and western blot against the capsid protein VP2 (**Figure 7**). Next, both viruses were incorporated into a novel bead-based multiplex assay to simultaneously monitor changes in serum antibodies specific for both RV-A strains in subjects who were experimentally infected with either RV-A16 or RV-A39 (**Figure 8**). By this method, increases in IgG, IgA, and IgM specific for the infecting strain (i.e. homotypic antibodies), were detected in the serum 21 days after experimental infection (IgG,  $p < 0.0001$ ; IgA,  $p < 0.0001$ ; IgM,  $p < 0.01$ ) (**Figure 9**). However, increases in antibodies to the heterotypic RV strain were not detected, with the exception of a modest rise in IgG ( $p < 0.01$ ). As expected, serum antibodies were unchanged in subjects who did not become infected (**Figure 10**), and no change was observed for serum antibodies to negative (mouse IgG) and positive (tetanus toxin c-terminal fragment) control antigens (**Figure 9**). Notably, serum antibodies to the capsid subunit, VP1, did not change after infection, indicating a lack of specificity for virus (**Figure 11**). These findings validated whole virus as a biologically relevant

target, and confirmed that IgG, IgA and IgM antibodies induced by RV infection in the serum are predominantly strain-specific.

*Dual-specific B-cells are Expanded in the Blood and Lack CXCR5*

Next, to identify RV-specific B-cells, virus was tagged with fluorophore and integrated into a B-cell surface-staining antibody panel for multi-color flow cytometry. B-cells were first analyzed in the blood of healthy uninfected subjects based on the premise that virus-specific memory B-cells would be detectable as a result of previous RV exposures. We elected to analyze RV-specific B-cells in the context of CXCR5, a chemokine receptor that is critical to the retention of B-cells within follicles of secondary lymphoid organs. We posited that the lack of expression of this marker might delineate those virus-specific B-cells with a tissue homing predilection capable of secreting antibodies at the infection site. This was based on the following: (1) low expression of CXCR5 on antibody secreting plasma cells, which facilitates their egress from lymphoid organs into the blood (151,116,99); and (2) previous reports of CXCR5<sup>-</sup> B-cells with putative tissue homing ability in chronic viral infections (160,245,165). Staining of PBMCs with whole virus revealed that RV-specific B-cells were predominantly IgD-negative (i.e. class-switched) memory cells, and enriched for CXCR5<sup>-</sup> cells (~30% of RV-specific B-cells versus <3% of total memory B-cells) that expressed higher levels of CD20 compared with their CXCR5<sup>+</sup> counterparts (**Figure 12a & b**). Analysis of total B-cells revealed CXCR5<sup>-</sup> cells that labeled with both RV-A16 and RV-A39, whereas cells that labeled with only a single virus were enriched for

CXCR5<sup>+</sup> cells (**Figure 13a**). This unexpected finding demonstrated the presence of CXCR5<sup>-</sup> dual-specific and CXCR5<sup>+</sup> mono-specific B-cell types. Within memory B-cells, the numbers of CXCR5<sup>+</sup> cells are typically >10-fold higher than CXCR5<sup>-</sup> cells, and calculation of the absolute percentages of mono-specific and dual-specific cells within memory B-cells confirmed their opposing profiles according to CXCR5 expression (**Figure 13b**). Upon further inspection, 75.2% ± 10.5% of dual-specific B-cells were CXCR5<sup>-</sup>, versus 23.7% ± 15.6% of mono-specific B-cells (**Figure 14**), while only 3.3% ± 0.8% of total memory B-cells were CXCR5<sup>-</sup>. Moreover, CXCR5<sup>-</sup> RV-specific B-cells (mono-specific + dual-specific) comprised 5.0 ± 2.7% of total CXCR5<sup>-</sup> memory B-cells, and dual-specific B-cells were the dominant subset (3.8 ± 2.0%) (**Figure 15**). Given that the frequency of B-cells with a given specificity is typically less than 0.1% of total B-cells (246–249), the relative abundance of dual-specific memory B-cells was striking, and likely reflected expansion from previous RV infections.

To ensure that labeling of B-cells by virus was occurring via surface B-cell receptor (BCR), and not via the major RV receptor ICAM-1, our staining method incorporated an excess of anti-ICAM-1 antibody. However, even when ICAM-1 blocking was omitted, a lack of correlation between virus binding and ICAM-1 staining indicated that binding of virus to B-cells by surface ICAM-1 was not a feature (**Figure 16**).

Next, to probe the functional relevance of a lack of CXCR5 expression on dual-specific B-cells, the phenotype of CXCR5<sup>-</sup> and CXCR5<sup>+</sup> cells within the

memory B-cell compartment was compared. This analysis revealed that CXCR5- memory B-cells expressed higher levels of the transcription factor T-bet, the myeloid marker CD11c, and Th1-associated receptors, CCR5 and CXCR3 (**Figure 17a**). Moreover, these cells were predominantly IgG+, and the percentage of IgG+ cells was higher as compared with CXCR5+ B-cells, whereas the percentage of IgA+ and IgM+ cells was lower (**Figure 17b**). Thus, CXCR5- B-cells fit the signature of T-bet+ B-cells reported in chronic viral infections (160,81,165,168). Such CXCR5- memory B-cells might constitute the B-cell equivalent of an “effector memory” subset, based on their trafficking potential and antibody profile (189,185,229).

*Dual-specific B-cells Rapidly Secrete Cross-Reactive IgG, but not IgA or IgM*

A cardinal feature of “effector memory” is the ability for cells to respond rapidly upon activation. To test for this quality, and to exclude the possibility of B-cell exhaustion, the capacity for dual-specific B-cells to secrete cross-reactive antibodies was assessed by culturing under conditions that differentiate plasma cells (241). Cells were FACS sorted to high purity to compare the function of B-cells with dual-specificity versus mono-specificity. To accomplish this, B-cells were first gated for binding of RV-A16 only, RV-A39 only, or both viruses. The remaining non-specific cells were gated into naïve, CXCR5+ memory, and CXCR5- memory B-cell types, to give a total of six sorted B-cell populations. Culture supernatants were collected every two days for antibody analysis. Dual-specific B-cells predominantly secreted IgG antibodies that were

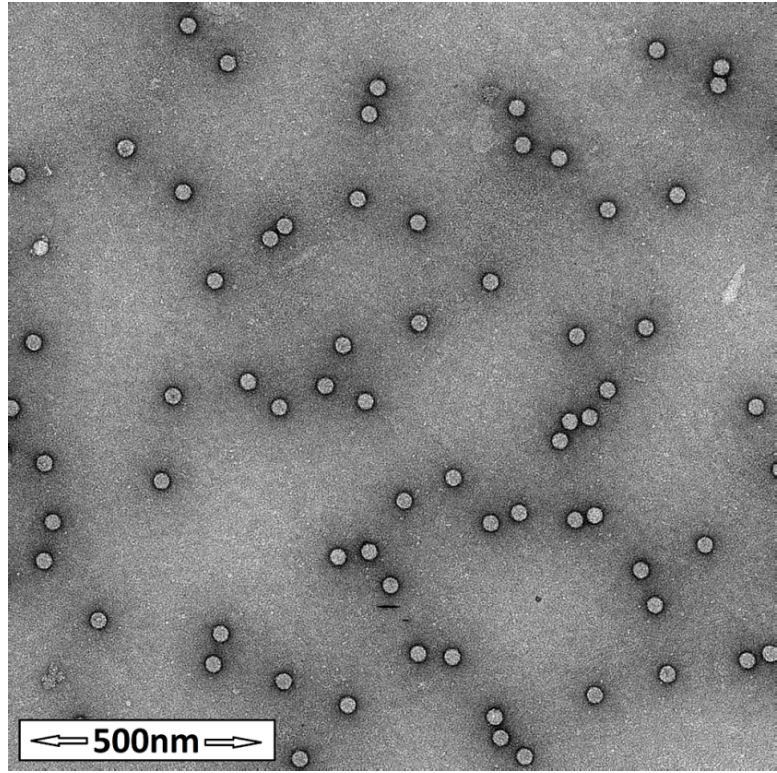
cross-reactive for RV-A16 and RV-39, while secretion of other RV-specific isotypes was minimal. The predominance of IgG was also a feature of non-specific CXCR5<sup>-</sup> memory B-cells. By contrast, mono-specific B-cells secreted strain-specific IgG, IgA and IgM antibodies, echoing the isotype profile of non-specific CXCR5<sup>+</sup> memory B-cells (**Figures 17b & 18-20**). Dual-specific B-cells responded more rapidly than their mono-specific counterpart, based on the detection of IgG as early as day 2 in culture, consistent with an "effector memory" function. In addition, non-specific CXCR5<sup>-</sup> memory B-cells differentiated more rapidly than non-specific CXCR5<sup>+</sup> memory B-cells under plasmablast differentiating conditions, as judged by upregulation of CD27 and downregulation of CD20 (**Figure 21**).

Weak signals for cross-reactivity were detected for mono-specific B-cells, but for IgG only (**Figures 18-20, top left panel**). This likely arose from contamination with dual-specific B-cells. Non-specific CXCR5<sup>+</sup> and CXCR5<sup>-</sup> memory B-cell subsets also gave signals for anti-RV IgG and IgA (CXCR5<sup>+</sup>) or anti-RV IgG only (CXCR5<sup>-</sup>), indicating the presence of residual RV-specific B-cells within these more abundant subsets (**Figure 17b**). As expected, these B-cell types also secreted tetanus-specific antibodies. Taken together, these findings established the ability for dual-specific memory B-cells to rapidly secrete cross-reactive IgG, and distinguished their specificity and antibody profile from mono-specific B-cells.

**Figure 5: Purified Whole Virus is Stable and Structurally Uniform**

**a.** Purified RV by electron microscopy at low (12,000x) magnification. **b.** Purified RV by electron microscopy at high (60,000x) magnification. Scale bars denote 500nm and 100nm, respectively.

**a**



**b**

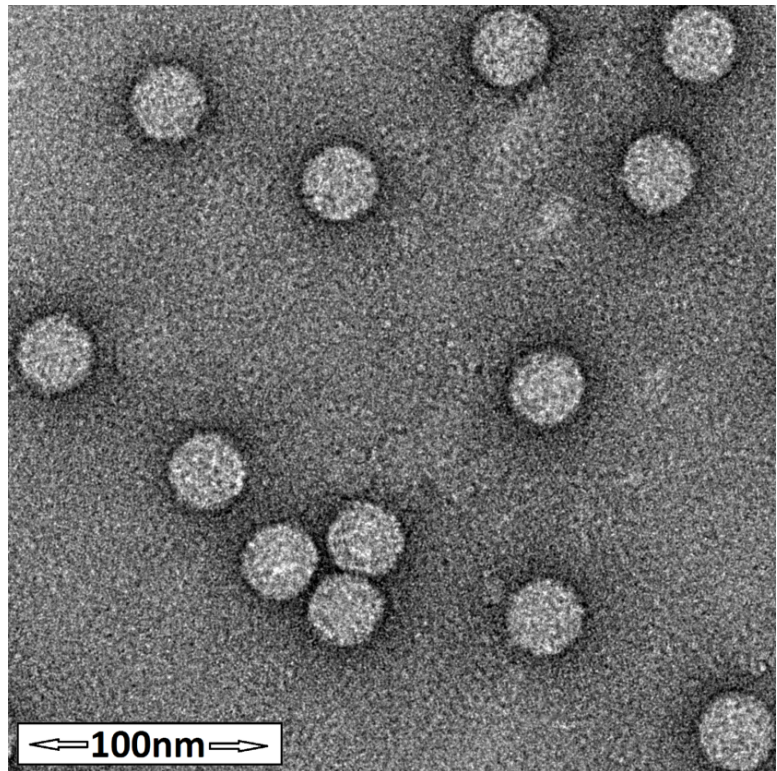


**Figure 6: Experimental RV Strains are Genomically and Structurally Distinct**

PCR analysis of strains RV-A16 and RV-A39 using strain-specific primers for a non-conserved exon region of the VP1 capsid subunit protein. Primer sequences are provided in Table 1.

**RT-PCR**

RV sample: A16 A39 A16 A39  
Primers: A16 A16 A39 A39

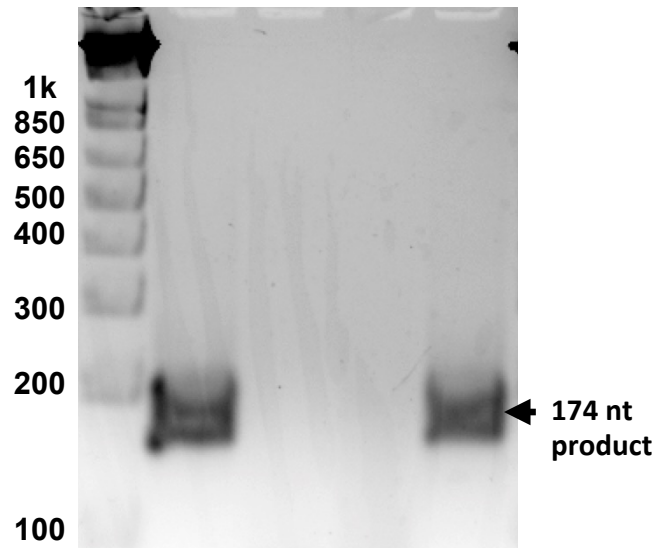


**Figure 7: Whole Virus is Isolated to High Purity**

SDS-PAGE analysis (at left) with silver staining of RV-A16 and corresponding western blot for VP2. RV was purified from cell lysates prepared in buffer with 0.01% BSA for virus stability, and subsequently isolated in pure PBS. RV preparations were analyzed before (RV-unconc.) or after (RV-conc.) concentration to confirm purity. The identity of RV-A16 was confirmed by western blot (at right) using anti-VP2 mAb. Higher molecular weight immature polyproteins containing uncleaved VP2 are denoted. Similar results were obtained for RV-A39.

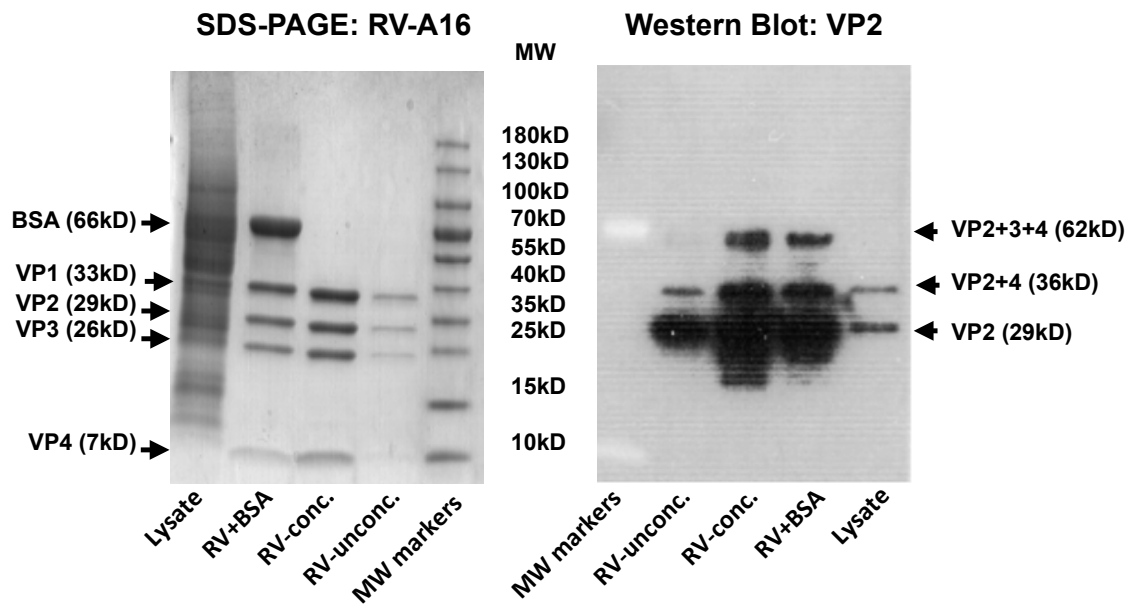


**Figure 8: Model of Experimental RV Infection in Humans**

Arrows denote time points for blood draws. Blood was available on day 7 only for subjects challenged with RV-A16.

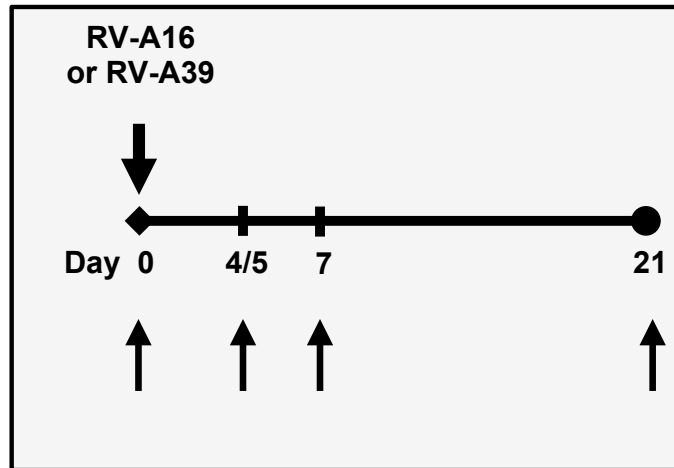


**Figure 9: Whole Virus Detects Multiple RV-specific Isotypes**

Longitudinal analysis of serum antibodies specific for homotypic or heterotypic whole virus (depending on infecting strain) at days 0, 4/5, 7 and 21 after RV inoculation (13 subjects infected with RV-A16 and 12 subjects infected with RV-A39; n=25 for all time points, except for day 7 (n=13)). Geometric mean  $\pm$  geometric SD. \*\*p<0.01 and \*\*\*\*p<0.0001 versus day 0.

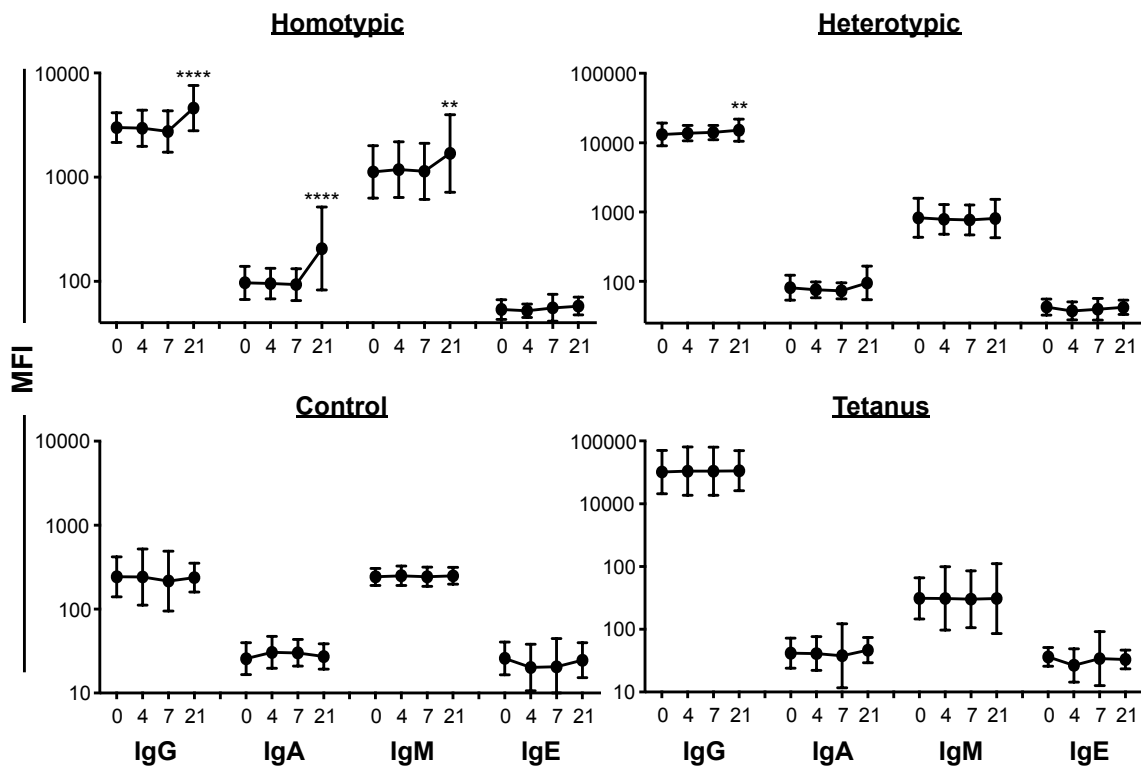


**Figure 10: Serum Antibodies Remain Unchanged in Uninfected Subjects**

Homotypic antibodies were measured by cytometric bead assay in serum from 5 uninfected subjects following RV challenge. Geometric mean  $\pm$  geometric SD.

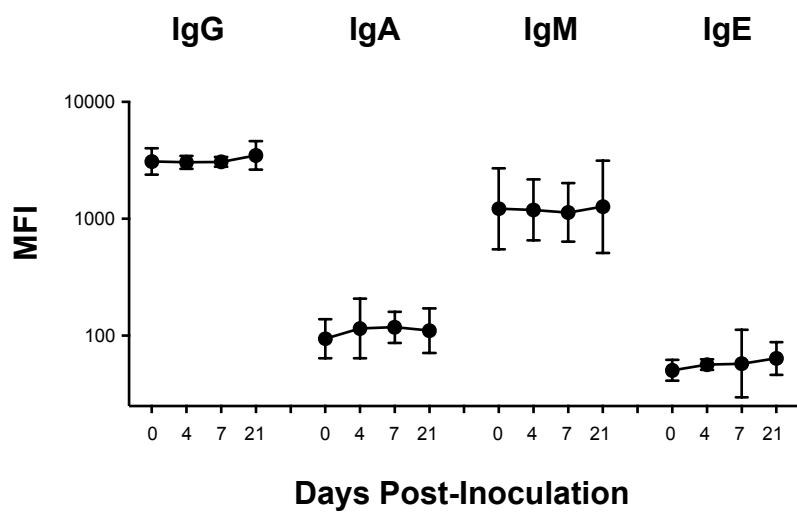


**Figure 11: VP1 Capsid Subunit Does Not Detect RV-specific Antibodies**

Longitudinal analysis of serum antibodies specific for RV-A16 VP1 in 13 subjects infected with RV-A16. Significance was determined by Wilcoxon matched pairs signed-rank test. Geometric mean  $\pm$  geometric SD.

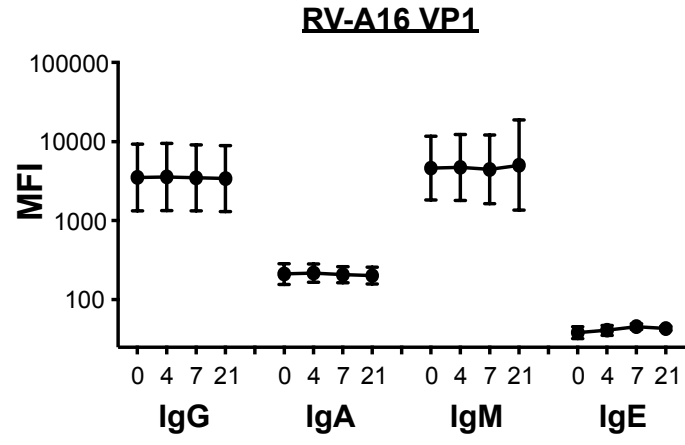


**Figure 12: RV-specific B-cells are Enriched in the CXCR5-neg Memory**

**a.** Gating strategy for virus-specific B-cells showing their enrichment within the IgD-negative subset in uninfected subjects. **b.** Comparison of the percentages of CXCR5+ and CXCR5- cells within virus-specific and total memory B-cells. Data is representative of 6 subjects.

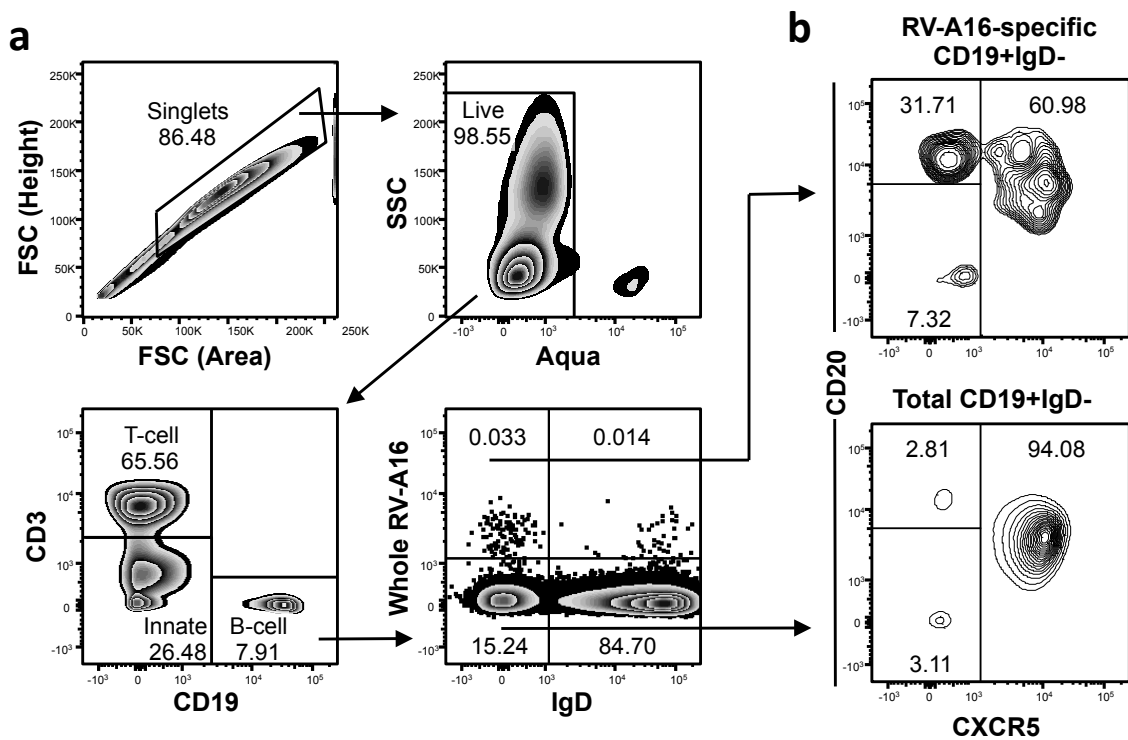


**Figure 13: Dual-specific B-cells are Expanded in Blood and Lack CXCR5**

**a.** Total B-cells from uninfected subjects stained for RV-A16 and RV-A39 and colored for CXCR5 expression. Data is representative of 6 subjects. **b.** Percentages of CXCR5+ and CXCR5- mono-specific and dual-specific B-cells within total memory B-cells (CD19+CD20+IgD-) (n=6). Significance was determined by Wilcoxon matched pairs signed-rank test. Geometric mean  $\pm$  geometric SD. \*p<0.05.

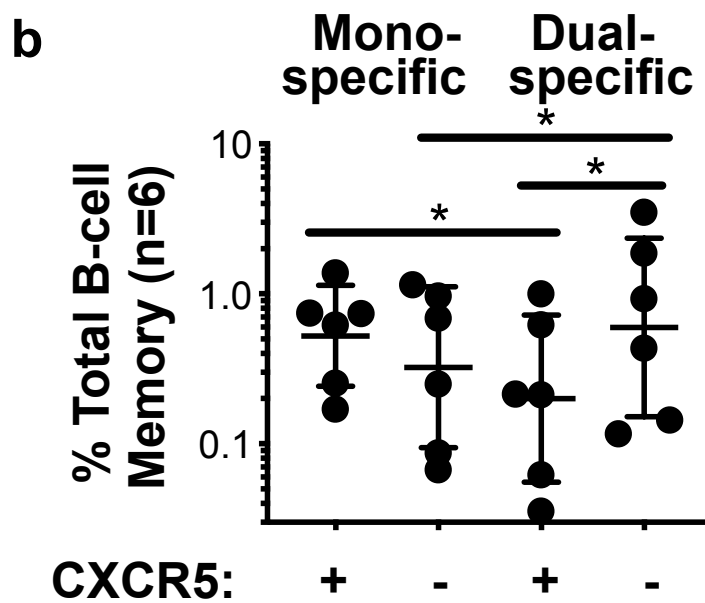
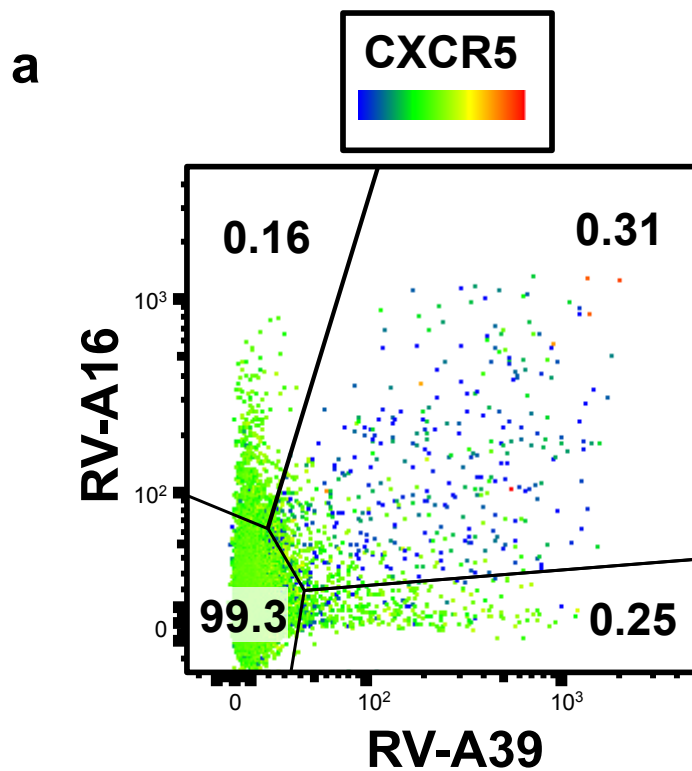


**Figure 14: Dual-specific B-cells are Highly Enriched in CXCR5- Memory**

The percentage of naive (IgD+), CXCR5+ memory and CXCR5- memory B-cells within RV-specific B-cells (n=6). Significance was determined by Wilcoxon matched pairs signed-rank test. Mean  $\pm$  SD. \*p<0.05.

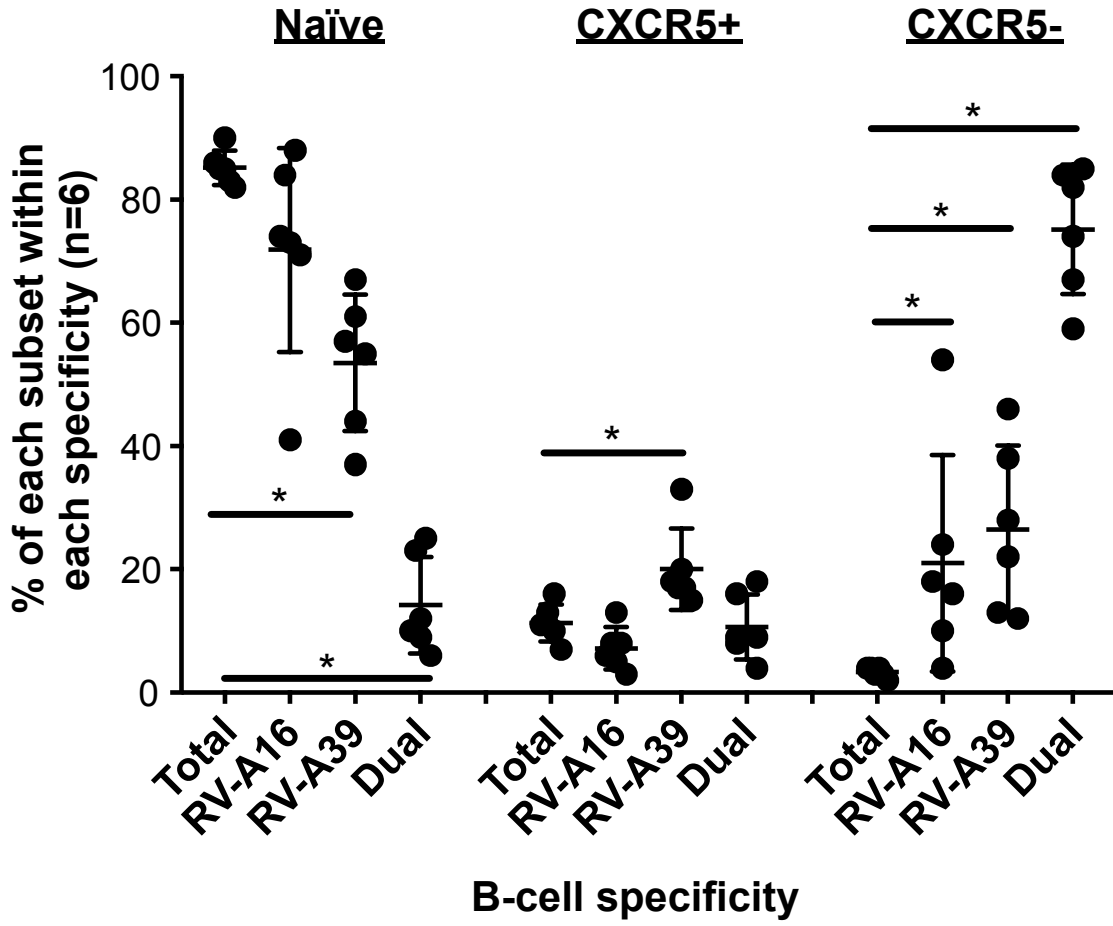


**Figure 15: Dual-specific B-cells are Predominantly CXCR5- Memory**

The percentage of mono-specific and dual-specific B-cells within naive, CXCR5+ memory and CXCR5- memory B-cell subsets (n=6). Significance was determined by Wilcoxon matched pairs signed-rank test. Geometric mean  $\pm$  geometric SD. \*p<0.05.

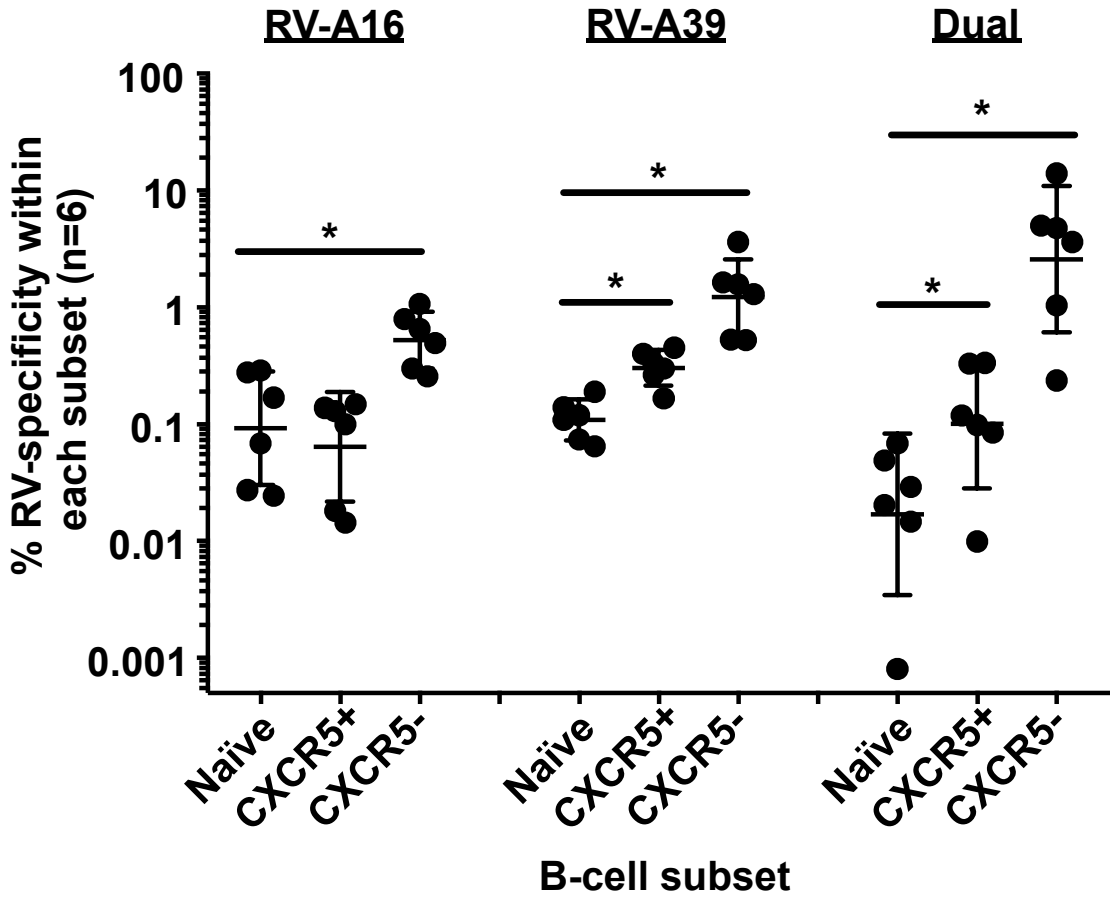


**Figure 16: B-cell Binding of RV is Independent of ICAM-1**

Total B-cells stained for RV-A16 and ICAM-1 without ICAM-1 blocking.

Data is representative of 6 subjects.

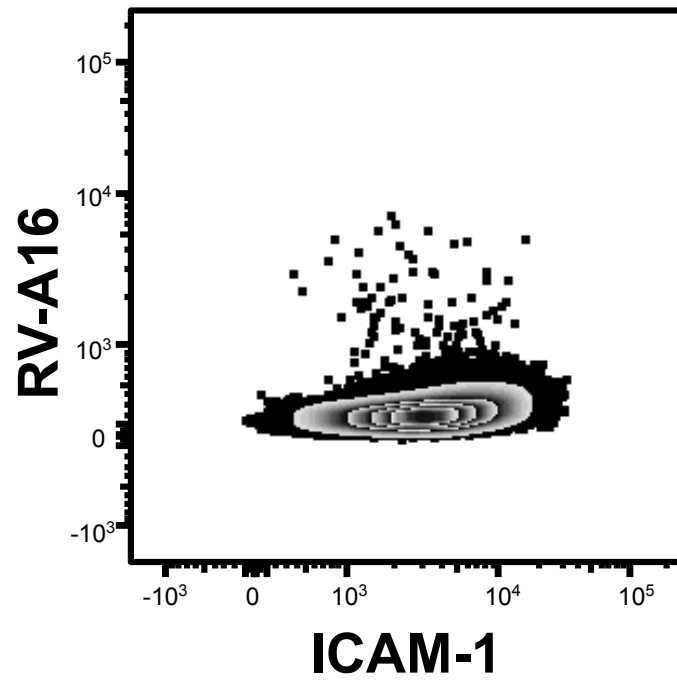


**Figure 17: CXCR5- B-cell Memory is Distinct from CXCR5+ Memory**

Comparison of surface markers (h) and antibody profiles (i) of CXCR5+ and CXCR5- subsets (n=8). Significance was determined by Wilcoxon matched pairs signed-rank test. Geometric mean  $\pm$  geometric SD (a). Mean  $\pm$  SD (b). \*p<0.05, \*\*p<0.01, \*\*\*p<0.001, \*\*\*\*p<0.0001.

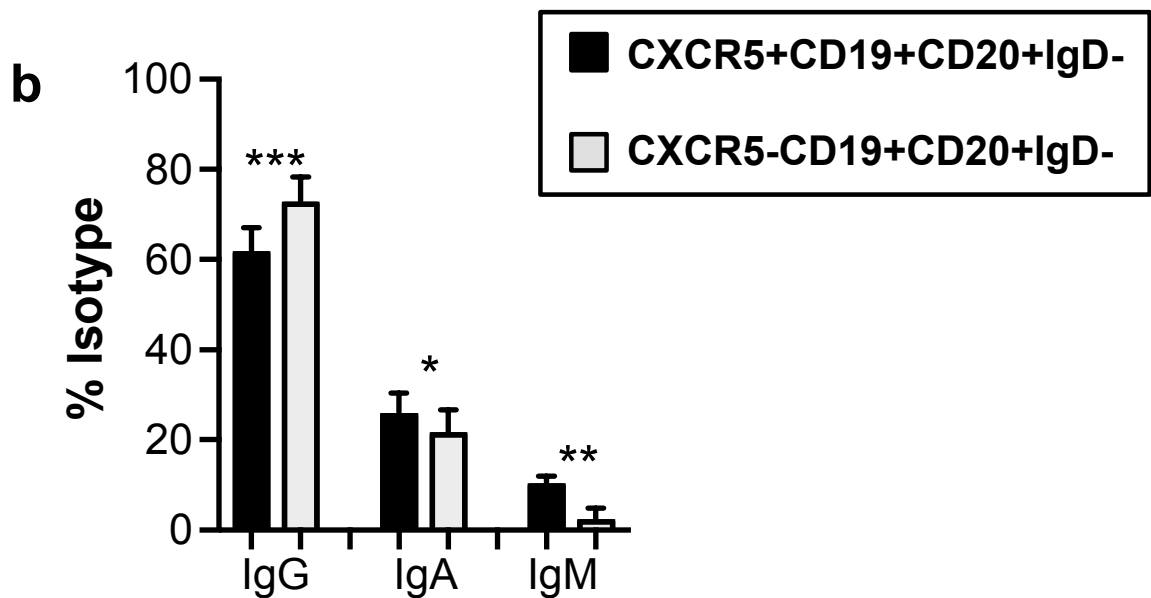
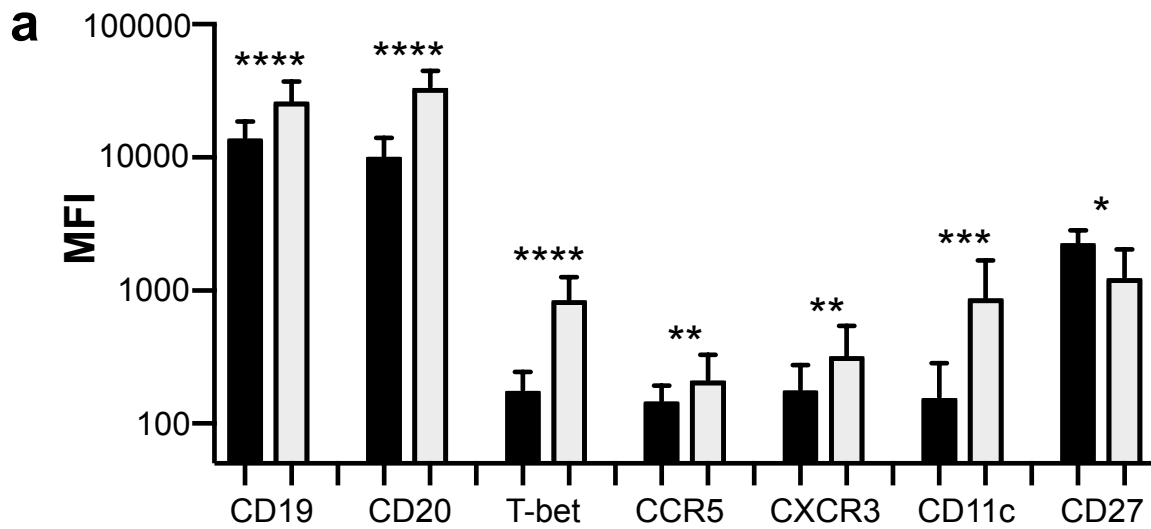


**Figure 18: Dual-specific B-cells Rapidly Secrete Cross-Reactive IgG**

Purified B-cell types were cultured for 10 days under plasma cell differentiating conditions and secretion of IgG was assessed every 2 days. Data is shown for the change over baseline in specific antibodies for RV-A16, RV-A39, tetanus toxin, and mouse IgG (control) (n=6 subjects). Significance was determined by Friedman multiple comparisons test. Geometric mean  $\pm$  geometric SD. \*p<0.05, \*\*p<0.01, \*\*\*p<0.001, \*\*\*\*p<0.0001 versus day 0.



**Figure 19: Dual-specific B-cells Do Not Rapidly Secrete Cross-Reactive IgA**

Purified B-cell types were cultured for 10 days under plasma cell differentiating conditions and secretion of IgA was assessed every 2 days. Data is shown for the change over baseline in specific antibodies for RV-A16, RV-A39, tetanus toxin, and mouse IgG (control) (n=6 subjects). Significance was determined by Friedman multiple comparisons test. Geometric mean  $\pm$  geometric SD. \* $p < 0.05$ , \*\* $p < 0.01$ , \*\*\* $p < 0.001$ , \*\*\*\* $p < 0.0001$  versus day 0.

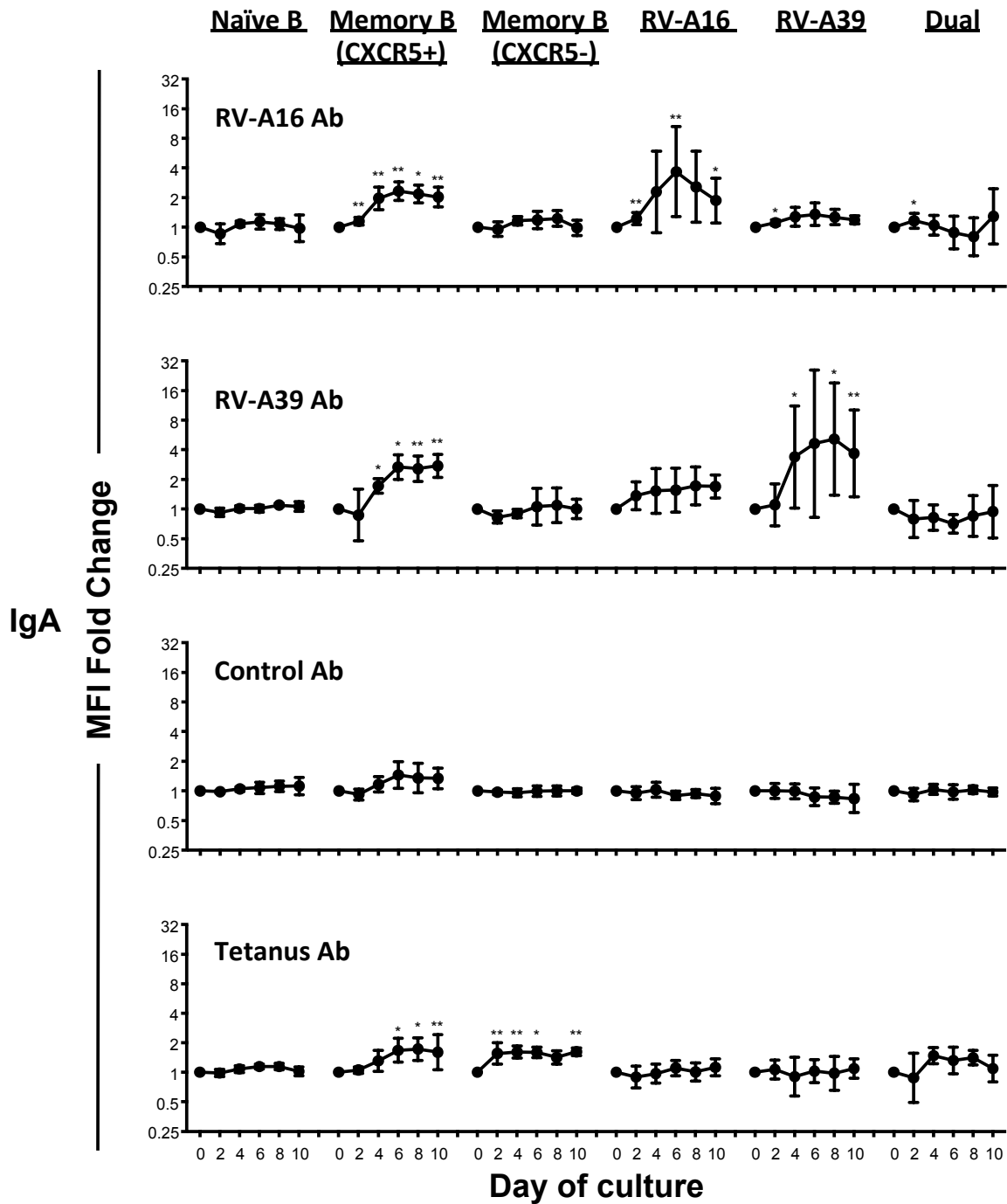


**Figure 20: Dual-specific B-cells Do Not Rapidly Secrete Cross-Reactive IgM**

Purified B-cell types were cultured for 10 days under plasma cell differentiating conditions and secretion of IgM was assessed every 2 days. Data is shown for the change over baseline in specific antibodies for RV-A16, RV-A39, tetanus toxin, and mouse IgG (control) (n=6 subjects). Significance was determined by Friedman multiple comparisons test. Geometric mean  $\pm$  geometric SD. \*p<0.05, \*\*p<0.01, \*\*\*p<0.001, \*\*\*\*p<0.0001 versus day 0.

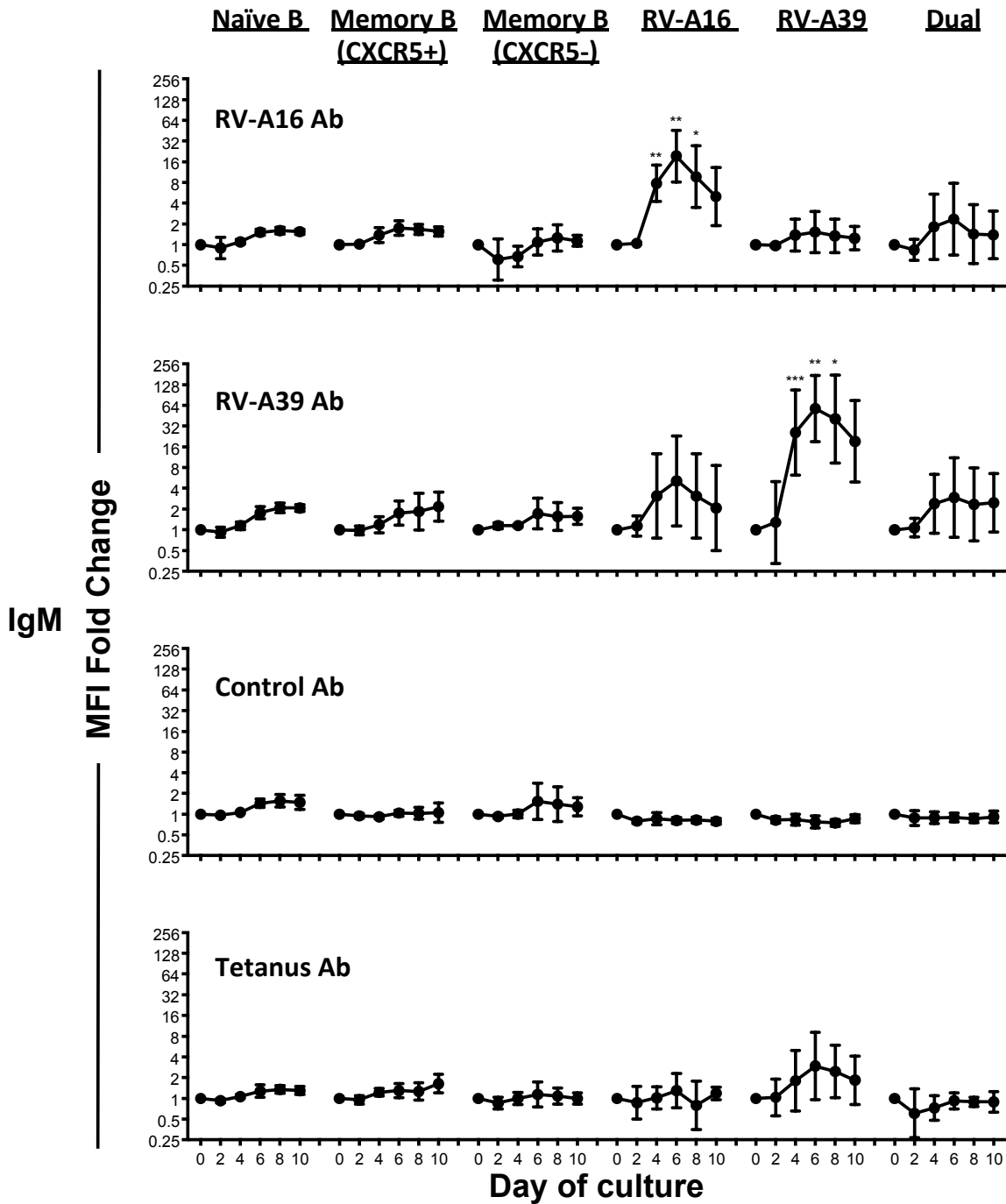
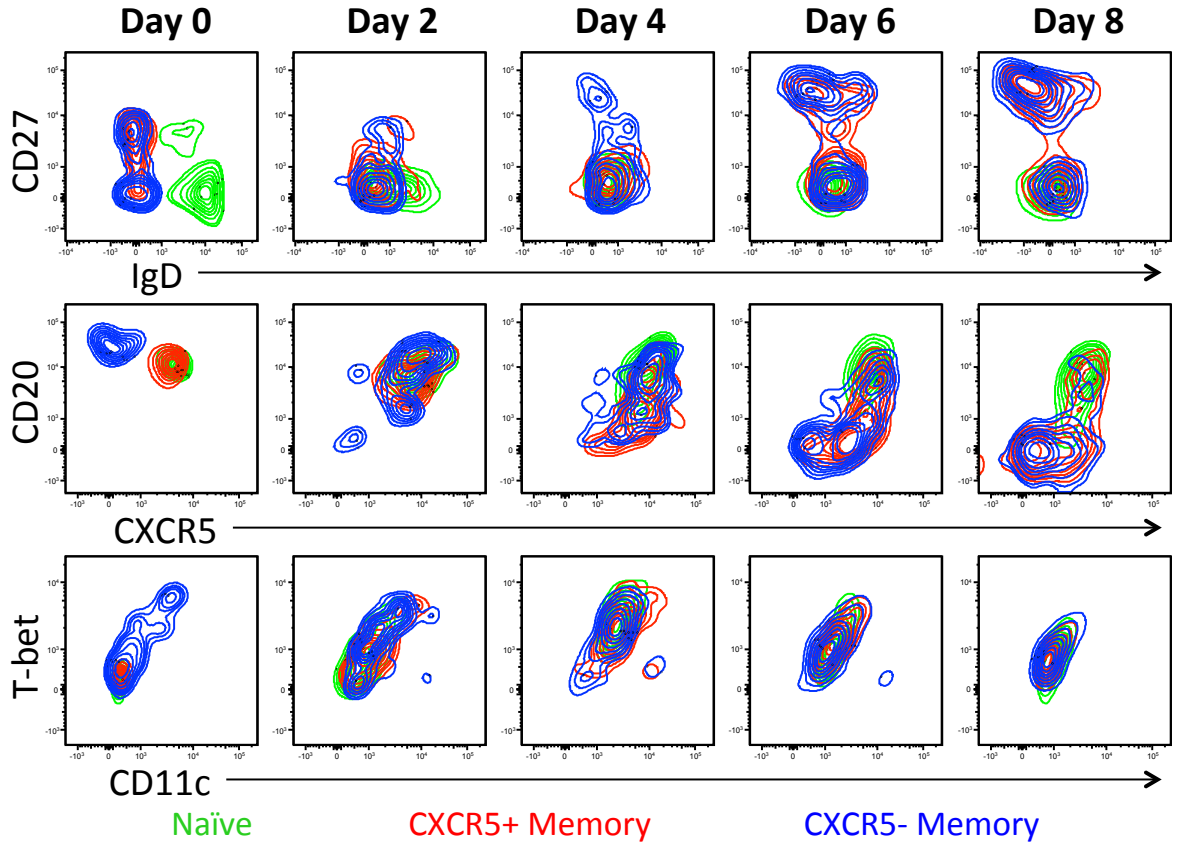


**Figure 21: CXCR5- Memory B-cells Transition Rapidly Under Plasma Cell Differentiating Conditions**

B-cell subsets were sorted to high purity and cell phenotypes monitored by multi-color flow cytometry every 2 days under plasma cell differentiating conditions. Representative data of 6 experiments is shown for naïve (green), CXCR5+ memory (red), and CXCR5- memory (blue) B-cells. Contour plots for each subset are superimposed for comparison.



### *Dual-specific B-cells Display "Effector Memory" by High Dimensional Analysis*

Our next step was to rigorously interrogate the molecular signature of dual-specific B-cells, and test their ability to respond to *in vivo* infection. To accomplish this, mass cytometry was applied to our experimental infection model. To ensure the sensitive and reliable detection of alterations in B-cell types during infection, including rare RV-specific cells, PBMC samples that were enriched for B-cells, were barcoded by a novel method that combined anti-CD45 and anti-MHCI antibodies labeled with 8 different metal isotopes. Samples were then pooled for mass cytometry analysis. This allowed all samples to be prepared under identical conditions and run in a single experiment, thereby minimizing batch effects that might obscure changes in rare B-cell subtypes. Seventy samples were analyzed from 24 subjects challenged with either RV-A16 (n=13) or RV-A39 (n=11), corresponding to 3 time points (day 0, pre-inoculation; day 4/5, acute infection; and day 21, convalescence).

By first analyzing pooled data for all subjects at all time points using stochastic neighbor embedding (SNE) (236), B-cells were classified into 5 main populations: (1) a major group of CXCR5+ memory B-cells; (2) plasmablasts with low CD20 expression; (3) CXCR5- memory B-cells with high CD20 expression; (4) a small group expressing CD20 and CD38, suggestive of extrafollicular plasmablasts (PB-X); and (5) contaminating non-B-cells with low CD20 expression (**Figure 22**). A deeper clustering analysis yielded 50 phenotypes based on differential expression of 35 markers (238,239) (**Figure 23**). A heatmap

display listed markers in order of priority based on their efficiency to discriminate phenotypes (**Figure 24**). Markers were selected that distinguished plasmablasts (CD20 (low), CD22 (low), CD38 (high), CD43 (high), and CD86 (high)) from conventional B-cells. Other markers were those expressed on cells that are activated or found at inflamed sites (CD27, CD95, and MHCII), and those involved in cell trafficking (integrins  $\beta$ 1 (airway) and  $\beta$ 7 (gut); CXCR5 and CCR7 (lymphoid organs); CCR5 and CXCR3 (inflamed airways); and CXCR4 (bone marrow)).

Four memory B-cell clusters were identified that lacked expression of CXCR5, which were IgG+ or IgA+, T-bet<sup>high</sup>, CD11c<sup>high</sup>, CD19<sup>high</sup>, and CD20<sup>high</sup> (#19, 20, 25 & 26) (**Figure 24**). Dual-specific B-cells constituted a single one of these clusters that was IgG+ (#19), and expressed integrin  $\beta$ 1, CCR5 and CXCR3, and markers of activation/inflammation (CD95<sup>high</sup>, CD40<sup>low</sup>, MHCII<sup>high</sup>). These cells also expressed low levels of the activating receptor CD21 and high levels of the inhibitory receptor, CD22, similar to other reports of T-bet+ memory B-cells (160,243,168). Virus labeling was not restricted to cluster #19; however, the algorithm assigned all other clusters a log-scaled value at least ~80% lower, indicating much lower numbers of RV-specific B-cells within other phenotypes. Thus, to allow assessment of CXCR5+ mono-specific B-cells, the algorithm was modified for manually-gated RV-specific cells only, clustered on the basis of CXCR5 and their labeling with the two virus strains. This analysis confirmed dual-specificity for CXCR5- T-bet+CD11c+ memory B-cells, and their enrichment

for IgG. By contrast, CXCR5<sup>+</sup> mono-specific B-cells were T-bet<sup>lo</sup>CD11c<sup>lo</sup> and CCR7<sup>+</sup>, consistent with LN homing, and CD21 was a prominent feature (**Figures 25 & 26**). These findings confirmed the distinctive "effector memory" signature of dual-specific B-cells.

#### *Dual-specific B-cells Expand After RV Infection*

Next, we assessed which B-cell phenotypes were modulated during RV infection. During acute infection (day 4/5 post-inoculation) CXCR5<sup>+</sup> circulating memory B-cell subsets decreased, consistent with their egress from peripheral blood into LNs. By contrast, plasmablasts and CXCR5<sup>-</sup> B-cell subsets were increased (**Figure 27**). The largest increase was observed for an extrafollicular plasmablast subset (cluster #38, +50% change over baseline,  $p < 0.0001$ ), consistent with an early extrafollicular response, given its upregulation of CD38 and residual CD20 (hence its designation PB-X) (**Figure 27-29**) (100). This subset resembled an IgM<sup>+</sup> plasmablast, except for its expression of CD20, and displayed low expression of Ki-67, CD27, and CD71, suggesting it had recently differentiated and mobilized, but had not undergone mitosis. This subset also expressed  $\beta 1$  integrin and CCR5, consistent with trafficking to the inflamed airways (151,152). The next most significant cluster was an IgA<sup>+</sup> CXCR5<sup>+</sup> memory B-cell subset (cluster #41) which decreased by 20% ( $p < 0.001$ ) (**Figure 27-29**), and whose change was inversely correlated with the increase in cluster #38, indicating a coordinated B-cell response (**Figure 30**). IgA<sup>+</sup> B-cells cannot give rise to IgM<sup>+</sup> PBs, but these acute fluxes reflect circulating CXCR5<sup>+</sup>

memory homing to LNs, while naïve B-cells receive stimulus, differentiate, and traffic to blood. Cluster #21 was a similar IgG<sup>+</sup> CXCR5<sup>+</sup> memory B-cell type that also contracted during acute infection (-17%,  $p < 0.01$ ). By contrast, three CXCR5<sup>-</sup> memory B-cell clusters expanded. These included two IgG<sup>+</sup> clusters (#20: +15%,  $p < 0.01$ ; and #26: +9%,  $p < 0.01$ ) that differed according to their expression of CD27, CD43, CD95, and CXCR3; and an IgA<sup>+</sup> cluster (#25, +12%,  $p < 0.01$ ). An IgA<sup>+</sup> plasmablast cluster was also expanded at this time point (#1, +16%,  $p < 0.01$ ) (**Figure 27-29**).

All clusters that were modulated at day 4 returned to baseline levels by day 21. RV-specific B-cells that were "dual-specific" (#19) were the only cluster that significantly increased at day 21 compared with day 0 (cluster #19, +23%,  $p < 0.001$ ) (**Figure 27-29**). Further analysis of cluster #19 revealed decreased expression of markers of tissue homing (CXCR3) and inflammation (CD27) during acute infection and their rebound at convalescence, consistent with egress of tissue homing B-cells from the periphery, and their subsequent return (**Figure 31**). To further examine fluxes in virus-specific B-cells that may not be appreciated by the algorithm, mono-specific and dual-specific B-cells were analyzed within CXCR5<sup>+</sup> and CXCR5<sup>-</sup> memory subsets by manual gating of mass cytometry data (**Figure 32**). As expected, the results confirmed an increase in dual-specific B-cells after RV infection, but also revealed significant increases in mono-specific B-cells, when analyzed in relation to challenge with homotypic, but not heterotypic virus. Together, the findings demonstrated highly coordinated

responses of diverse B-cell types during RV infection, and confirmed the response of dual-specific B-cells to heterotypic virus.

**Figure 22: B-cells Analyzed by Mass Cytometry in Experimental Infection**

t-SNE distribution for total memory B-cells and plasmablasts (CD19+ IgD- cells) colorized by CD20 expression (plasmablasts (low), CXCR5+ memory (mid), CXCR5- memory (high)) and CXCR5 expression (plasmablasts (low), CXCR5+ memory (high), CXCR5- memory (low)). Data was pooled from 70 samples analyzed from 24 subjects.

CD19+IgD-

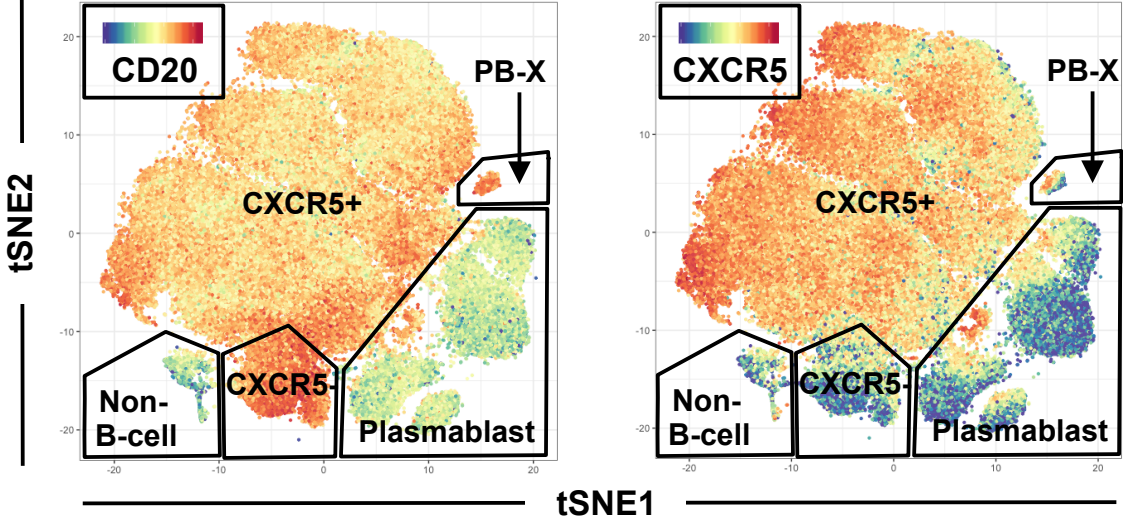


**Figure 23: Visual Representation by t-SNE of B-cell Phenotypes Identified by FlowSOM**

Total memory B-cells and plasmablasts clustered into 50 phenotypes by FlowSOM algorithm, and overlaid on t-SNE map. Data was pooled from 70 samples analyzed from 24 subjects.

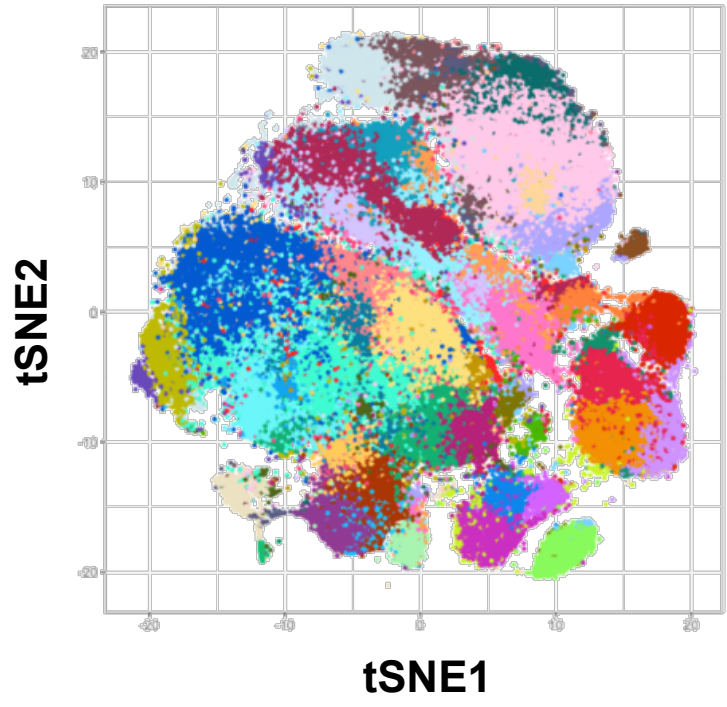


**Figure 24: Dual-specific B-cells Display "Effector Memory" Phenotype by High Dimensional Analysis**

Heatmap of phenotypes according to expression of all markers assessed by FlowSOM algorithm. Colors in the left column correspond to cluster phenotypes in Figure 23. Arrowheads denote CXCR5- memory B-cell clusters that include a subset dual-specific for RV-A strains (cluster #19).

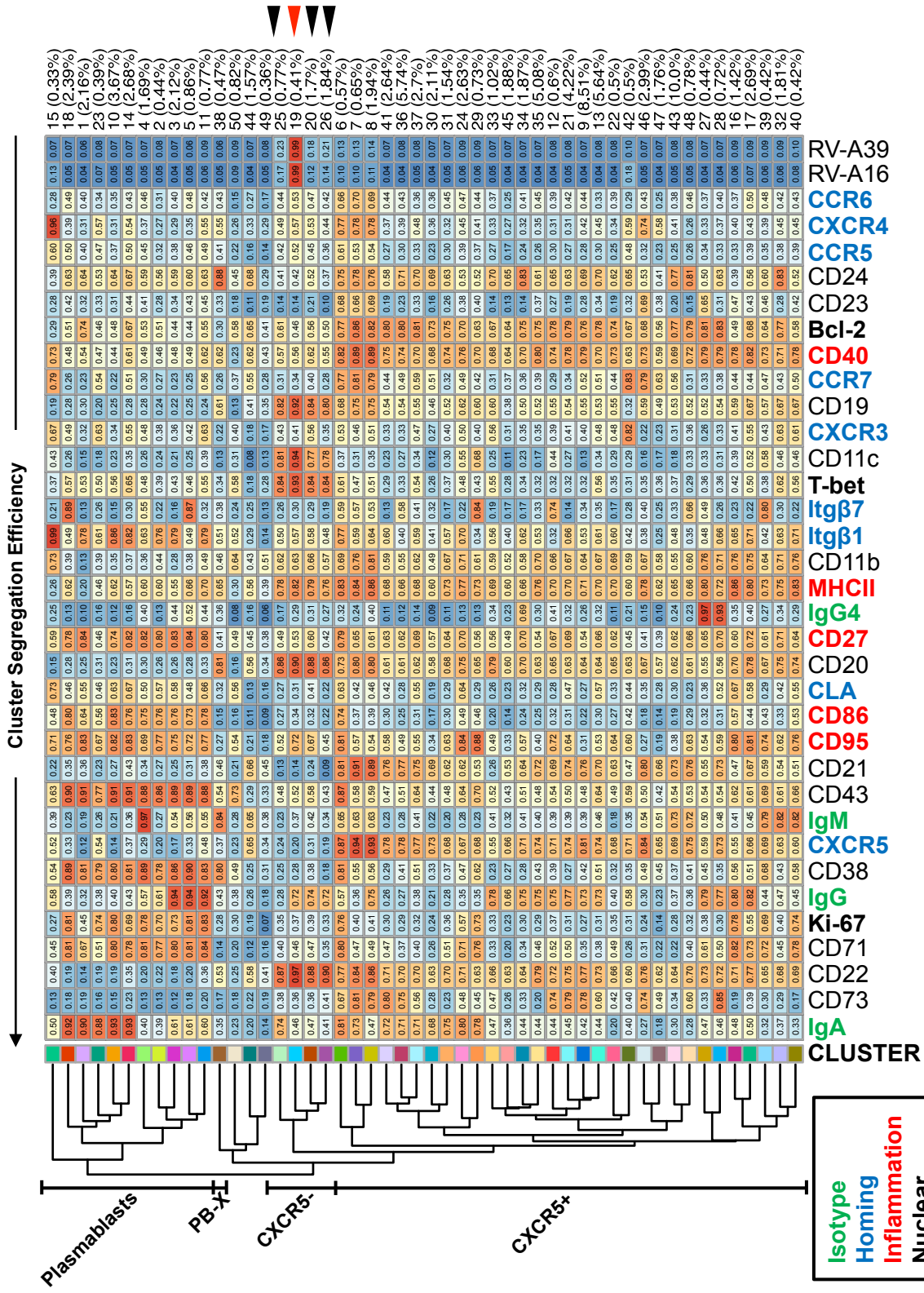


**Figure 25: RV-specific CXCR5+ Memory B-cells Primarily Target a Single Strain**

Comparison of dual-specific and mono-specific phenotypes within total RV-specific memory B-cells, showing only those markers used in multi-color flow cytometry (Figure 17). Cells were clustered solely according to CXCR5 expression and binding of the two RV strains, to demonstrate that CXCR5+ B-cells can efficiently be segregated into two mono-specific populations.

Dual-specific	0.25	0.57	0.62	0.84	0.85	0.16	0.41	0.44	0.57	0.46	0.33	0.76	0.35	1 (56.3%)
Mono-specific	0.87	0.00	0.56	0.40	0.38	0.85	0.62	0.72	0.46	0.57	0.53	0.58	0.34	2 (24.3%)
	0.90	0.77	0.00	0.31	0.31	0.87	0.64	0.77	0.47	0.65	0.53	0.53	0.37	3 (19.4%)
	CXCR5	RV16	RV39	T-bet	CD11c	CD21	CD27	CCR7	CCR5	CXCR3	IgM	IgG	IgA	

Isotype
Homing
Inflammation
Nuclear

**Figure 26: Dual-specific B-cells are T-bet+**

Pooled total B-cells stained for RV-A16 and RV-A39, and colored for T-bet expression.

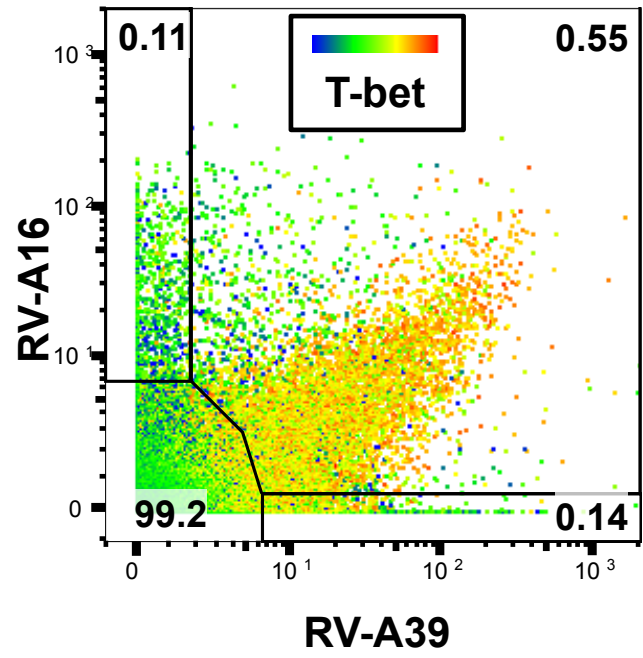


**Figure 27: Discrete Circulating B-cell Clusters Fluctuate in Response to Infection**

Volcano plots showing the percentage change in B-cell clusters that were significant during acute infection (day 4/5, n=24) and convalescence (day 21, n=22) ( $p < 0.05$ ). Numerical cluster titles are generated stochastically by the FlowSOM algorithm. Significance was determined by Wilcoxon matched pairs signed-rank test.

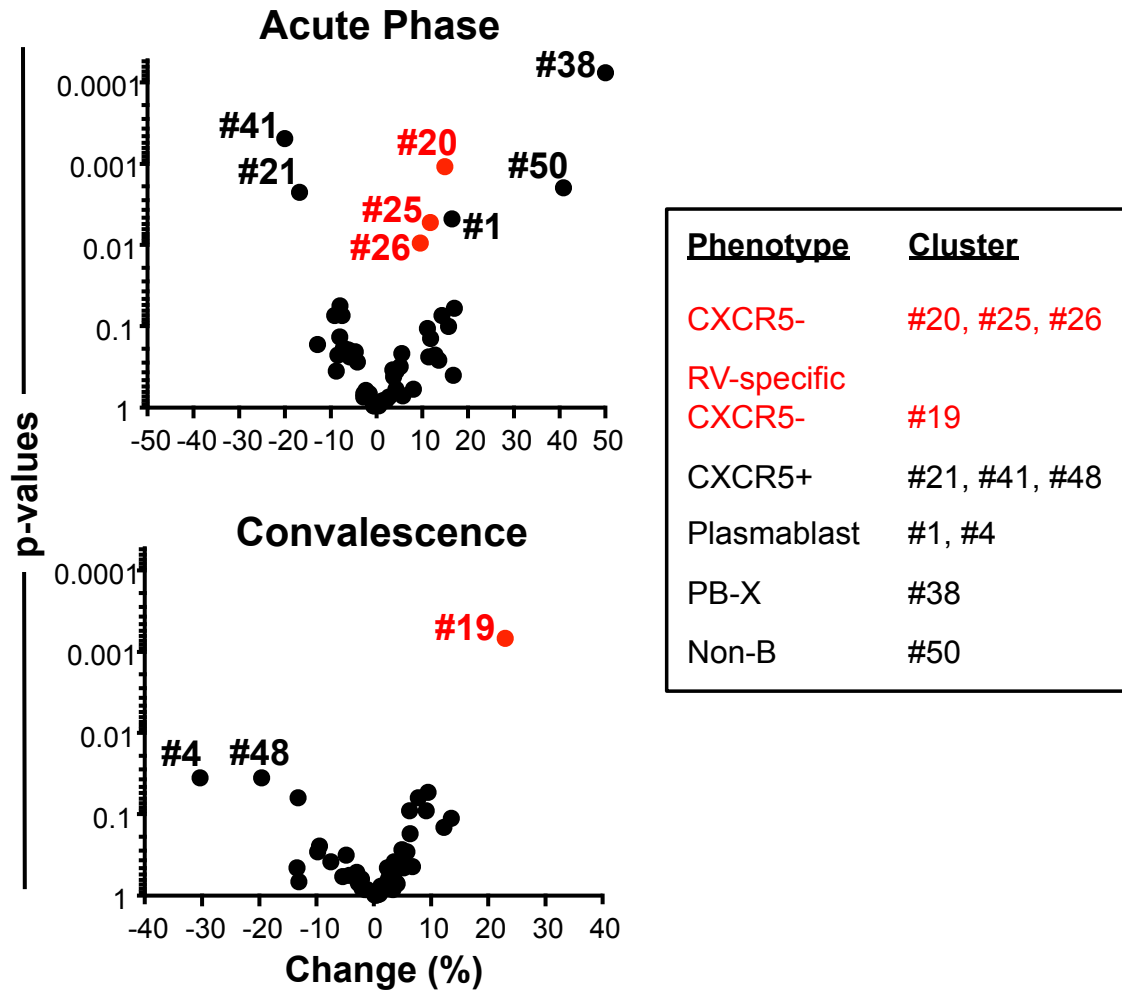


**Figure 28: Change in Frequency of Selected Clusters During Infection**

Cluster frequencies among total IgD<sup>-</sup> cells are provided across all time points for each subject. Geometric mean  $\pm$  geometric SD indicated in red. Significance was determined by Wilcoxon matched pairs signed-rank test. \*\*\* $p < 0.001$ , \*\*\*\* $p < 0.0001$ .

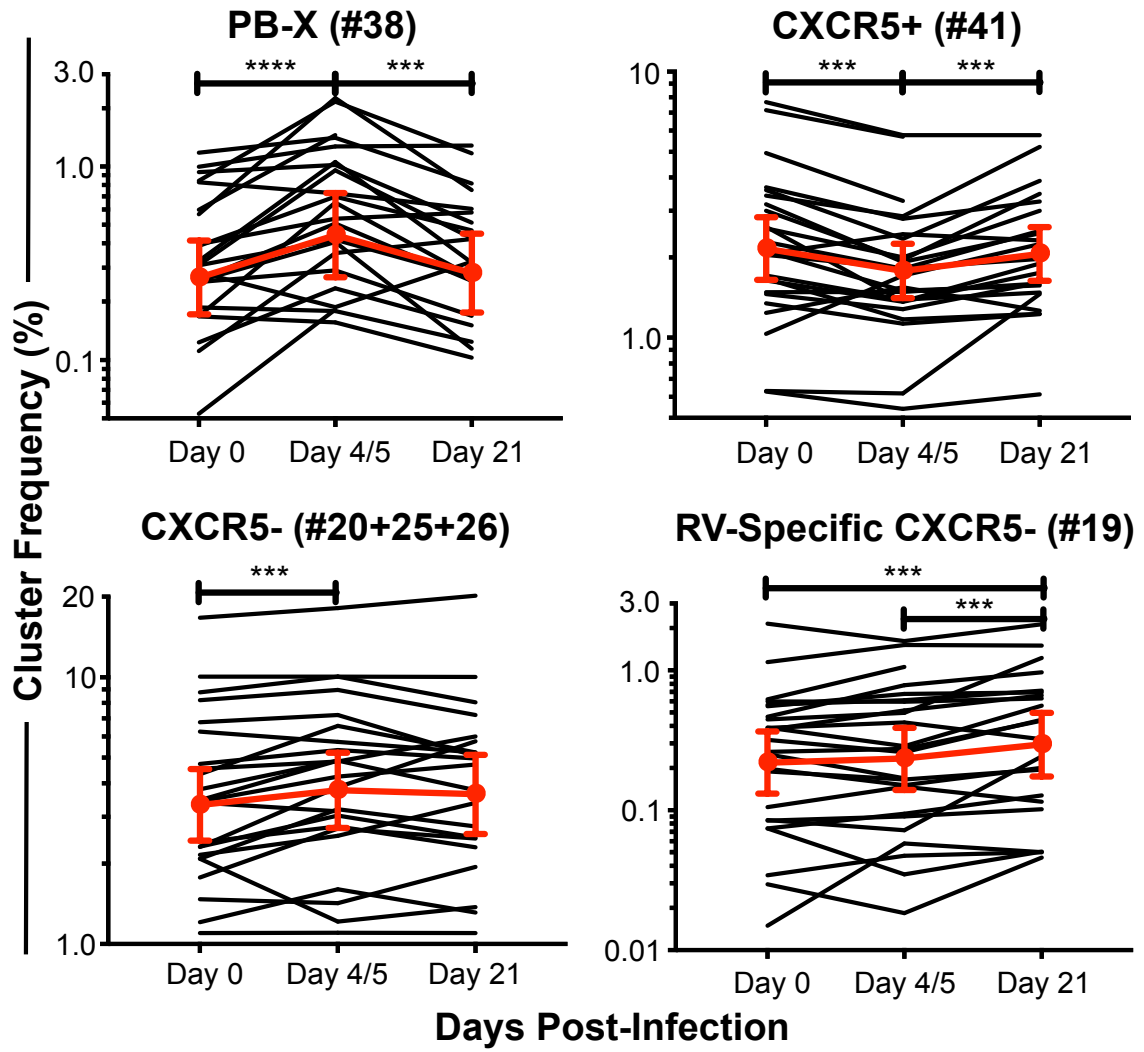


**Figure 29: Overlay of B-cell Clusters Related to RV Infection on t-SNE Maps**

Only B-cell clusters that changed significantly ( $p < 0.01$ ) during infection are shown for each time point.

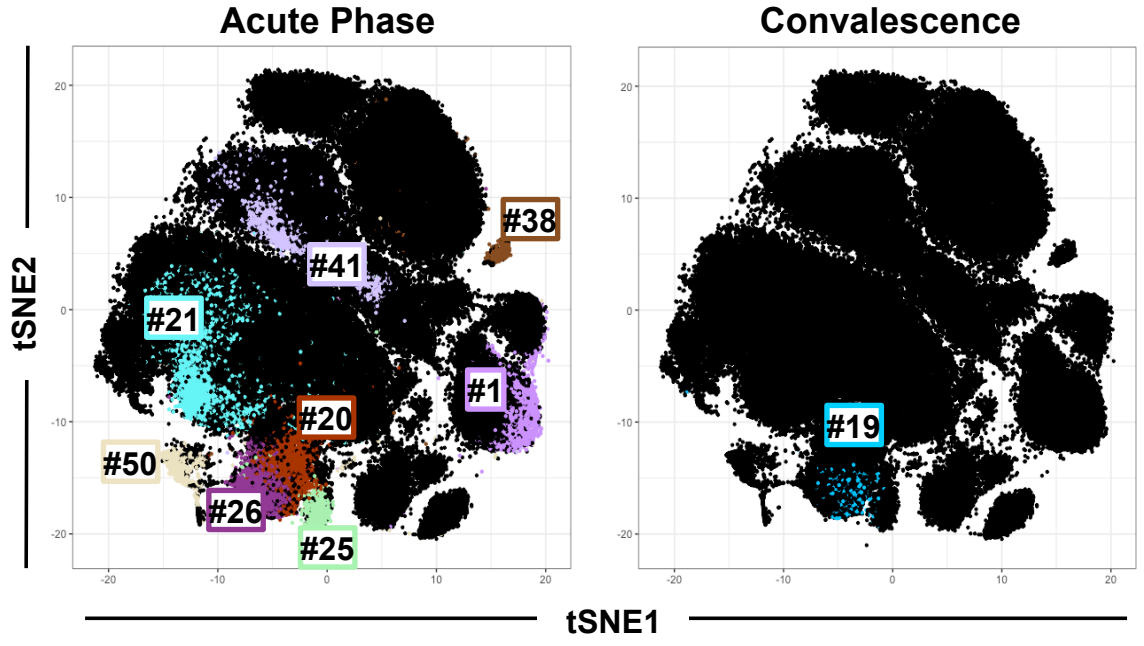


**Figure 30: Expansion of Circulating Extrafollicular Plasmablasts Coincides with a Decrease in a CXCR5+ Memory B-cell Cluster**

Correlation between the percentage in PB-X (cluster #38, expanded) and IgA+ CXCR5+ memory B-cells (cluster #41, contracted) during the acute phase (n=24). Significance was determined by Spearman correlation.

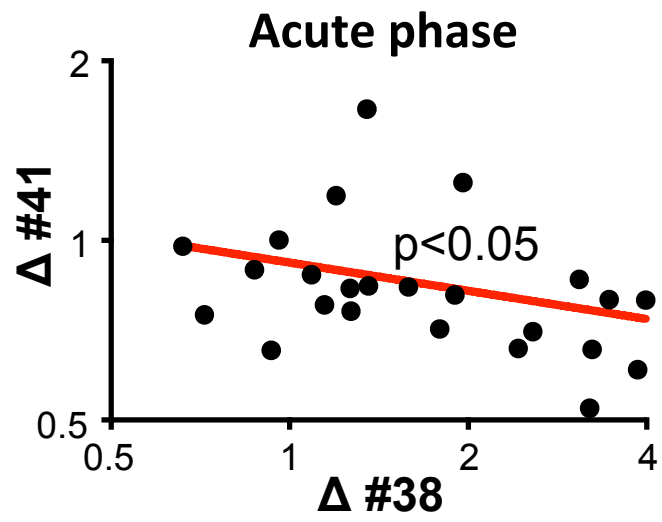


**Figure 31: Change in the Signature of Dual-specific B-cells (Cluster #19)  
During RV Infection**

The MFI for each marker is shown at day 0, day 4/5, and day 21 (n=70 specimens). Arrows denote marker significance, as determined by Wilcoxon matched pairs signed-rank test. Geometric mean  $\pm$  geometric SD. \*p<0.05, \*\*p<0.01.

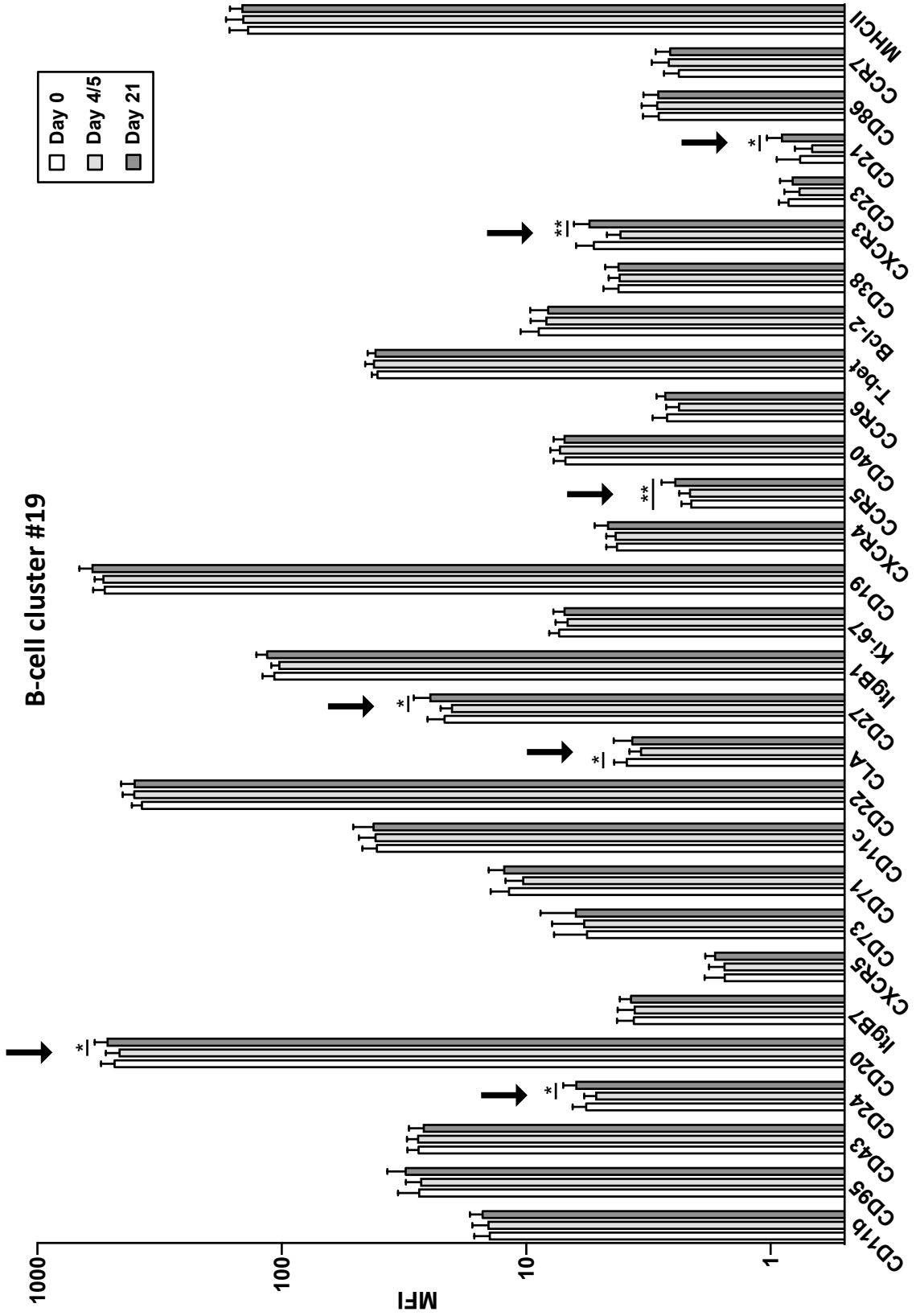
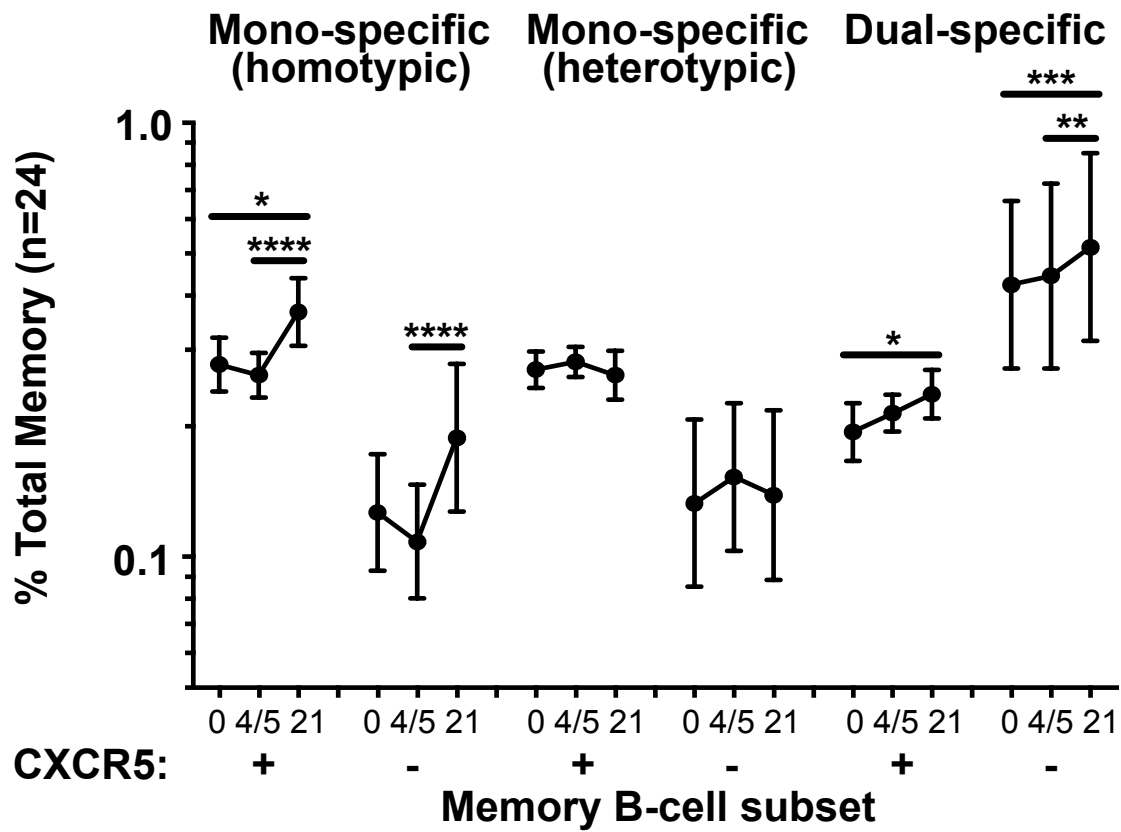


**Figure 32: Change in Percentages of CXCR5+ and CXCR5- Mono-specific and Dual-specific Memory B-cells during RV Infection**

Determined by manual gating (n=24). Mono-specific B-cells were analyzed in relation to challenge with homotypic and heterotypic RV-A strains. Significance was determined by Wilcoxon matched pairs signed-rank test. Geometric mean  $\pm$  geometric SD. \*p<0.05, \*\*p<0.01, \*\*\*p<0.001.



*Early Antibody Responses to RV in the Nose are Cross-reactive, Limited to IgG, and Coincide with B-Cell Infiltrates*

To establish a role for B-cells at the site of infection, nasal biopsies were obtained during acute infection for immunohistochemistry analysis. The results revealed dense infiltrates of CD19<sup>+</sup> B-cells that co-localized with virus and CD3<sup>+</sup> T cells in the nasal mucosa of infected subjects (**Figures 33-37**). Infiltrating B-cells expressed CD20, indicating a phenotype consistent with CXCR5<sup>-</sup> memory B-cells, rather than plasma cells (**Figure 38**), although expression of CD11c and T-bet was not detected, suggesting acquisition of a transitional phenotype *in situ* (**Figure 21**). B-cells were absent in tissue from healthy controls.

Analysis of nasal wash specimens obtained from infected subjects revealed a rapid cross-reactive response that was restricted to IgG, peaked at days 4/5, and was followed by a 2nd peak at day 21 (**Figure 39**). These antibodies matched the features of dual-specific B-cells. By contrast, increases in strain-specific IgA and IgM were restricted to day 21, and matched the antibody profiles of mono-specific B-cells and those in the serum (**Figures 9 & 18-20**). Anti-viral responses in the nose were accompanied by weak IgG responses to tetanus, suggesting bystander activation of tetanus-specific memory B-cells. Surprisingly, in subjects who tested negative for RV infection, weak anti-viral IgG responses were also detected in the nose, suggesting that viral exposure can recruit low numbers of CXCR5<sup>-</sup> memory B-cells, without hallmarks of infection

(**Figure 40**). Taken together, these findings are consistent with the rapid recruitment of dual-specific B-cells to the nose. The differences in nasal and serum antibody profiles suggest the division of labor between dual-specific and mono-specific B-cells in the production of local and systemic antibodies respectively.

*Dual-specific B-cells are Clonally Distinct from Their Mono-specific Counterparts*

In order to gain further insight into the features of dual-specific B-cells and their relationship to mono-specific cells, RV-specific B-cell subsets were purified by cell sorting, and subjected to single-cell BCR mRNA sequencing. We theorized that dual-specific B-cells would display high rates of hypermutation given their ability to respond to different RV strains. As expected, hypermutation was evident for these cells; however, it was highest for IgA<sup>+</sup> CXCR5<sup>+</sup> cells (**Figure 41**). Since IgG1 and IgA1 were the main subclasses expressed by virus-specific B-cells, this likely reflects IgG1 switch to IgA1 (95), and affinity maturation of IgA<sup>+</sup> cells in germinal centers.

Given that clonal families of B-cells share VDJ usage, we next compared VDJ segment usage for mono-specific and dual-specific cells. The results revealed a high degree of divergence between antibodies expressed by mono-specific and dual-specific cells, suggesting that dual specificity did not arise from hypermutation of a mono-specific clone, but rather through discrete recombination events in naive B-cells (**Figure 42**). Moreover, dual-specific cells displayed reduced antibody diversity compared with their mono-specific

counterparts. Such oligoclonality of cross-reactive B-cells may reflect the evolution of VDJ segments that mediate binding to conserved conformational epitopes of the viral capsid. These findings, coupled with the phenotypic and functional attributes described herein, support the evolution of a discrete cross-reactive tissue homing memory B-cell lineage that is rapidly mobilized and expanded in response to different RV strains.

**Figure 33: Uninfected Nasal Biopsies Stain Sparsely for B-cells and T-cells**

Immunofluorescence analysis of nasal tissue analyzed for CD19 (green), CD3 (white), RV (red), and DNA (blue). Panel (a) was prepared without primary antibodies. Data is representative of 5 uninfected subjects.

**CD3** **CD19** **RV-A16**

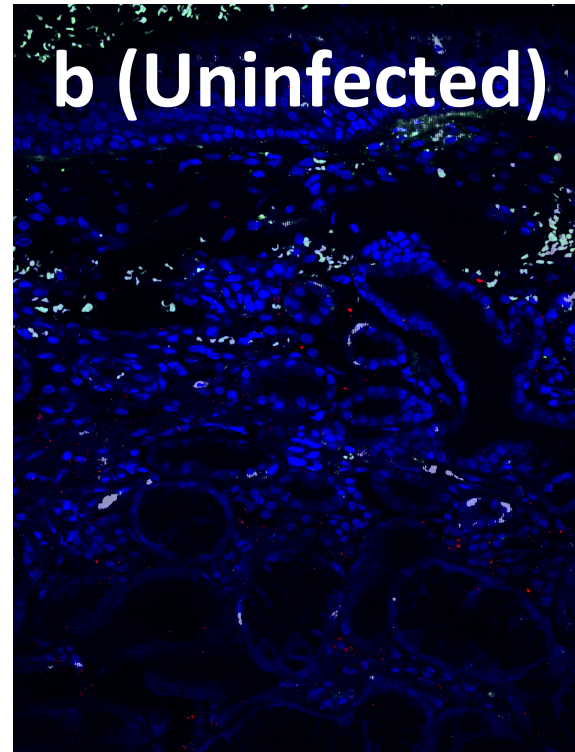
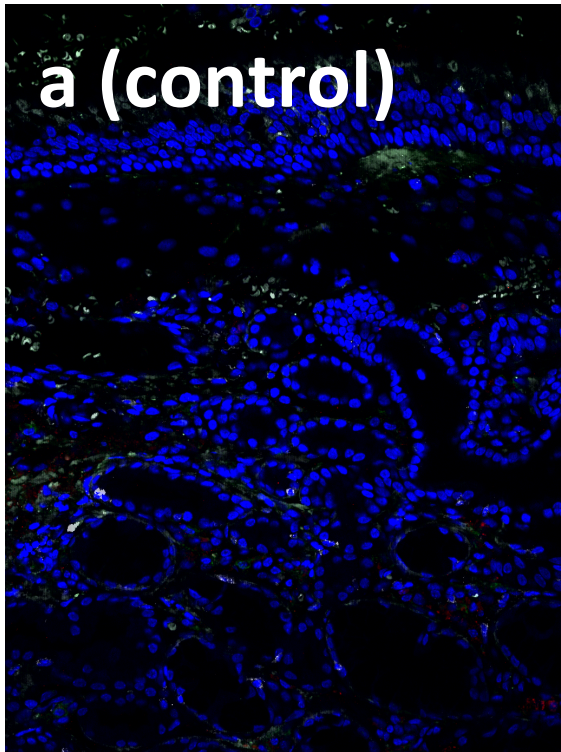


**Figure 34: Infected Inferior Turbinate Stains Densely for B-cells and T-cells**

Immunofluorescence analysis of inferior turbinate (IT) tissue analyzed for CD19 (green), CD3 (white), RV (red), and DNA (blue). Panel (a) was prepared without primary antibodies. Data is representative of 5 infected subjects.

**CD3 CD19 RV-A16**

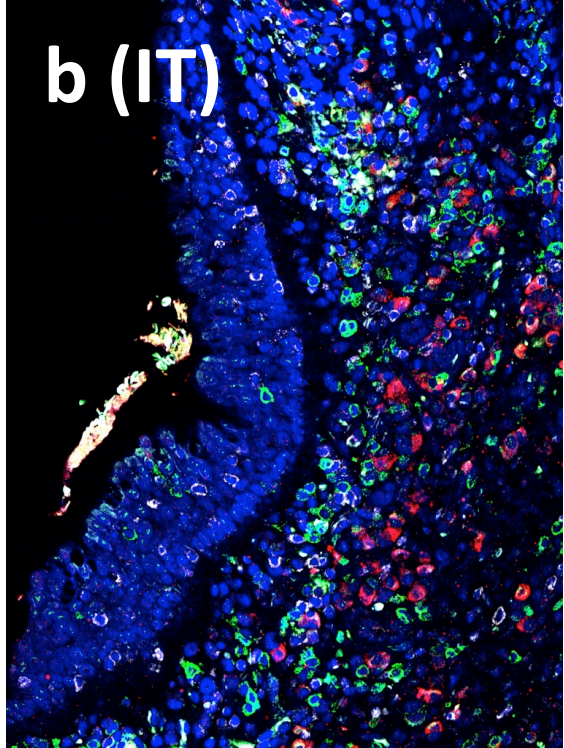
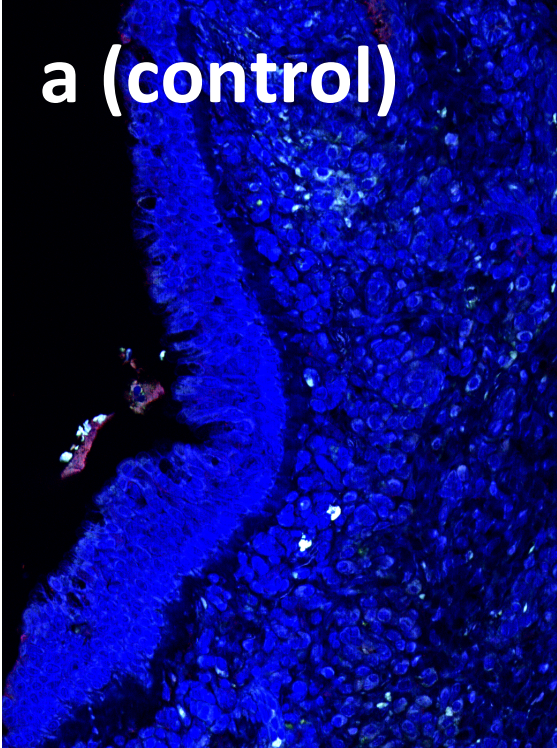


**Figure 35: Infected Middle Turbinate Stains Densely for B-cells and T-cells**

Immunofluorescence analysis of middle turbinate (MT) tissue analyzed for CD19 (green), CD3 (white), RV (red), and DNA (blue). Panel (a) was prepared without primary antibodies. Data is representative of 5 infected subjects.

**CD3 CD19 RV-A16**

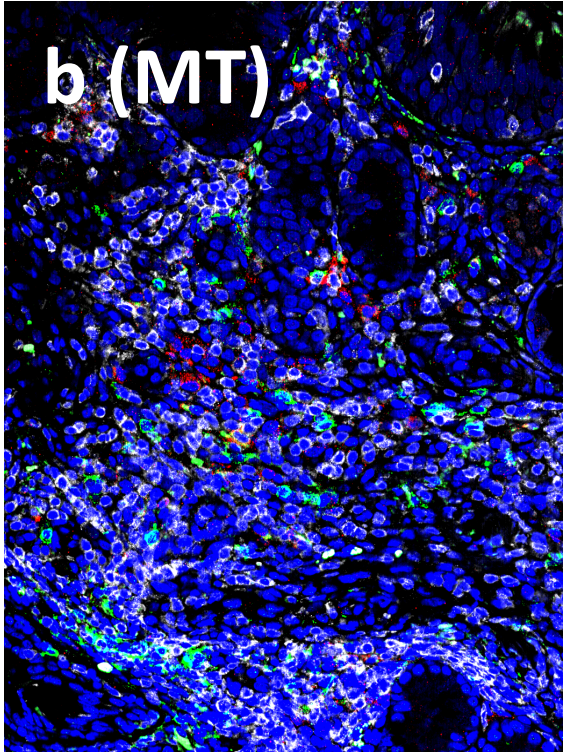
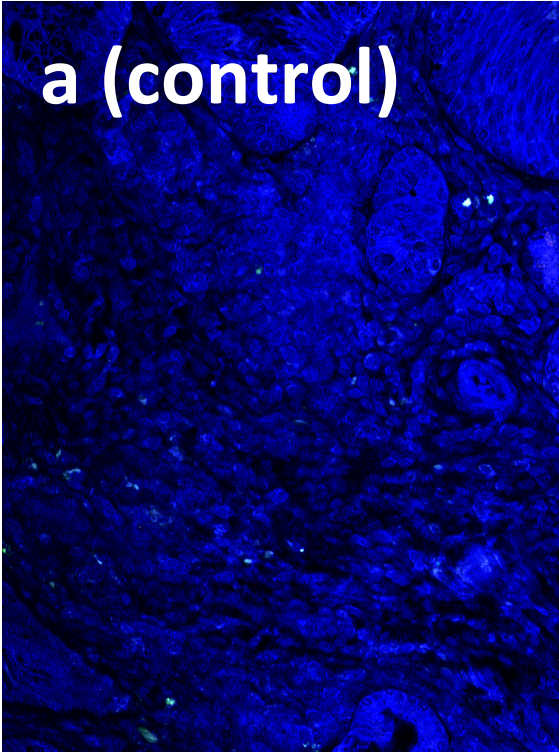


**Figure 36: Infected Nasopharynx Stains Densely for B-cells and T-cells**

Immunofluorescence analysis of nasopharynx (NP) tissue analyzed for CD19 (green), CD3 (white), RV (red), and DNA (blue). Panel (a) was prepared without primary antibodies. Data is representative of 5 infected subjects.

**CD3** **CD19** **RV-A16**

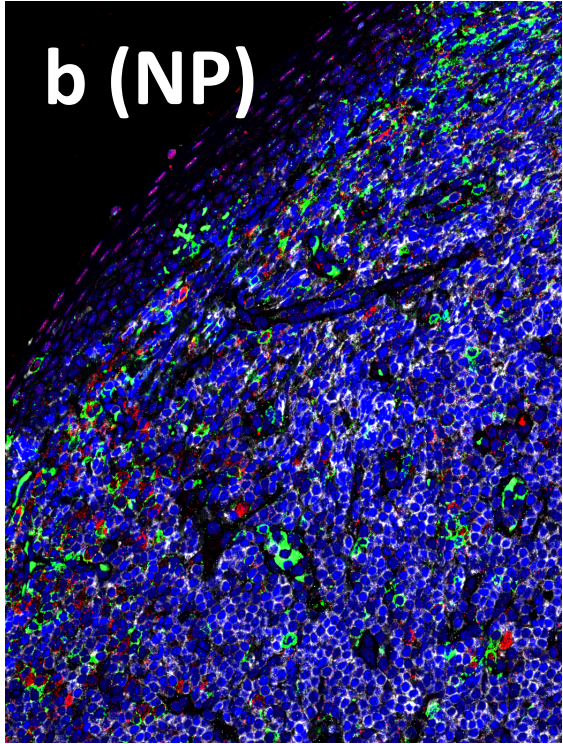
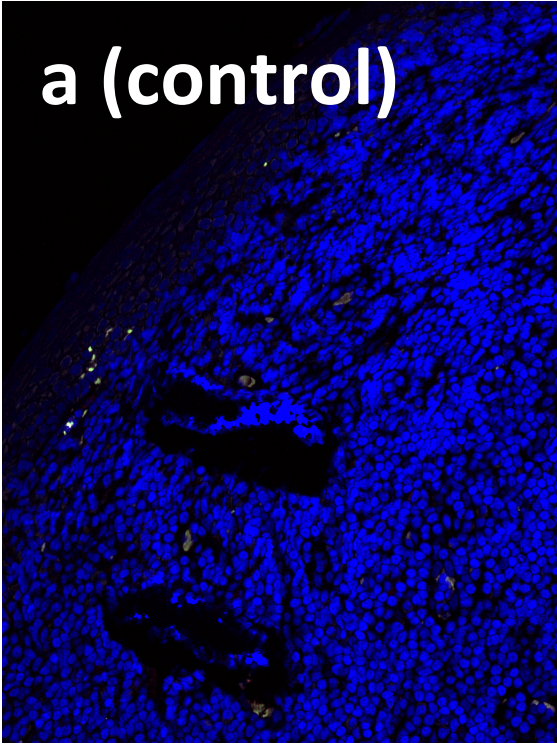


**Figure 37: Infected Nasal Tissue Demonstrates Dense Lymphocytic Infiltrates**

Cell counts in nasal biopsies from infected subjects after RV challenge and in uninfected (Un) healthy controls (5 per group). Specimens from uninfected subjects were available for a single nasal site only. Averages for each subject were calculated from four image locations within each biopsy. Significance was determined by Mann Whitney ranked-sum test. \* $p < 0.05$ , \*\* $p < 0.01$  versus uninfected tissue.

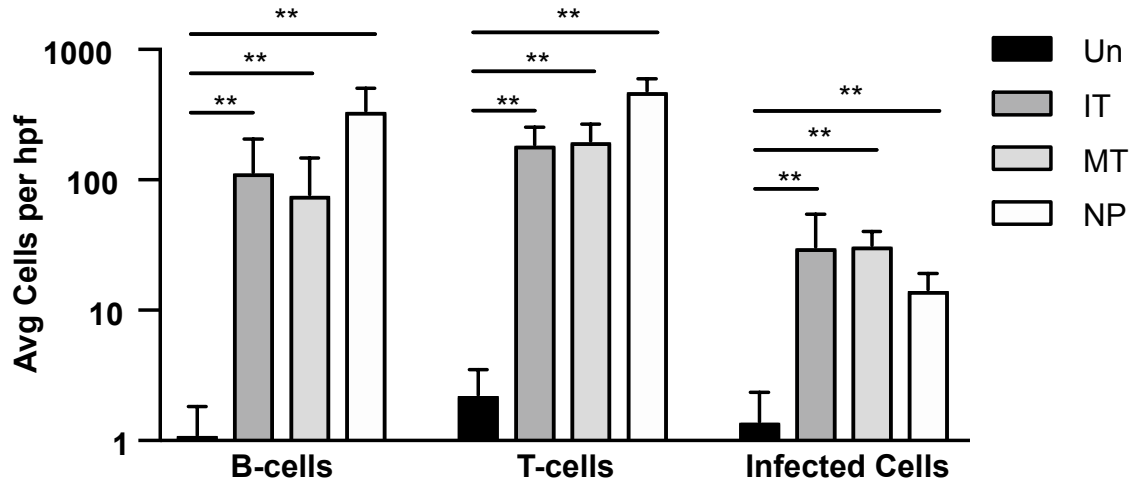


**Figure 38: Immunofluorescence Analysis of CD20 in Nasal Biopsy Specimens from RV-Infected Subjects**

Representative images from 5 infected subjects showing co-expression of CD19 and CD20 in infiltrating B-cells, consistent with an effector memory phenotype. Panel (a) is presented without CD20 channel signal for contrast.

**CD3 CD19 CD20**

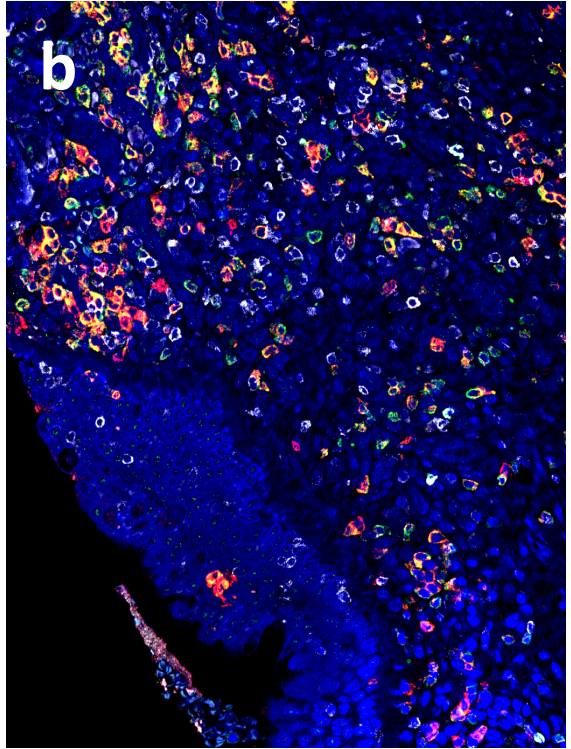
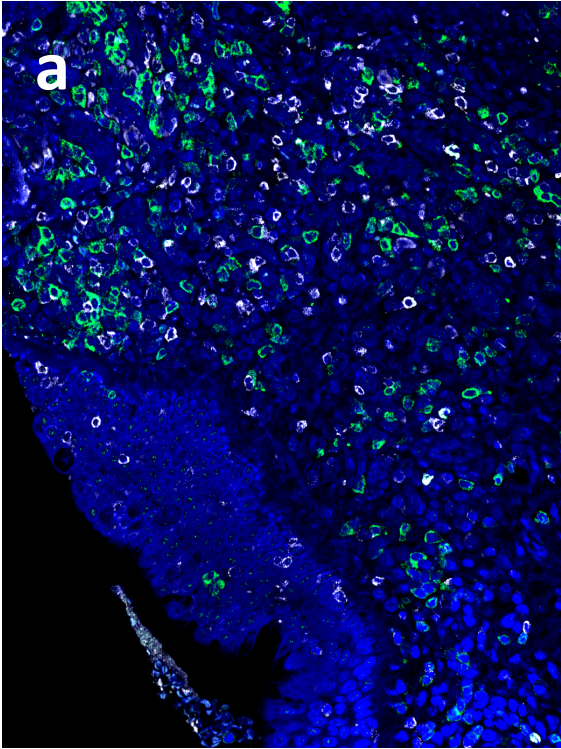


**Figure 39: Early Antibody Responses to RV in the Nose are Cross-reactive and Limited to IgG**

Longitudinal analysis of antibody isotypes specific for homotypic or heterotypic virus (depending on infecting strain) in nasal washes during RV infection (subjects infected with RV-A16 and RV-A39 = 13 and 12 respectively; n=25 for all time points). Significance was determined by Wilcoxon matched pairs signed-rank test. Geometric mean  $\pm$  geometric SD. \*p<0.05, \*\*p<0.01, \*\*\*p<0.001, \*\*\*\*p<0.0001 versus day 0.

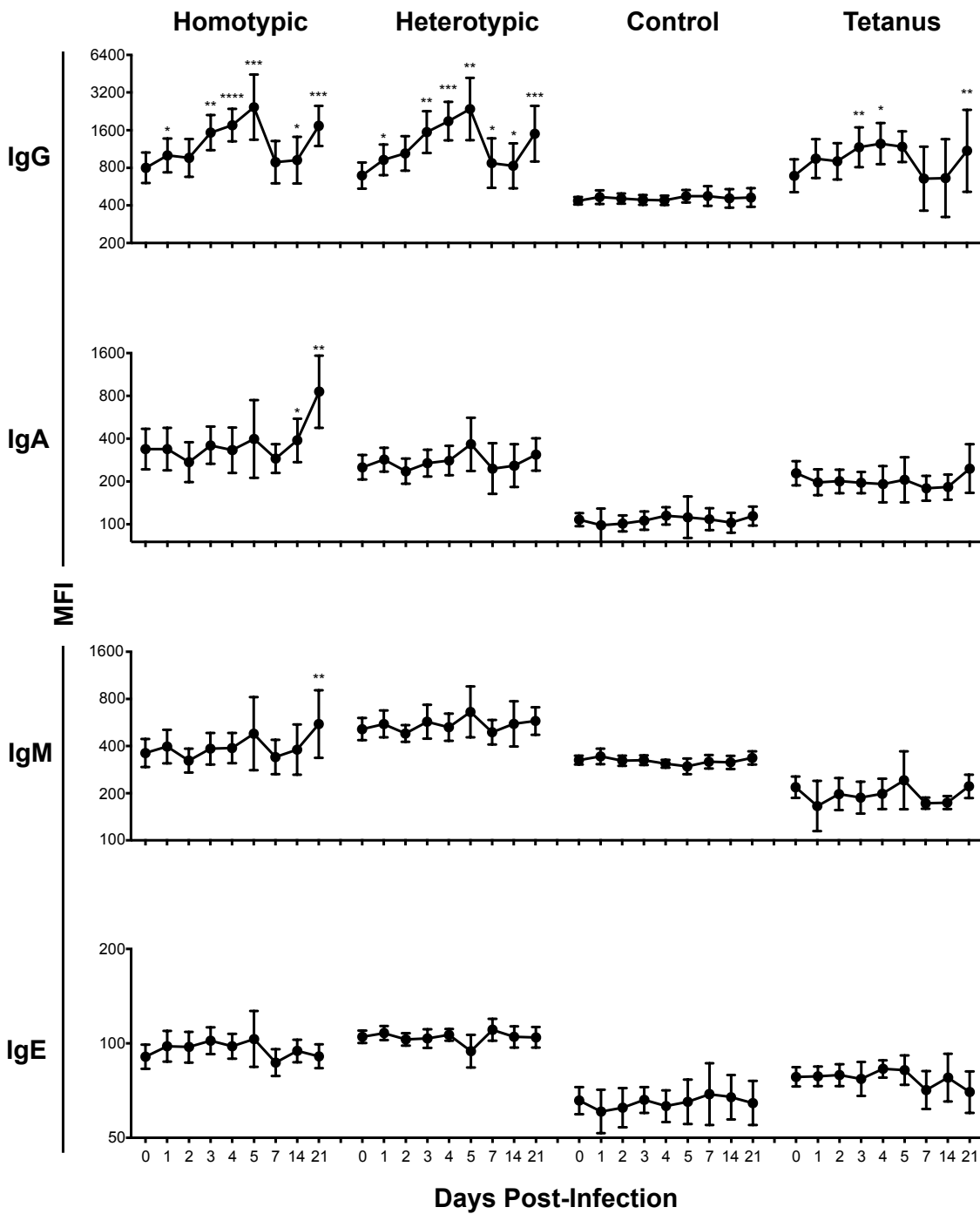


**Figure 40: Weak IgG Responses to Rhinovirus are Present in the Nose of Uninfected Subjects After RV Challenge.**

IgG antibodies were measured longitudinally in nasal washes obtained from 5 subjects who remained uninfected after RV challenge. Geometric mean  $\pm$  geometric SD.

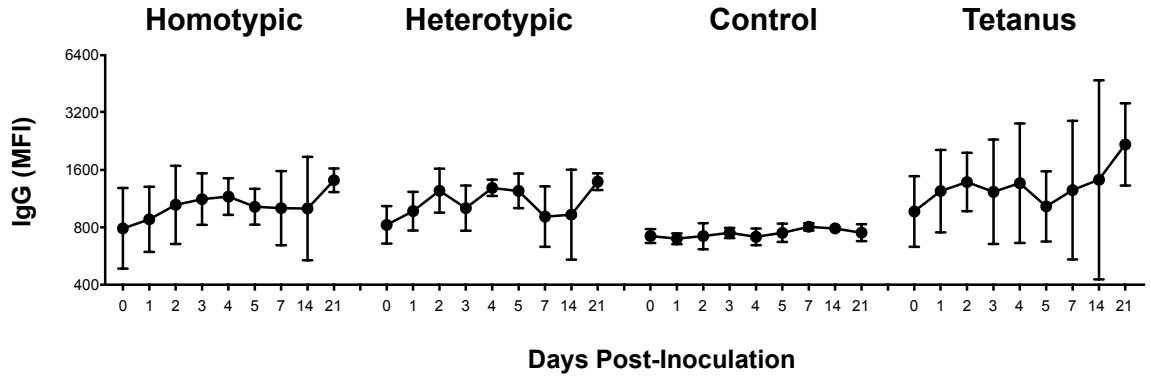


**Figure 41: Dual-specific and CXCR5<sup>-</sup> B-cells are Hypermutated at Similar Levels as their Mono-specific and CXCR5<sup>+</sup> Counterparts**

Somatic hypermutation counts at immunoglobulin heavy chain loci in FACS-sorted RV-specific single B-cells. Dual-specific B-cells were sorted as a separate phenotype for CXCR5<sup>-</sup> IgG<sup>+</sup> cells only. Significance was determined by Mann-Whitney ranked-sum test. Mean  $\pm$  SD. \*p<0.05, \*\*p<0.01, \*\*\*p<0.001, \*\*\*\*p<0.0001.

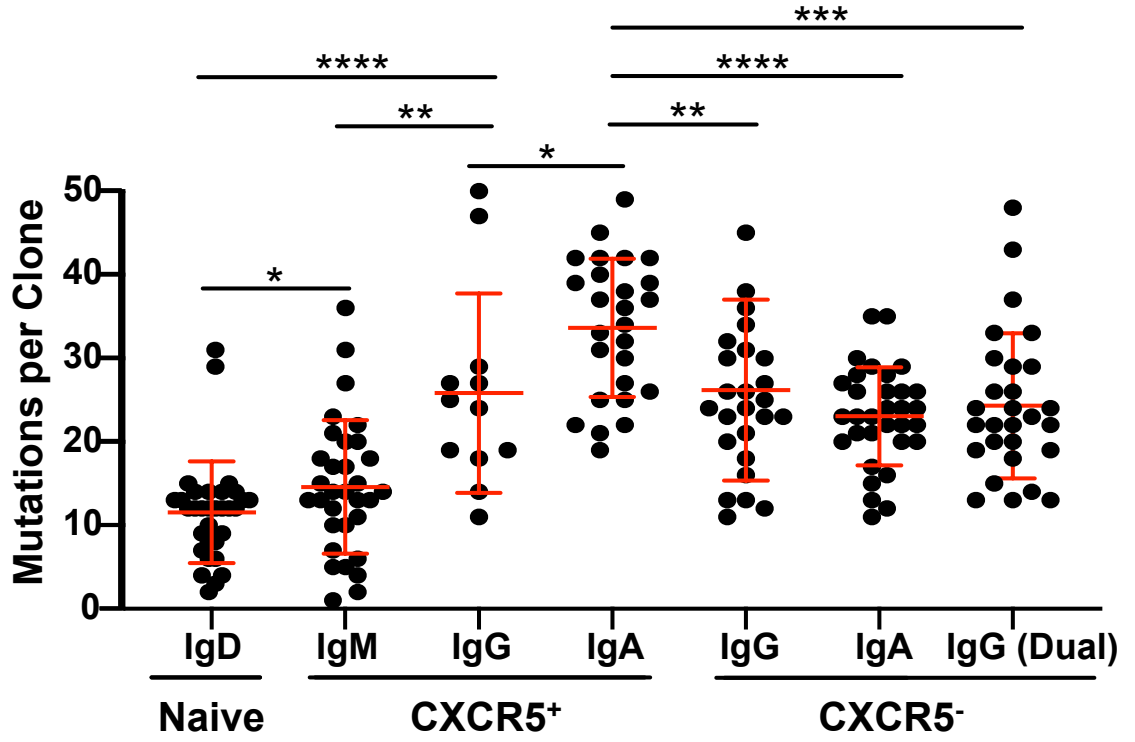
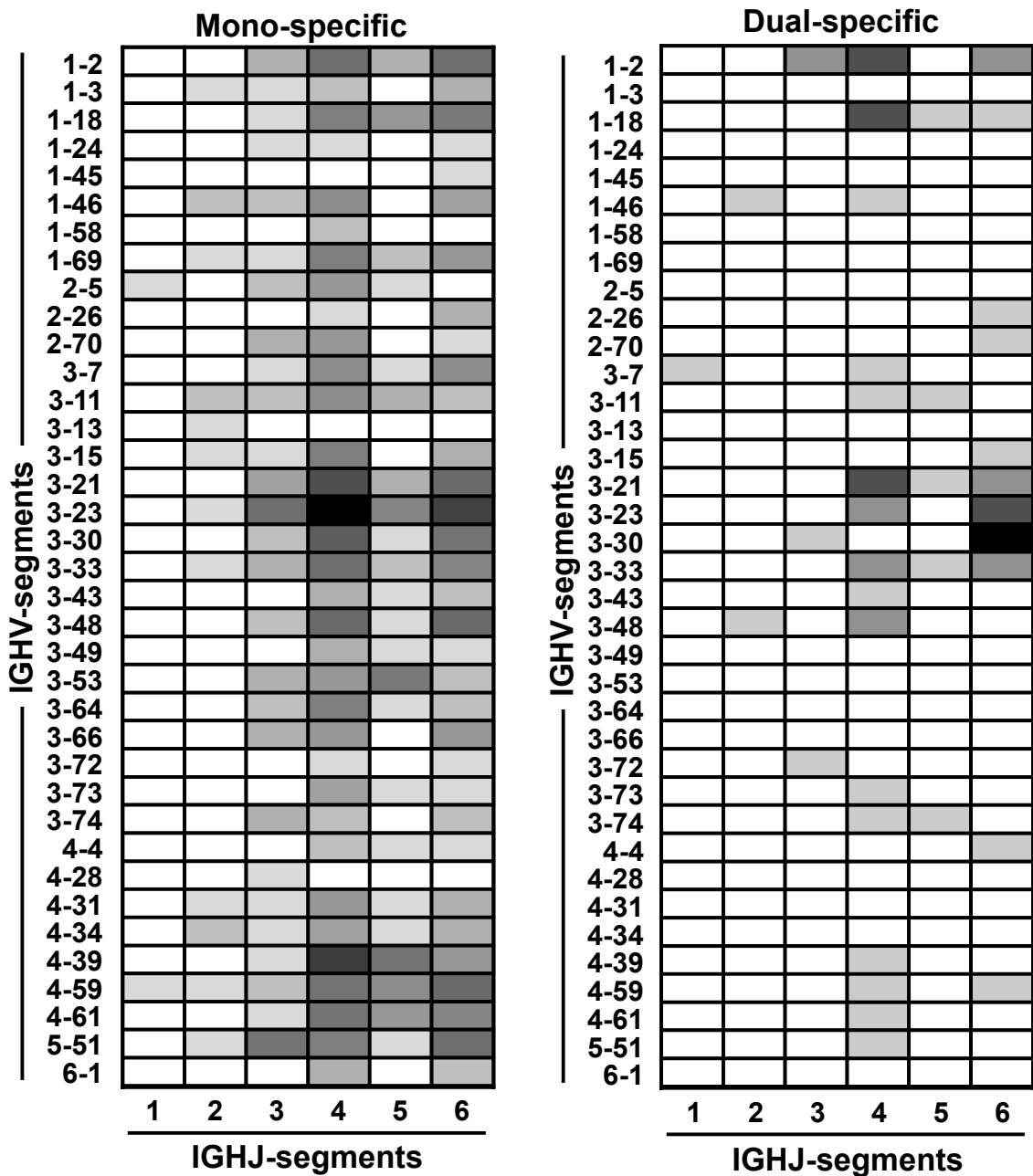


**Figure 42: Dual-specific B-cells are Clonally Distinct from Their Mono-specific Counterparts**

VDJ segment selection in mono-specific and dual-specific B-cells (734 and 180 cells respectively).



## Discussion

Here we report the first comprehensive analysis of RV-specific B-cells and humoral immunity in humans. By assessing B-cells in parallel with antibodies of all isotypes, we identify a pivotal role for dual-specific cells in mediating cross-reactive responses to different RV strains in the nose. This was made possible by using intact RV capsid to measure antibodies, and to label B-cells. By applying a multi-faceted approach in both the absence and presence of infection, we demonstrate that RV-specific B-cells, that cross-react with two distinct RV-A strains, constitute a major functional subset of tissue homing memory cells. The high number of these cells likely arises from previous RV infections. We provided several lines of evidence to support the pivotal role of dual-specific B-cells in the adaptive response including: (1) their ability to rapidly secrete IgG antibodies specific for both RV-A16 and RV-A39; (2) outgrowth following *in vivo* infection; (3) a molecular signature commensurate with tissue-trafficking T-bet<sup>+</sup> B-cells; and (4) antibody profiles in the nose that matched those secreted by dual-specific B-cells. The molecular characteristics of dual-specific B-cells echo the features of RV-specific Th1 effector memory cells previously described by our group (228,229). With this in mind, these dual-specific memory B-cells may constitute a subset analogous to "effector memory", which was borne out by their functional properties.

Dual-specific B-cells express receptors for ligands induced by RV in nasal secretions, which would be expected to aid in their recruitment to the site of

infection (229). In the present study, the presence of dense B-cell infiltrates in nasal biopsies, coupled with the production of cross-reactive IgG antibodies (but not IgA or IgM) in the nose during acute infection, provided compelling evidence for the influx of dual-specific “effector memory” cells. Moreover, the dichotomous antibody profiles in the nose versus the serum fit with the different antibody profiles of dual-specific and mono-specific B-cells respectively. Together, these findings indicate a spatial and temporal division of labor between distinct virus-specific B-cell subsets that mediate antibody responses during the acute phase at the site of infection, and those that contribute to the systemic antibody repertoire after virus has cleared.

The persistence of dual-specific T-bet<sup>+</sup> B-cells in steady state, that are poised to rapidly differentiate and secrete cross-reactive IgG, contrasts with the portrayal of T-bet<sup>+</sup> B-cells as exhausted, poorly functional, or pathogenic (243,164,165,167). This discrepancy may be explained by the ability to re-activate B-cells upon repeated RV infections, as opposed to the induction of B-cell anergy by chronic antigenic stimulation in certain disease settings (163,245). Our study is not the first to define the trait of tissue homing “effector memory” B-cells. Previous studies have referred to B-cell phenotypes as “tissue-like memory” based on signatures of surface proteins that included the lack of CXCR5, although features of cell trafficking and differentiation were not elucidated (160,250,170,243).

Expression of inhibitory receptors on T-bet<sup>+</sup> B-cells has been interpreted as a sign of exhaustion (160,243,168). One example is the BCR co-receptor CD22, which was also highly expressed on dual-specific B-cells. This molecule inhibits BCR signaling, but also has functions in B-cell homeostasis, survival and migration (251–253). Similarly, the loss of expression of B-cell activating molecules such as CD21 and CD27 on "tissue-like memory" B-cells has also been linked to exhaustion based on reduced proliferation capacity, despite the ability to secrete antibodies (245). Low expression of these proteins was a feature of dual-specific B-cells in the present study. On the other hand, high expression of molecules that amplify BCR signaling (e.g. CD19 and CD20) was also a feature. With these aspects in mind, the functional relevance of inhibitory molecules may be more nuanced in those cases where T-bet<sup>+</sup> B-cells rely on alternative pathways to modulate BCR signaling (e.g. TLR pathway) (170,80,164). Regardless, when considered together, much of the phenotypic and functional data related to T-bet<sup>+</sup> B-cells indicates an effector function (168,169,167). The rapid benefits of anti-CD20 therapy (rituximab) in autoimmune disease aligns with this view. This treatment would not be expected to ablate CD20<sup>-</sup> plasma cells, but would be expected to target CD20<sup>high</sup> B-cells, such as those with an "effector memory" signature. Indeed, successful anti-CD20 therapy demonstrates lasting ablation of IgD<sup>-</sup> CD27<sup>-</sup> B-cells that resemble "effector memory" cells (254,255).

Our study raises new questions regarding the provenance of LN homing and tissue homing B-cells that are virus-specific, especially considering their different specificities. One possibility is that these subsets are lineally divergent, a theory supported by the disparate VDJ usage of mono-specific and dual-specific B-cells. Interestingly, we identified a rare naive (IgD<sup>+</sup> IgM<sup>+/-</sup>) subset that was CXCR5<sup>-</sup> and T-bet<sup>+</sup> that would fit the profile of a precursor of "effector memory" B-cell (**Figure 43**). While the dichotomy of mono- and dual-specificity is puzzling, it is possible that the cross-reactive RV epitope recognized by dual-specific cells, and that drives its expansion at sites of infection, is not maintained on viral antigen that primes those B-cells in draining LNs. Variation in the nature of antigen encountered in the tissues versus the LNs might also explain the different antibody profiles of dual-specific and mono-specific B-cells respectively.

The discrete antibody profiles of mono- and dual-specific B-cells were also striking. The interferon axis in the nose would be expected to favor CSR in tissue homing dual-specific B-cells to IgG. In mice, IFN- $\gamma$  produced by T-cells induces T-bet-dependent CSR to IgG2a in B-cells, which is the antibody subclass most closely related to human IgG1 (161,256,176,80). On the other hand, denatured virus within draining LNs may drive CSR to IgG and IgA in LN homing B-cells during resolution of inflammation (79). In addition to its role in CSR, T-bet has been implicated in regulating the balance between systemic and mucosal antibody responses, possibly by influencing B-cell migration to tissues via

upregulation of CXCR3 (180,256). This feature might further contribute to the discrepancy between strain-specific antibody profiles in the serum and cross-reactive antibodies in the nose reported here.

Importantly, our findings help to explain why humans can resolve RV infections, but remain susceptible to re-infection throughout their lives. Adaptive immunity to different RV-A strains is intact in all adults we have tested to date. Beyond B-cells, circulating memory T-cells that are RV-A-specific are cross-reactive, based on their recognition of peptide epitopes that are highly conserved across the RV-A species (228). Repeat infections likely arise from waning of cross-reactive B-cell responses over time, as a result of the return of dual-specific B-cells to the circulation, spleen, or other reservoir (**Figure 44**). Indeed, our data indicate that nasal B-cells are not retained indefinitely, as evidenced by sparse B-cells in nasal tissue from healthy controls. Moreover, our data imply that dual-specific B-cells fail to give rise to LLPCs that might provide durable cross-protection, given that cross-reactive antibody responses in nasal secretions did not extend to the serum. Instead, cross-reactive antibodies are induced locally and briefly, but do not persist systemically, whereas longer lasting narrow spectrum antibodies target the infecting strain, but do not cross-protect. This may reflect evolution of the “ideal” relationship between host and virus that is mutually beneficial.

Clinical observations in patients with primary hypogammaglobulinemia provide compelling evidence of the importance of B-cells, as opposed to

systemic antibodies, in resolving RV infections. This condition results in defects in the production and survival of B-cells, and acute respiratory tract infections are common. In these patients, RV was found to be the most common virus, and positive PCR for RV, including that for the same strain, persisted for several months, despite adequate immunoglobulin replacement therapy (257). Given that RV-specific antibodies would be expected to be present in the immunoglobulin treatment, owing to high rates of seropositivity to specific RV strains in the population (~40%), this scenario highlights the inability for systemic antibodies to clear virus in the nose, and the importance of antibodies secreted by mucosal B-cells.

A key question remains regarding the neutralizing capacity of cross-reactive antibodies in our system. If we consider that viral surface epitopes involved in host-cell entry are less likely to mutate than other epitopes (208,204–206), conserved epitopes of RV-A16 and RV-A39 might be expected to interact with the major RV receptor, ICAM-1. Thus, we might predict that dual-specific B-cell clones are more likely to neutralize virus than their mono-specific counterparts. However, neutralization may be dispensable, as long as opsonization occurs. In keeping with the capacity to opsonize virus, we have demonstrated the ability for dual-specific B-cells, as well as their secreted antibodies, to bind whole virus. It should be noted that the nature of neutralizing antibodies remains ill-defined in RV infection, including their isotype. However, knowledge of antibodies against influenza, another common respiratory viral

pathogen, could yield clues. In this context, IgA is more cross-reactive and more neutralizing than IgG, primarily as a result of its more efficient secretion into the airways, and its divalence, which enhances avidity and complex formation with virus (258–260). Interestingly, whereas IgA outperforms IgG in neutralizing influenza when secretions isolated from the upper airways are considered, the reverse may be true in the lower airways during acute infection (261). Given that influenza primarily infects the lungs rather than the nose, this would fit with a model of rapid secretion of neutralizing IgG at the infection site by "effector memory" B-cells. With respect to RV, a previous report noted initiation of neutralizing activity in nasal secretions as early as 4 days post-infection, whereas a rise in neutralizing activity in the serum required more than 7 days, consistent with our timeline (262).

In summary, we have characterized a novel T-bet<sup>+</sup> B-cell subset that is cross-reactive for different RV strains. These cells respond rapidly to RV infection *in vivo*, and differ from their mono-specific counterparts based on their tissue homing potential and enrichment for IgG. Through comprehensive assessment of antibody profiles both *in vivo* and *ex vivo* we define a role for dual-specific "effector memory" B-cells in the induction of cross-reactive IgG in the nasal mucosa as early as 1 day post-infection, whereas mono-specific B-cells drive subsequent IgG, IgA, and IgM responses systemically. Such division of labor among dichotomous B-cell types that are virus-specific provides unprecedented insight into the B-cell response to RV.

**Figure 43: T-bet and CXCR5 Expression in IgD+ and IgD- B-cells**

Representative flow cytometry data from an uninfected human subject demonstrating the presence of T-bet+ CXCR5- B-cells in both CD19+IgD- and CD19+IgD+ subsets.

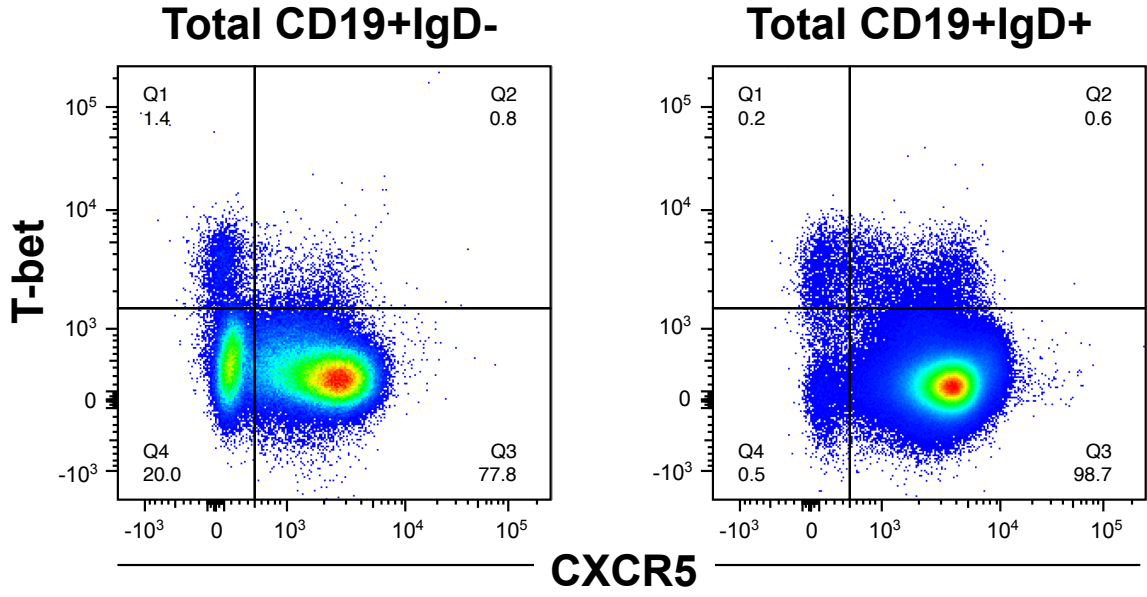
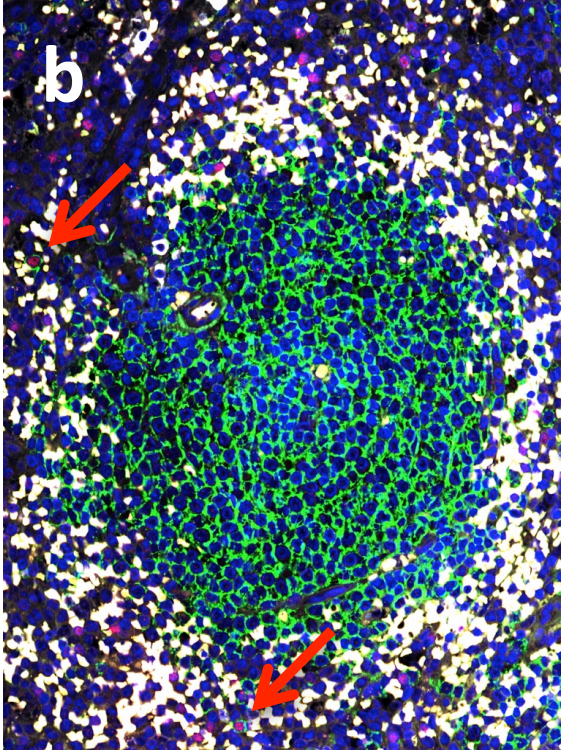
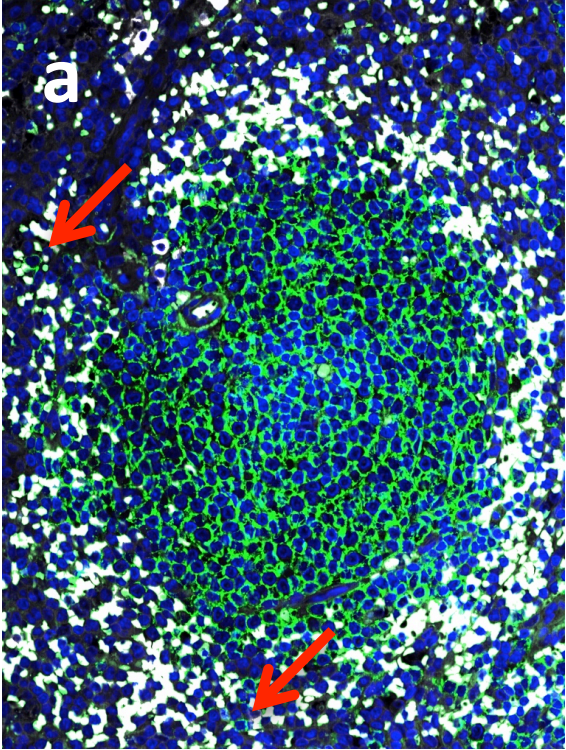


**Figure 44: Immunofluorescence Analysis of T-bet<sup>+</sup> B-cells in Spleen**

Representative images from deidentified healthy splenic tissue demonstrating nuclear T-bet and surface CD19 co-expressed on the margins of B-cell zones (see arrows). Sections are stained for CD19 (green), T-bet (red, purple overlay on nuclei), and DNA (blue). RBCs are unstained, but autofluoresce intensely (white). Panel (a) is presented without T-bet channel signal for contrast.

**RBC CD19 T-bet**



## Conclusions and Future Directions

We have addressed a major knowledge gap in the field of adaptive immunity to RV by characterizing the B-cell response to infection. In particular, we demonstrate the presence of mixed-isotype single-strain specificity in CXCR5<sup>+</sup> memory cells and convalescent serum, and IgG-restricted cross-reactivity in CXCR5<sup>-</sup> B-cells and acute nasal secretions. These results indicate a lack of humoral cross-protection at steady state, somewhat mitigated by a broadly-reactive localized response rapidly induced upon infection. This begins to explain human susceptibility to repeated RV infections, which are relatively brief, and occasionally even asymptomatic. Our most generalizable finding going forward is novel evidence for the existence of an effector memory phenotype in B-cells (Bem), most easily recognizable by its lack of lymphoid homing receptor CXCR5. By utilizing this term, we invoke the well-established T-cell subset (Tem) that circulates through peripheral tissues and blood, rapidly differentiating toward effector activity upon engagement with cognate antigen at sites of inflammation. This is precisely what we observe in B-cells responding to RV: a stably circulating population with a characteristic surface phenotype (in several ways reminiscent of Tem), that mobilizes upon acute infection, as evidenced by the accumulation of B-cells and secretion of corresponding antibodies within infected nasal tissue, as early as day 1 post-infection (**Figure 45**). This is in contrast to conventional memory B-cells, or, to extend our T-cell analogy, central memory (Bcm). These cells also circulate in blood, but

continuously traffic through lymphatic tissue and receive stimulus in LN follicles. Our ability to link our findings in the blood with those in the nose was strengthened significantly by the cross-reactive specificity exhibited by putative Bem, and its absence in Bcm. At first this would seem purely fortuitous, but in fact there is recent evidence that this may be a common feature of tissue-homing B-cells. Prior to our work, CXCR5- T-bet+ B-cells, analogous to the Bem subset we have defined, were described as exhausted “age-associated” B-cells (ABC), given their inferior proliferative capacity, and accumulation with advanced age, or else in chronic infection or autoimmunity. We acknowledge that the suggestion of this novel phenotype and functional capability in B-cells is provocative, however, in this chapter, we will argue in support of this notion, and propose future work to provide confirmation and to further explore its implications for the immunology field.

### **Effector Memory and Symmetry in Lymphocytes**

The literature is littered with evidence indicating that ABCs are functional, poised for rapid effector activity, traffic to inflamed tissues, and share many mechanistic and descriptive characteristics with Tem (80,81,159–170). This work is the first to demonstrate and synthesize all of these observations within a unifying model, and it does so in the setting of experimental human infection. While the theory absolutely requires confirmation through replication, and generalization to additional models of immunization including infection (other than RV), vaccination, autoimmune disease, allergy, and possibly even cancer, it

would not be a surprising phenomenon if borne out. It denotes symmetry in T-cells and B-cells, two cell-types sharing an ancient lineage. Given the evolutionary complexity that now separates these cells, the patterns of trafficking represented by central memory, effector memory, resident memory, and effector cells (PCs vis-à-vis B-cells) are comparably simple, and likely predate the T-B schism. Furthermore, the ability of B-cells to respond immediately with opsonizing (and most likely neutralizing) antibodies and limit the spread of infection is an advantage that evolution would be expected to conserve. Physicists perhaps have a monopoly on the aphorism “nature loves symmetry”, but this physical truth extends far beyond their limited purview. Although, in fairness to physicists, life and immunity are manifestations of physics, as quantum mechanics dictate electron orbitals, and thus molecular bonding and biochemistry. Symmetry amplifies the applications of established building blocks and the utility of genetically encoded information. Thus Occam’s razor may be restated: “the most symmetrical solution is the most likely solution.” If T-bet drives an antiviral immune program, it would do so most efficiently by initiating a parallel program in Th1, CD8+ T-cells, NK-cells, and B-cells. CXCR3 expressed by any of these cells is the same gene product and employs the same homing mechanism.

### **Theoretical Benefits of B-Effector Memory**

Arguably there is not an absolute need for Bem: B-cells are capable of acting at a distance through immunoglobulin secretion to control local infections,

whereas cytotoxic T-cells and NK-cells are not, as they require direct synapse with infected cells (174,186). However, CD4+ T-cells' immune orchestrating role conceivably could also be restrained to endocrine function in the draining LN. Yet, to the contrary, these cells are well known to contribute Tem that home directly to nascent sites of inflammation, providing immediate and undiluted support to other effector lymphocytes and phagocytic myeloid cells. No one would dispute the value of this feature in CD4+ T-cells, and certainly the humoral response would also benefit from such proximity. To this point, distinctions are often made between specific antibodies and neutralizing antibodies, however, any antibody of any affinity will neutralize at high enough concentration. The RV capsid is a 60-mer of VP1-4 complexes (~100kD total, each), and thus might contain up to 60 binding sites for a single antibody clone, if we assume one epitope per monomer subunit (though as few as 12 sites at five-fold vertices). If 60 sites were occupied, given sufficient IgG concentration, the opsonins would total ~10MD, while the capsid itself would be a mere ~6MD, and thus neutralization would be a foregone conclusion. Bem offers both immediacy and many orders of magnitude higher concentration of antigen-specific antibodies at the site of infection, where effector activity is most vital. The restriction on pathogen outgrowth would no doubt be profound, compared with the lack of this, albeit theoretical, B-cell subset. However, as above, all the requisite pieces of immune machinery are present, and the T-cell analog exists; if Bem are not present in humans (or mice), the most likely explanation is that they were not

preserved by evolution. Perhaps we should be asking why we never appreciated their contributions previously, and, more pointedly, why we neglected to look for them.

### **Evaluating the Practical Role of B-Effector Memory**

While we may freely speculate at the value of Bem, given the clear advantages they would ostensibly confer, ultimately it will be necessary to more rigorously test their importance in immunity. Studies in human patients lacking B-cells and receiving passive humoral immunity via transfusion demonstrate chronic viral infections, including RV, that are absent in healthy, B-cell competent individuals (257). This is highly consistent with a role for Bem in clearance of infection. However, these subjects also lack what we might call “central memory” B-cells (Bcm or conventional, lymphoid-homing memory). Thus, their infections do not receive an influx of Bem immediately upon infection, but they also do not receive lymphoid-derived humoral immunity beginning a week later. Further work is needed to elucidate the distinction between central and effector memory B-cells. It is unlikely that naturally-occurring human genetic variants (spontaneous knockouts) will be informative in this regard. Similarly, while there are a variety of human conditions (particularly cancer and autoimmune disease) wherein treatments effectively knock out B-cells by targeting CD19 or CD20, these too will not suffice, as they ablate Bem as well as Bcm. In light of these limitations, it will be necessary to pursue murine models of infection, which regrettably will not make use of ICAM-1-tropic strains of RV (such as RV-A16

and RV-A39), as they infect humans exclusively. RV strains tropic for the LDL-receptor are a possibility, however (263). Also Coxsackie viruses, which are closely related to RV (picornavirus family, enterovirus genus) have been applied to mouse models of infection and immunity (219). Given the drastic change of model, it will first be necessary to confirm in mice all of the observations made in this work. ABCs are documented in mice, and it is reasonable to suggest that T-bet<sup>+</sup> B-cells in mice function equivalently as in humans, but there must be verification that the murine infection successfully generates functional Bem, before these cells are further probed in that context. Provided the mouse model of serial RV or Coxsackievirus infection demonstrates the outgrowth of Bem after primary infection, and rapid localization and IgG secretion in infected tissue after secondary infection, novel experiments may be undertaken. Ideally, this model will also allow for antigen-specific B-cell labeling, as demonstrated herein, with whole capsid, tagged fluorescently or otherwise. The expansion of Bem in mice may be quite profound given their relatively pathogen-free environment, and, in this case, antigen labeling may not be necessary. However, if mice, as humans, have a considerable circulating cohort of Bem at baseline, antigen-specificity may be crucial to identify responding cells. At this point, establishing the relative importance of Bem and Bcm should be straightforward. Virus-specific (or bulk) Bem and Bcm will be sorted from mice previously infected one or more times. These cells will be transferred separately (and both or neither as controls) to congenic naïve animals to be subsequently infected. This also presents an

opportunity to test the dependence upon memory CD4+ T-cells, which could be transferred in parallel. Bcm are likely to depend upon Tcm, but it is an open and intriguing question whether Bem depend upon Tem. Both cell types are clearly present in the nasal biopsies we collected from RV-infected human subjects, but this does not necessarily imply immune synapse and T-dependent B-cell activation. Control of viral growth should be assessed by qPCR of infected tissues and animal health by weight loss and survival. Infectious doses of virus may need to be titrated to reveal measurable health effects. Alternatively, the model may require a more virulent pathogen. By all readouts, however, our hypothesis is that Bem is more important for early clearance and acute-phase wellbeing than Bcm. Given literature tracking the outgrowth of PCs from GCs and the concordance in our own data between Bcm specificity and serum antibodies, we expect that Bcm, is likely instead crucial for production of bone marrow-resident LLPCs and subsequent protection from initiation of infection upon future exposure (21,27–29,51,151). Still, the relationship between PCs within various anatomic niches should be tested for their differential derivation from Bem or Bcm. This could easily be determined from a congenic transfer model, as described above.

### **Association of Specificity and Phenotype**

One curious finding of our work is that Bcm and Bem largely target distinct RV epitopes, the former being strain-specific and the later cross-reactive. This may be a unique peculiarity of human RV infection, but the immunological

mechanism accounting for it is likely broadly applicable, even if it does not always result in such stark dichotomous specificity. The essential question this observation poses concerns the state of antigen draining to LNs, and how it varies from native antigen at the site of infection. Our data suggest that the cross-reactive epitope between RV-A16 and RV-A39 may be compromised by the time viral protein reaches a lymphoid follicle, having drained passively through lymphatic vessels, or having been carried actively by a DC. This is difficult to probe because the same antigen may be present in both locations, even proteolytically intact, while its conformation may be altered. Methods will require preservation of tertiary and quaternary structure in protein gathered at either location. One simple approach in mice (as above) would be to purify RV or Coxsackievirus from infected tissue and from the draining LNs by the same density gradient approach used to harvest RV from HeLa cells (232), and then to quantify by qPCR. Alternatively, homogenized tissue could be used in a plaque assay to determine the presence of viable virus. Based on the narrow specificity of Bcm, our expectation would be that intact virus rarely migrates to the LN, however, if it is found there, another possibility is that it is infecting DCs or some other draining cell. This notion is consistent with our finding that some RV-infected cells in our biopsy samples are weakly CD11c-positive, though their precise identity and trafficking pattern are unknown (**Figure 46**). While this may at first appear as a negative outcome for the host, it is possible that such infection is the most efficient mechanism to provide antigen to central

(LN-resident) lymphocytes, allowing their eventual outgrowth and production of Teff and PCs to induce late clearance and long-term protection. Other possible assays would involve harvesting supernatants from homogenized infected tissue and LNs. These would be run on native gel and blotted, or coated on ELISA plates, to be detected with immunoglobulin harvested from plasmablast differentiation cultures of Bem and Bcm, as performed in this work. Here we might expect antibodies derived from Bem to demonstrate augmented binding to samples derived from infected tissue, and Bcm to favor lymphoid antigen.

One theory to account for the discrepancy in specificity between Bem and Bcm is a temporal shift between disrupted antigen and intact viral capsid flowing to the GC, the latter of which could be sourced from infected cells in the LN, as suggested above. Early in the infection, only opsonized fragments flowing through lymphatic vessels may reach the LN, but this supply of protein may shift toward whole virus if LN-homing cells become infected and begin releasing intact viral particles before the GC has run to completion. This hypothesis is consistent with a study of influenza vaccination which compared the IGH gene sequences of memory B-cells (Bcm) and ABCs (in this case, “activated B-cells” but phenotypically consistent with our Bem) (264). Here the authors found a temporal untethering of immunoglobulin heavy chain sequence families between memory B-cells and ABCs, which was profound in the first two weeks, but faded away in the coming months as memory B-cells and ABCs looked increasingly similar and clonally related. Their interpretation was that ABCs lose their activation status

over time and become conventional memory B-cells. It is difficult to compare our data to theirs, given the incongruence in experimental models and time points, but both of our studies may be consistent with other work demonstrating that memory is first to leave the GC and PCs are last, and that each have divergent specificities (138,139). Logically, Bem may form sometime in between, and thus if the quality of antigen was changing over the course of that period, it could affect the specificity of PCs versus Bem versus Bcm. Further studies might address this question, as above, by harvesting supernatants from LN homogenates at various time points across infection, and assaying by qPCR, native gel blot, or ELISA.

Once Bem are established, it is possible that they maintain their population by forming local GCs in respiratory tissue in the setting of infections. This is consistent with our biopsy results, which demonstrate dense infiltrates of both T-cells and B-cells (**Figures 34-37**). It is also consistent with a murine influenza study finding that cross-reactive B-cells are highly enriched in lung tissue compared with LN and spleen (265). These dual-specific B-cells persisted in the lungs for at least 2 months post-infection, and could be found in GC-like structures. When GC clonal selection was analyzed in each site, it was found to vary significantly between lung and lymphoid tissue. These results again argue for the presence of distinct viral antigen at the site of infection, compared with draining LNs. In this case, the authors maintain that antigen persists longer in lung tissue than in lymphoid tissues, and that this extended period of GC

competition promotes the development of cross-reactivity. Certainly it should increase affinity for the infecting (homotypic) strain, but we are somewhat skeptical that time alone would augment cross-reactivity because protracted SHM could just as easily diminish affinity for homologous, but structurally distinct epitopes on the heterotypic strain. However, the idea of transient tertiary lymphoid centers within infected tissue is highly intriguing, and could help to explain the specificity of Bem, particularly if it is found that intact virus does not appreciably migrate to LNs at any time point. This histological finding should be confirmed in a murine model of RV or Coxsackievirus, and the prevalence of cross-reactive RV-specific B-cells should also be determined in freshly excised human tonsils or adenoids, given their respiratory/lymphoid hybrid nature.

### **Association of Specificity and Isotype**

Although we demonstrate a trend in Bem toward cross-reactivity and Bcm toward mono-strain specificity, these are not mutually exclusive. The more absolute rule, however, is for cross-reactivity in IgG<sup>+</sup> B-cells, and its absence with other isotypes. This is apparent in our assays of plasmablast differentiation culture supernatants and in nasal washes. Lack of cross-reactivity in B-cells with isotypes other than IgG is particularly notable, given the presence of naïve cells found to bind both RV strains. This suggests that when dual-specific B-cells are activated, it is in the context of signals that strongly induce CSR to IgG. This is precisely what ought to happen under the control of a Th1 anti-viral response, but it is impressive how consistent CSR to IgG is for dual-specific B-cells

(79,81,165). This finding is consistent with the theory above that only certain B-cells come into contact with whole virus, which would contain both the cross-reactive capsid epitope and viral RNA. Such B-cells binding intact virions, upon internalization of those viral particles, might receive innate TLR-derived signals from the viral RNA. RV RNA would most likely signal through TLR-7, which is known to activate pre-established T-bet<sup>+</sup> B-cells (80,164,167). Unmethylated DNA, another viral DAMP, while not present in RV, has been shown to induce T-bet expression in B-cells via TLR-9, and it is likely that TLR-7 is capable of functioning the same way (162). Again, if there were a temporal switch in quality of antigen flowing to GCs, early draining material may simultaneously lack the cross-reactive epitope as well as the IgG- and T-bet-inducing viral RNA. As a first step toward establishing a role for the RNA genome in inducing the Bem phenotype, it would be worth confirming the reports of T-bet induction and CSR to IgG in B-cells using TLR-7 ligands (e.g. resiquimod) in place of CpG (the TLR-9 ligand used previously). Next, as a more complete experiment, naïve human B-cells should be *in vitro* co-cultured with RV-specific CD4<sup>+</sup> T-cells using various antigen preparations including whole virus (with intact RNA), whole virus lacking RNA, fractionated virus with RNA, and fractionated virus without RNA (266). T-cells would be gathered by sorting for Tetramer labeling, as previously established in our lab (228,229). RNA would be removed by digestion with benzonase (nuclease). Our hypothesis in this case would be that B-cells are induced to expand, differentiate, and secrete when

stimulated with all forms of RV antigen, but that when viral RNA is present, CSR is fairly uniform to IgG, whereas it might be more mixed with IgM and IgA otherwise. Furthermore, dual-specific B-cells should only grow out when whole capsid is present. It is important to remember here that fractionated virus with RNA is an unphysiological control condition; naked RNA would not be expected to survive long *in vivo*, as it drains through lymphatic vessels.

### **T-Helper Skewing Applied to B-Effector Memory**

In arguing for effector memory parallels between T-cells and B-cells, we have a major problem with our theory in that CD4<sup>+</sup> Tem come in a variety of subtypes: Th1, Th2, Th17, etc. While B-cells do as well, in the form of isotypes, we are arguing that T-bet both drives the Bem phenotype as well as IgG. Thus Bem are necessarily Th1-skewed by our argument. This may be the case, but it seems more likely that Bem can exist with other isotypes, and driven by other Tfh subtypes (Th1-like/IgG, Th2-like/IgE, Th17-like/IgA) (79). A subset of Bem is IgA<sup>+</sup>, but it is not clear whether this indicates Th17 skewing in its GC of origin, or simply that IFN- $\gamma$ -driven CSR to IgG makes occasional errors. By sole virtue of the elegance of symmetry, we are in favor of Bem existing with equivalent diversity as exists in T-helper cells. It could easily be that Bem type-1 is just the most prevalent phenotype, as Th1 is among CD4<sup>+</sup> T-cells. Also, our viral model, by definition, favors type-1 responses, potentially blinding us to others. It would be convenient if T-bet clearly induced either an effector memory homing phenotype, as in CD8<sup>+</sup> T-cells, or a type-1 (IgG1) skewing phenotype, as in

CD4<sup>+</sup> T-cells, but it seems to do both. Thus it is difficult to separate our variables. Notably, within our own data, we detect a tetanus-specific IgG signature in Bem plasmablast differentiation cultures and in nasal washes during RV infection, suggesting that even the Th2 adjuvant, alum, induces type-1 Bem. Certainly we are open to a breakdown of symmetry, but it will be worthwhile to probe tissue-homing B-cells in other inflammatory contexts before dismissing the possibility of the type-2 (Th2-induced, IgE<sup>+</sup>) or type-3 (Th17-induced, IgA<sup>+</sup>) Bem. Since the most basic definition of effector memory has nothing inherent to do with T-bet or IgG, only tissue-trafficking and rapid immunoglobulin secretion, we propose further mouse experiments immunizing with adjuvants known to induce Th1, Th2, and Th17 responses (e.g. KLH+NP with CpG DNA, alum, or flagellin, respectively) (267,268). Circulating NP-specific B-cells should be phenotyped (with particular attention to CXCR5 expression) prior to and after serial immunizations, and the site of immunization should be assayed by fluorescence microscopy and enzymatically digested for further flow cytometric analysis. Ideally these experiments would be carried out in a variety of locations and tissue types to determine whether those have any bearing on Bem phenotypes. In addition to our upper-respiratory data, previous work suggests that a Bem-like response may be elicited in the lung by influenza infection, but this should be confirmed (261). Here we expect that CXCR5-negative memory B-cells will be induced, and that these will traffic to site of immunization upon re-exposure. It is difficult to imagine, however, what the detailed phenotype of these cells might be

when stimulated with Th2 and Th17 adjuvants. Certainly we expect Th17 to elicit IgA, but this may be heavily dependent upon the site of immunization (79). After all, IgA would seem to have evolved more specifically for mucosal surfaces than for particular PAMPs, though these factors are not entirely disentangled from one another, as pathogens often demonstrate strong preferences for anatomical niches. IgE is also difficult to predict, given that its expression as a membrane bound BCR is intrinsically pro-apoptotic, which explains the effective absence of IgE<sup>+</sup> memory cells in circulation (269,270). Still, short-lived IgE<sup>+</sup> Bem would present a fascinating result, and their detection may require a high-frequency repeat immunization schedule, with close attention to early time points.

### **Induction of B-Effector Memory**

While the theory above that Bem arise midway through a GC response satisfies many of our observations, as well as those of others, it does not account well for the existence of IgD<sup>+</sup> B-cells lacking CXCR5 and expressing T-bet (**Figure 43**). If these are indeed GC-experienced cells, they would be expected to have undergone CSR, although this is not an absolute requirement (68,69,101,102). Still, we should consider other more likely possibilities than a GC origin. One option is that these are the result of an extrafollicular response, and that they did not receive adequate CD40L, IL-4, and IL-21 to undergo CSR. Alternatively, they may represent T-independent responses, which are similarly less prone to CSR. This could occur by either of the two routes: type 1 with activation through an innate PAMP receptor (e.g. TLR), or type 2 with massive

crosslinking of BCR by a highly repetitive antigen (54,60). These mechanisms could be easily tested *in vitro*, and supplementation with IFN- $\gamma$  may be required to elicit T-bet. It would also be interesting to determine if SHM rates in these cells differ from other IgD+ true naïve B-cells, where it is essentially absent. Given the lack of CSR, and the interrelation of these processes through AID, it would be surprising if SHM were elevated. Additional comparisons should be made between IgD+ “Bem” and naïve B-cells, particularly encompassing *in vitro* activation and immunoglobulin secretion. If these cells are previously activated, they should initiate secretion more rapidly than true naïve cells, and there would likely be some disparity in their rate of surface phenotype differentiation, as well. A final possibility is that T-bet+ CXCR5- B-cells are a pre-existing lineage prior to any engagement with antigen or activation event. This would be difficult to verify, given the complex lives of lymphocytes, and the activation events that necessarily occur en route to maturity, but a simple approach would be to evaluate bone marrow for T-bet expression and determine its presence in immature B-cells. We do not favor this possibility, but it should be considered. Setting IgD expression aside, a theory that dominated the early ABC literature was that T-bet+ B-cells were the exhausted products of repeated stimulation (160,170,245,250). Though it seems unlikely, given more recent reports pointing to roles for TLR signaling and T-cell-derived IFN- $\gamma$ , this hypothesis should nevertheless be tested (80,81,163,165,167–169,242). Human B-cells could be stimulated *in vitro* under culture conditions favoring memory expansion (rather

than PC differentiation), and the expression of CXCR5 and T-bet could be assessed for the outgrowth of a Bem phenotype (271–273). In parallel, murine congenic virus-specific Bcm could be transferred to naive mice and tracked upon repeated challenge. Maintenance of phenotype or conversion to Bem could inform the influence of chronic activation on Bcm stability.

### **B-Effector Memory in Tissue and Beyond**

Many questions remain unresolved concerning the nasal biopsy samples collected from infected subjects. We are extremely curious about the RV-infected cells that sit interspersed among the responding lymphocytes. The cells staining positive for RV have so far defied clear staining with all T-cell, B-cell, and myeloid markers that we have attempted (CD11c is questionable, **Figure 46**). Unexpectedly, the RV staining of epithelial cells is mild in comparison. The cytoplasm of these RV+ cells appears thick with viral antigen (capsid subunit VP2, specifically), suggesting genuine infection, rather than simple endocytosis. This relates to our hypothesis above about supply of intact capsid to LNs; if these cells drain through lymphatic vessels, they may explain the temporal shift in specificity between Bcm and Bem. Given our failure so far to identify these cells, taking a step back and attempting basic CD45 staining seems appropriate. Another method that would help in identifying these RV-infected cells, as well as further confirming the Bem phenotype of the B-cells infiltrating infected nasal tissue, would be to enzymatically digest and homogenize freshly biopsied tissue, rather than subjecting it to formalin fixation. Unfixed cells could be stained for

cytometry, allowing the use of our expansive panel of phenotyping antibodies. Though it may be below the limit of detection for fluorescence microscopy, day 4 differentiated Bem may still express residual T-bet and CD11c, and this may be appreciable by cytometric analysis. Furthermore, fixed samples are not amenable to staining cells for IgG, given that by day 4 of RV infection, secreted IgG thoroughly coats the tissue, and B-cells do not stand out above background signals. Digested tissue evaluated by cytometry could confirm whether infiltrating B-cells are exclusively IgG+, or if the representation is more mixed, and perhaps IgD+ Bem (as above) are present. Mitotic markers such as Ki-67 will also be informative when considering the origin and expansion of Bem. Extending biopsy time points would also help to determine what becomes of these cells after the resolution of acute infection. From *in vitro* stimulation experiments, we expect that many Bem differentiate toward a PC phenotype, but *in vivo* this may not be the case, or it may only be reflective of a subset of the infiltrating cells. Another possibility is that after PC differentiation and secretion of cross-reactive IgG, these cells de-differentiate and resume their Bem phenotype. An analogous process has been proposed in T-cells, with T<sub>eff</sub> surviving contraction to supply the T<sub>em</sub> pool (274). Pursuing the ultimate fate of tissue-trafficking cells will likely again require an animal model, however. To this end, we envisage a photoactivatable approach wherein Bem responding to rechallenge with virus or other immunogen (e.g. NP-KLH) at an accessible site, such as the murine ear, are photolabeled. Such cells could then be pursued for their eventual phenotype

in circulation or in LNs. We were at first surprised by our observation that stimulated Bem temporarily upregulate CXCR5 before assuming a PC phenotype, however, given that leukocytes are not known to traffic into blood vessels, other than in the unique context of the thoracic duct, the lymphatic route may represent the only way back into circulation for effector memory. Indeed, Tem are known to recirculate from peripheral tissue via lymphatic vessels by re-expressing CCR7 (275–277). Alternatively, CXCR5 may aid Bem in localizing with Tem within inflamed tissues. Its ligand, CXCL13 may be secreted directly by Tfh-like Tem or by myeloid cells orchestrating that interaction; both cell types are known to perform this function (25,99,278,279). This also suggests further avenues for determining the T-cell dependence of Bem, given that this interaction could be restrained *in vivo*, either by directly blocking synapse or by inhibiting trafficking patterns.

### **Harnessing B-Effector Memory**

From our data relating to tetanus and others' to influenza, it does seem that Bem are induced by vaccination (including inactivated formulations), but some analysis of the expansion of Bcm and Bem should be performed to compare the differential effects of infection, live-attenuated vaccines, and inactivated vaccines (264,169). Specificity will be of particular interest, given that one would expect the antigen binding of Bcm and Bem to be more uniform with a cross-linked target that should be conformationally identical in immunized tissue as in the draining LN. This could help to confirm above theories of differential

antigen quality and access between B-cell memory subtypes, given that no such temporal or spatial disparity should occur in this setting. As previously, the expected province of Bem is clearance of infections, not necessarily prevention, so this phenotype possibly becomes less important with pathogens that cause lifelong disease, such as HIV. Alternatively, because Bem are hypothesized to be less dependent upon T-cell help than Bcm, they may play an important role in the initial control of HIV and prolonging latency. Their expansion in HIV is well appreciated, but this has not been compared with health outcomes (160,168,170,250). Testing this will require a primate model, and should be extended to studies inoculating with recombinant cytomegalovirus that protects against simian immunodeficiency virus (SIV) exposure by incorporating immunogenic SIV epitopes (280). HIV aside, Bem ostensibly presents the greatest benefits in reducing the duration and extent of infections that humans regularly clear, but nonetheless cause significant morbidity and mortality. Depending on the results of mouse experiments described above, evaluating the respective contributions of Bcm and Bem, vaccine strategies may be enhanced by favoring the outgrowth of Bem, or by increasing their longevity. Though alum seems reasonably conducive to tetanus-specific Bem, given our *in vitro* stimulation and nasal wash data suggesting anti-tetanus IgG secretion by Bem, it will be valuable to compare the effects of various adjuvants in a murine model, particularly those that favor a Th1 response, as proposed above. Lastly, given the putative role for Bem in causing autoimmune pathology, studies of the

alleviating effects of TLR inhibitors in such diseases should expand their scope to include Bem (281). Ablation of ABCs individually, upon total B-cell ablative treatment, is known to correlate with improved remission outcomes, but such aggressive treatment leaves patients severely immunocompromised (254,255). Blocking the DAMP-dependent activation of Bem may provide more narrowly targeted, yet efficacious therapy.

### **Humoral Immunity to Rhinovirus**

While the implications of Bem are highly generalizable, it is worth considering the individual context of RV infection, given that it is the primary concern of the Woodfolk lab. Reflecting on our initial thoughts going into this work, we had surmised the presence of an inherent defect in the humoral response to RV that could account for the repeated infections to which humans are subject. In particular, we theorized that when a subject is reinfected with a heterotypic strain of RV, cross-protective Tfh-memory cells might be monopolized by the dominant reservoir of memory B-cells expanded at the previous infection. Such B-cells, we imagined, would largely be of low-affinity or non-neutralizing with respect to the new viral strain, and might block access to Tfh-cells for higher-affinity memory and naïve B-cells that are relatively scarce. There was also widespread evidence in our field to suggest that most individuals produce high levels of antibodies against a buried RV epitope on the VP1 capsid subunit protein N-terminus that is unexposed on live virus (202,215,216,282). Thus, we further conjectured that when a subject is reinfected with RV, the early

response might be dominated by B-cells expanded at previous infections, which target this “decoy” epitope on dead virus. The VP1 N-terminus is highly conserved, and we expected B-cells targeting it to be cross-reactive. Alas, these would succeed only in opsonizing broken, inactive viral particles, and might block access to Tfh-cells for scarce memory and naïve B-cells with neutralizing potential. However, in light of our data presented herein, it seems that rather than the VP1 N-terminal “decoy” being the object of misguided B-cells, it was the research focused upon it that was misguided. Our work instead supports the idea that antibodies binding this motif do so through a nonspecific interaction resulting from its hydrophobicity. Our own experience and others’ (unpublished) suggests that monomeric VP1 is a poorly soluble protein, highly prone to aggregation, and this precisely reflects the hydrophobic quality that leads to nonspecific binding of immunoglobulin. Furthermore, our bead-based immunoassay demonstrated marked increases in serum antibodies against intact capsid after RV infection, but detected no such change with respect to VP1. This indicates that the changes in serology brought about by the humoral immune response against RV have no relationship to the VP1 monomer, which appears to bind antibodies in a non-specific fashion. Indeed, the publications touting the high antibody binding capacity of VP1 failed to demonstrate change in binding across infectious time points, consistent with our findings (202,215,216,282). Their data is intriguing in that asthmatics have higher levels of binding than controls, but this may reflect

the properties of serum of allergic asthmatics that makes antibodies more prone to bind non-specifically in solid phase assays.

Another goal of ours was to detect cross-reactivity, which we succeeded in doing. As discussed at length, there is quite a bit of nuance to this observation, as cross-reactivity was heavily enriched in a B-cell subset highly consistent with effector memory. The consequence of this distribution of specificity is that cross-reactivity is exclusively within the IgG isotype, and is primarily expressed at the site of infection, rather than systemically. Lastly, overall we did not see evidence of original antigenic sin. Conventional B-cell memory and naïve cells responded as expected to novel strains with mono-strain specificity, and we did not observe heterotypic responses in mono-specific B-cells. Heterotypic signals were largely confined to dual-specific Bem, and were the result of balanced cross-reactivity, with no reason to doubt the neutralizing or opsonizing capacity for either viral strain. Thus, if a B-cell defect exists, it is the lack of cross-reactivity in Bcm and in IgA. Bem seems well equipped for clearance, but its effect appears only temporary. If cross-reactive Bcm could accumulate and predominate over the course of many discrete infections, cross-protective LLPCs might develop. Given that Bem represent a novel concept, there is cause to question dogma dictating that LLPCs are primarily Bcm derived. However, this notion conflicts with our own results indicating a lack of cross-reactive serum antibodies (**Figure 9**), and with numerous studies linking LLPCs to lymphoid GCs (283–286). The most likely explanation is that while RV-specific Bem efficiently

generate PCs, these traffic to respiratory tissue, an environment much less conducive to longevity than bone marrow (29,148–150). Furthermore, RV-specific Bem would be expected to produce almost exclusively IgG+ PCs. Compared with IgG, IgA has shown greater capacity for neutralization, given its divalence and mucosal secretion efficiency (259–261). Thus, broadly protective cells are two steps away from reality: Bem, while in some ways exciting, are the wrong phenotype and the wrong isotype. We could envisage a highly artificial scenario wherein IgA+ Bcm are engineered with immunoglobulin genes isolated from Bem, but hopefully the experiments proposed above will provide alternatives to such a heavy-handed intervention by elucidating the mechanisms by which Bcm and Bem are created, and how their specificities develop. The ultimate goal remains a fairly traditional vaccine model, but will require the appropriate antigen, adjuvant, and delivery, to be determined by future work.

### **B-Effector Memory and Rhinovirus**

Many questions remain concerning the unique role Bem seems to play in RV infection and clearance. The issue of neutralization is foremost, though as discussed earlier, any antibody at sufficient concentration to enforce saturation of a viral capsid with icosahedral symmetry should neutralize. Given that there is no objectively appropriate immunoglobulin concentration to test neutralization, such assays are somewhat meaningless. We fully expect the antibodies secreted by Bem are instrumental in clearance of multiple RV strains, which is consistent with the mild course most infections take. Moreover, there is some evidence that RV

infection is frequently subclinical, without sufficient symptoms to alert the host, and Bem may explain this phenomenon. In our own study, subjects who failed to become infected (negative seroconversion and viral culture/PCR at day 1 post-inoculation) nevertheless demonstrated cross-reactive nasal IgG secretion, indicative of Bem activity. It would be a simple matter to apply cellular analysis to such subjects. We strongly suspect that resistance to symptomatic infection may correlate with Bem frequency. While this arguably conflicts with our stated opinion that Bem are more important for clearance than for prevention, it is important to note here that subclinical infection and early clearance, in the strictest sense, still represent affirmative infection. It would certainly be worthwhile to explore time points prior to 1 day post-infection for nasal biopsies and washes. Bem may become active even within hours of exposure.

Another important step will be to establish the extent of cross-reactivity in Bem, particularly with minor group RV-A strains using the LDL-receptor to infect host cells, and also with RV-B and RV-C family viruses. It would be highly surprising if viruses using entry receptors other than ICAM-1 could be targeted by the same Bem cells highlighted by our study, given that receptor binding epitopes are by far the most likely to be conserved and cross-reactive. Even if Bem are not pan-RV-specific, there are roughly 100 major group RV-A strains, and simultaneously targeting all or most of those would be an impressive feat (1). Furthermore, there may be other Bem cells that target RV-B or RV-C broadly.

These questions can be answered using the same methods developed for the work herein.

### **Rhinovirus, B-cells, and Asthma**

Finally, a major focus of our lab is determining why asthmatics suffer increased morbidity (and occasional mortality) from RV, and future work will consider this. Essentially our full analysis should be repeated in asthmatic subjects, with particular consideration for disparities between their responses and healthy controls. Given that asthmatics are known to generate increased frequencies of PC effectors, we are curious to see if their Bem responses are also augmented. Certainly this is the trend in lupus, which is known to share many mechanistic qualities with allergy, though of course targeting a very different class of antigens (161,163,167,242). Prior to pursuing this considerable undertaking, however, several pieces of data we have already collected are informative. For one, according to our bead-based immunoassay, asthmatics produce RV-specific IgE in their serum after infection, whereas healthy control subjects do not (**Figure 9 and 47**). This alone could account for increased mast cell- and basophil-mediated symptoms after infection. On a related note, we register a strong bystander response against tetanus in nasal washes, which likely extends to a host of allergens and nasal bacteria (287). Benign environmental or commensal antigens that are chronically present will lead to symptoms, provided increased specific IgE secretion; this is the very definition of allergy. We have not confirmed IgE+ Bem, but this is a strong possibility,

particularly when considering allergic or asthmatic subjects. Just as it has been enlightening to determine the phenotypes of RV-specific B-cells, a similar approach considering allergen-specific cells would be valuable, and in asthmatics we expect to see B<sub>em</sub> specific to allergen, as well as RV and tetanus.

### **Summary**

We have demonstrated the presence of rare dual-strain rhinovirus-specific B-cells universally circulating in adult human subjects, which expand following resolution of RV infection. These cells exhibit an IgG<sup>+</sup> T-bet<sup>+</sup> phenotype consistent with published accounts of “age-associated B-cells”, and additionally lack CXCR5, indicative of peripheral tissue-homing. In contrast, we detected CXCR5<sup>+</sup> memory cells of all isotypes with single-strain RV-specificity. Supporting the proposed localization of the T-bet<sup>+</sup> cells, we found B-cell bodies and cross-reactive IgG at acute time points in nasal biopsies and washes, respectively, from human subjects experimentally infected with RV. Serum antibodies were not detected until convalescence, and were single-strain specific and of mixed isotypes, matching CXCR5<sup>+</sup> B-cells. Analysis of memory B-cell subsets *in vitro* demonstrated that CXCR5<sup>-</sup> B-cells secrete immunoglobulin more rapidly upon stimulation than CXCR5<sup>+</sup> B-cells. Taken together, these findings are highly suggestive of the existence of dichotomous memory B-cell types, as previously established in T-cells. T-effector memory is known to contribute to early control of infections by trafficking directly to sites of inflammation and rapidly initiating immune effector functions. Thus, a novel cross-reactive

B-effector memory cell type, coupled with a lack of cross-protective serum antibodies may explain the long documented phenomenon of frequent RV infections with rapid clearance in humans. Beyond shedding light on the nature of adaptive responses to RV, this also presents new questions relating to the origins of B-effector memory and its cross-reactive specificity. If this phenotype and its proposed capabilities are confirmed, there will be broad implications for the field of immunology. It will suggest new strategies for vaccination, as well as for treatment of autoimmune disease, and will challenge established dogma concerning the roles and functions of B-cells and secreted antibodies. There is more to be done to cement our theory, but this work, in a human model, is compelling, and, if myriad prior studies are reconsidered in light of our conclusions, there is truly striking congruence between them all. The most symmetrical solution is the most likely solution.

**Figure 45: Schematic of B-cell Memory Subsets Responding Acutely to RV**

According to our theoretical model, naïve B-cells and Bcm specific for individual viral strains traffic to LNs and form GCs, while Bem home directly to inflamed nasal tissue, immediately activate effector function, and begin elaborating cross-reactive IgG, contributing to RV clearance. PBs leaving GCs at later time points are predominantly mono-specific and may home to nasal mucosa or bone marrow. Upon convalescence, Bcm drain through efferent lymphatics and recirculate, while Bem transiently express LN-homing receptors to exit nasal tissue via afferent lymphatics, and follow Bcm back into circulation.

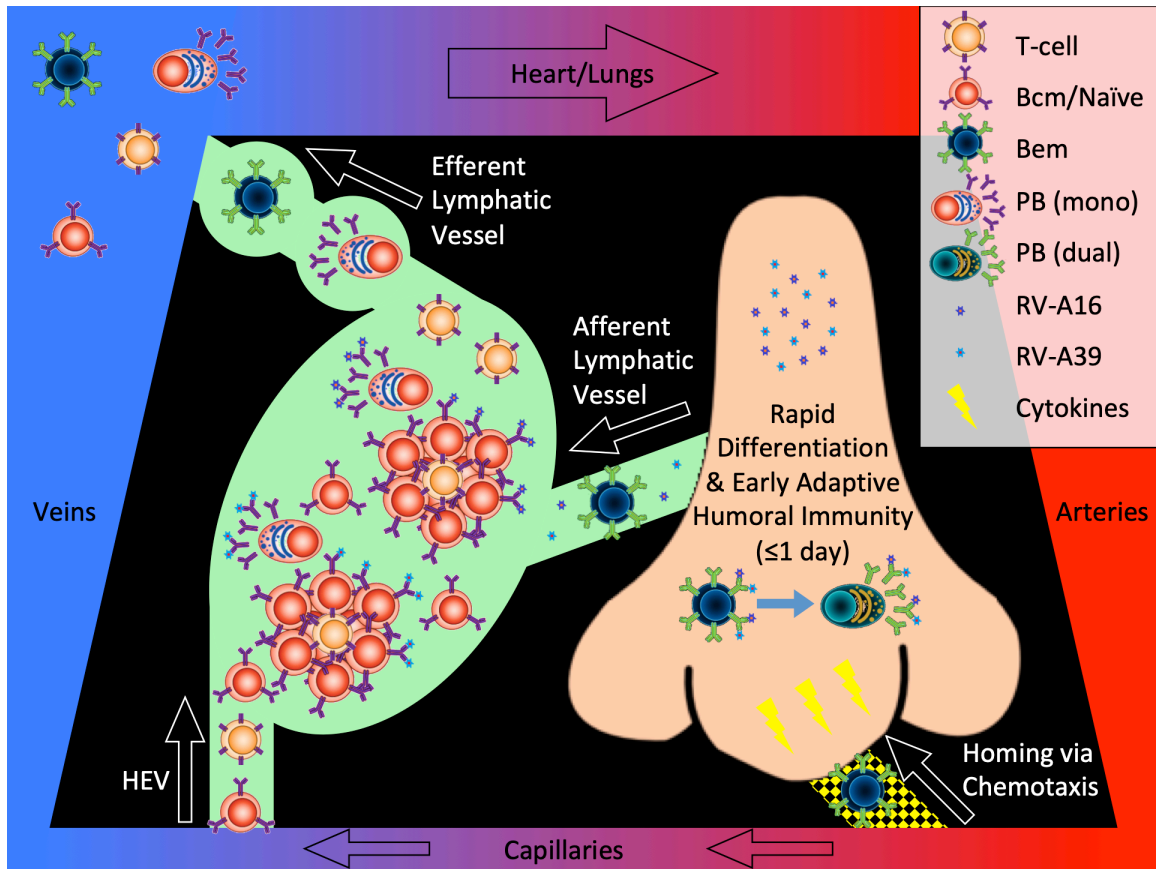


**Figure 46: CD11c is Expressed by Infiltrating non-B-cells**

Representative images from 5 infected subjects showing CD11c staining within RV-infected tissue. CD11c+ cells include some positive for RV (indicated by yellow arrows). Panel (a) is presented without RV channel signal for contrast.

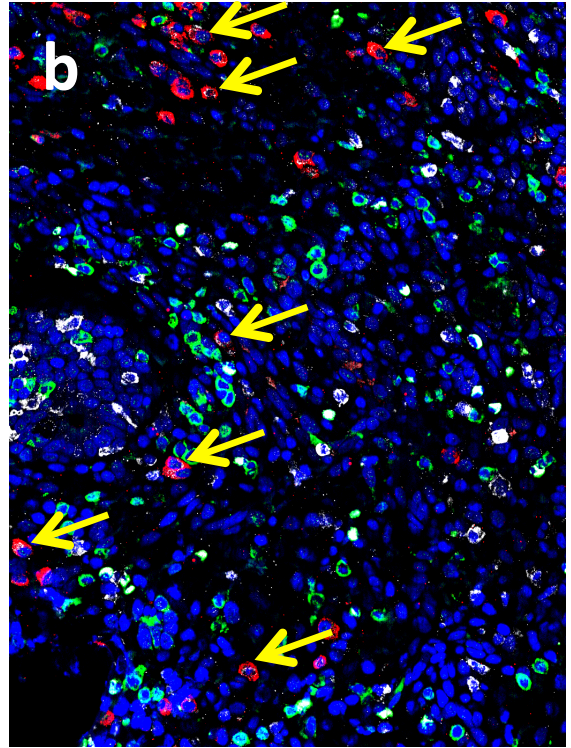
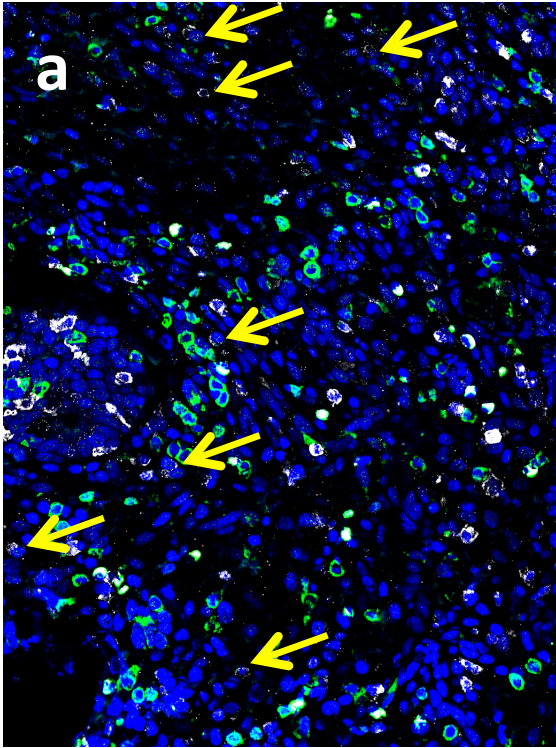
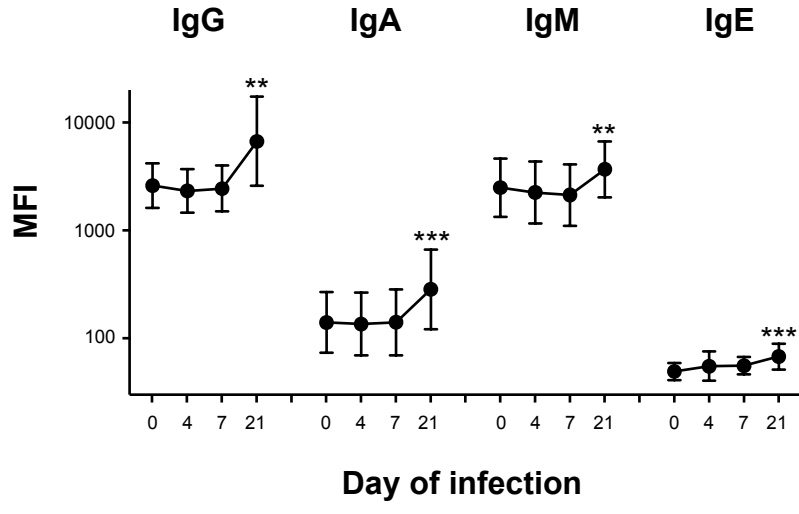


**Figure 47: RV-Infected Asthmatic Subjects Produce Serum IgE Against RV**

Longitudinal analysis in asthmatics of serum antibodies specific for homotypic whole virus at days 0, 4, 7 and 21 after RV inoculation (12 asthmatic subjects infected with RV-A16). Geometric mean  $\pm$  geometric SD. \*\* $p < 0.01$  and \*\*\* $p < 0.001$  versus day 0.



## References

1. Jacobs SE, Lamson DM, George KS, Walsh TJ. Human Rhinoviruses. *Clin Microbiol Rev.* 2013 Jan 1;26(1):135–62.
2. Fendrick A, Monto AS, Nightengale B, Sarnes M. The economic burden of non-influenza-related viral respiratory tract infection in the united states. *Arch Intern Med.* 2003 Feb 24;163(4):487–94.
3. Calhoun WJ, Dick EC, Schwartz LB, Busse WW. A common cold virus, rhinovirus 16, potentiates airway inflammation after segmental antigen bronchoprovocation in allergic subjects. *J Clin Invest.* 1994 Dec 1;94(6):2200–8.
4. Zambrano JC, Carper HT, Rakes GP, Patrie J, Murphy DD, Platts-Mills TAE, et al. Experimental rhinovirus challenges in adults with mild asthma: Response to infection in relation to IgE. *J Allergy Clin Immunol.* 2003 May;111(5):1008–16.
5. Iwane MK, Prill MM, Lu X, Miller EK, Edwards KM, Hall CB, et al. Human Rhinovirus Species Associated With Hospitalizations for Acute Respiratory Illness in Young US Children. *J Infect Dis.* 2011 Dec 1;204(11):1702–10.
6. Soto-Quiros M, Avila L, Platts-Mills TAE, Hunt JF, Erdman DD, Carper H, et al. High titers of IgE antibody to dust mite allergen and risk for wheezing among asthmatic children infected with rhinovirus. *J Allergy Clin Immunol.* 2012 Jun 1;129(6):1499-1505.e5.

7. Heymann PW, Kennedy JL. Rhinovirus-induced asthma exacerbations during childhood: The importance of understanding the atopic status of the host. *J Allergy Clin Immunol*. 2012 Dec 1;130(6):1315–6.
8. Cox DW, Bizzintino J, Ferrari G, Khoo SK, Zhang G, Whelan S, et al. Human Rhinovirus Species C Infection in Young Children with Acute Wheeze Is Associated with Increased Acute Respiratory Hospital Admissions. *Am J Respir Crit Care Med*. 2013 Aug 30;188(11):1358–64.
9. Agrawal R, Wisniewski J, Yu MD, Kennedy JL, Platts-Mills T, Heymann PW, et al. Infection with human rhinovirus 16 promotes enhanced IgE responsiveness in basophils of atopic asthmatics. *Clin Exp Allergy*. 2014;44(10):1266–73.
10. Zhu J, Message SD, Qiu Y, Mallia P, Kebabze T, Contoli M, et al. Airway inflammation and illness severity in response to experimental rhinovirus infection in asthma. *Chest*. 2014 Jun 1;145(6):1219–29.
11. Lemanske Jr. RF, Jackson DJ, Gangnon RE, Evans MD, Li Z, Shult PA, et al. Rhinovirus illnesses during infancy predict subsequent childhood wheezing. *J Allergy Clin Immunol*. 2005 Sep;116(3):571–7.
12. O'Callaghan-Gordo C, Bassat Q, Díez-Padrisa N, Morais L, Machevo S, Nhampossa T, et al. Lower Respiratory Tract Infections Associated with Rhinovirus during Infancy and Increased Risk of Wheezing during Childhood. A Cohort Study. *PLoS ONE*. 2013 Jul 31;8(7):e69370.

13. Rajewsky K. Clonal selection and learning in the antibody system. *Nature*. 1996 Jun;381(6585):751.
14. Edelman GM. Antibody Structure and Molecular Immunology. *Science*. 1973;180(4088):830–40.
15. Breman JG, Henderson DA. Diagnosis and Management of Smallpox. *N Engl J Med*. 2002 Apr 25;346(17):1300–8.
16. Faber C, Shan L, Fan Z, Guddat LW, Furebring C, Ohlin M, et al. Three-dimensional structure of a human Fab with high affinity for tetanus toxoid1The coordinates of B7-15A2 are available from the Brookhaven Protein Data Bank using ID code 1AQK.1. *Immunotechnology*. 1998 Jan 1;3(4):253–70.
17. Saphire EO, Parren PWHI, Pantophlet R, Zwick MB, Morris GM, Rudd PM, et al. Crystal Structure of a Neutralizing Human IgG Against HIV-1: A Template for Vaccine Design. *Science*. 2001 Aug 10;293(5532):1155–9.
18. Goodnow CC, Sprent J, de St Groth BF, Vinuesa CG. Cellular and genetic mechanisms of self tolerance and autoimmunity. *Nature*. 2005 Jun 1;435:590–7.
19. Jacob J, Kelsoe G, Rajewsky K, Weiss U. Intraclonal generation of antibody mutants in germinal centres. *Nature*. 1991 Dec;354(6352):389.
20. Odegard VH, Schatz DG. Targeting of somatic hypermutation. *Nat Rev Immunol*. 2006 Aug;6(8):573–83.

21. Okada T, Cyster JG. B cell migration and interactions in the early phase of antibody responses. *Curr Opin Immunol*. 2006 Jun 1;18(3):278–85.
22. Phan TG, Gray EE, Cyster JG. The microanatomy of B cell activation. *Curr Opin Immunol*. 2009 Jun 1;21(3):258–65.
23. Schwickert TA, Victora GD, Fooksman DR, Kamphorst AO, Mugnier MR, Gitlin AD, et al. A dynamic T cell–limited checkpoint regulates affinity-dependent B cell entry into the germinal center. *J Exp Med*. 2011 Jun 6;208(6):1243–52.
24. Parker DC. T Cell-Dependent B Cell Activation. *Annu Rev Immunol*. 1993;11(1):331–60.
25. Victora GD, Nussenzweig MC. Germinal Centers. *Annu Rev Immunol*. 2012;30(1):429–57.
26. Shulman Z, Gitlin AD, Targ S, Jankovic M, Pasqual G, Nussenzweig MC, et al. T Follicular Helper Cell Dynamics in Germinal Centers. *Science*. 2013 Aug 9;341(6146):673–7.
27. Sciammas R, Davis MM. Blimp-1; Immunoglobulin Secretion and the Switch to Plasma Cells. Singh H, Grosschedl R, editors. *Mol Anal B Lymph Dev Act*. 2005;290:201–24.
28. Shapiro-Shelef M, Calame K. Regulation of plasma-cell development. *Nat Rev Immunol*. 2005 Mar;5(3):230–42.

29. Moser K, Tokoyoda K, Radbruch A, MacLennan I, Manz RA. Stromal niches, plasma cell differentiation and survival. *Curr Opin Immunol*. 2006 Jun 1;18(3):265–70.
30. Brandtzaeg P. Role of secretory antibodies in the defence against infections. *Int J Med Microbiol*. 2003 Jan 1;293(1):3–15.
31. Karakawa WW, Sutton A, Schneerson R, Karpas A, Vann WF. Capsular antibodies induce type-specific phagocytosis of capsulated *Staphylococcus aureus* by human polymorphonuclear leukocytes. *Infect Immun*. 1988 May 1;56(5):1090–5.
32. Ravetch JV, Clynes RA. DIVERGENT ROLES FOR Fc RECEPTORS AND COMPLEMENT IN VIVO. *Annu Rev Immunol*. 1998;16(1):421–32.
33. Ravetch JV, Bolland S. IgG Fc Receptors. *Annu Rev Immunol*. 2001;19(1):275–90.
34. Dahlgren C, Karlsson A. Respiratory burst in human neutrophils. *J Immunol Methods*. 1999 Dec 17;232(1):3–14.
35. Bogdan C, Röllinghoff M, Diefenbach A. Reactive oxygen and reactive nitrogen intermediates in innate and specific immunity. *Curr Opin Immunol*. 2000 Feb 1;12(1):64–76.
36. Busslinger M. Transcriptional Control of Early B Cell Development. *Annu Rev Immunol*. 2004;22(1):55–79.

37. Hozumi N, Tonegawa S. Evidence for somatic rearrangement of immunoglobulin genes coding for variable and constant regions. *Proc Natl Acad Sci U S A*. 1976 Oct;73(10):3628–32.
38. Weigert M, Perry R, Kelley D, Hunkapiller T, Schilling J, Hood L. The joining of V and J gene segments creates antibody diversity. *Nature*. 1980 Jan;283(5746):497.
39. Agrawal A, Schatz DG. RAG1 and RAG2 Form a Stable Postcleavage Synaptic Complex with DNA Containing Signal Ends in V(D)J Recombination. *Cell*. 1997 Apr 4;89(1):43–53.
40. Jung D, Giallourakis C, Mostoslavsky R, Alt FW. Mechanism and Control of V(d)j Recombination at the Immunoglobulin Heavy Chain Locus. *Annu Rev Immunol*. 2006;24(1):541–70.
41. Komori T, Okada A, Stewart V, Alt FW. Lack of N regions in antigen receptor variable region genes of TdT-deficient lymphocytes. *Science*. 1993 Aug 27;261(5125):1171–5.
42. Gauss GH, Lieber MR. Mechanistic constraints on diversity in human V(D)J recombination. *Mol Cell Biol*. 1996 Jan 1;16(1):258–69.
43. Strasser A, Bouillet P. The control of apoptosis in lymphocyte selection. *Immunol Rev*. 2003;193(1):82–92.

44. Grawunder U, Leu TMJ, Schatz DG, Werner A, Rolink AG, Melchers F, et al. Down-regulation of RAG1 and RAG2 gene expression in PreB cells after functional immunoglobulin heavy chain rearrangement. *Immunity*. 1995 Nov 1;3(5):601–8.
45. Monroe JG. ITAM-mediated tonic signalling through pre-BCR and BCR complexes. *Nat Rev Immunol*. 2006 Apr;6(4):283–94.
46. Bankovich AJ, Raunser S, Juo ZS, Walz T, Davis MM, Garcia KC. Structural Insight into Pre-B Cell Receptor Function. *Science*. 2007 Apr 13;316(5822):291–4.
47. Melamed D, Benschop RJ, Cambier JC, Nemazee D. Developmental Regulation of B Lymphocyte Immune Tolerance Compartmentalizes Clonal Selection from Receptor Selection. *Cell*. 1998 Jan 23;92(2):173–82.
48. Casellas R, Shih T-AY, Kleinewietfeld M, Rakonjac J, Nemazee D, Rajewsky K, et al. Contribution of Receptor Editing to the Antibody Repertoire. *Science*. 2001 Feb 23;291(5508):1541–4.
49. Ansel KM, Cyster JG. Chemokines in lymphopoiesis and lymphoid organ development. *Curr Opin Immunol*. 2001 Apr 1;13(2):172–9.
50. Cyster JG, Ansel KM, Reif K, Ekland EH, Hyman PL, Tang HL, et al. Follicular stromal cells and lymphocyte homing to follicles. *Immunol Rev*. 2000 Aug;176:181–93.
51. Cyster JG. Chemokines, Sphingosine-1-Phosphate, and Cell Migration in Secondary Lymphoid Organs. *Annu Rev Immunol*. 2005;23(1):127–59.

52. Rosen H, Goetzl EJ. Sphingosine 1-phosphate and its receptors: an autocrine and paracrine network. *Nat Rev Immunol*. 2005 Jul;5(7):560–70.
53. Spiegel S, Milstien S. The outs and the ins of sphingosine-1-phosphate in immunity. *Nat Rev Immunol*. 2011 Jun;11(6):403–15.
54. Bekeredjian-Ding I, Jego G. Toll-like receptors – sentries in the B-cell response. *Immunology*. 2009;128(3):311–23.
55. Defranco AL, Richards JD, Blum JH, Stevens TL, Law DA, Chan VW-F, et al. Signal Transduction by the B-Cell Antigen Receptor. *Ann N Y Acad Sci*. 1995;766(1):195–201.
56. Kurosaki T. Functional dissection of BCR signaling pathways. *Curr Opin Immunol*. 2000 Jun 1;12(3):276–81.
57. Shaw AS, Filbert EL. Scaffold proteins and immune-cell signalling. *Nat Rev Immunol*. 2009 Jan;9(1):47–56.
58. Mond JJ, Lees A, Snapper CM. T Cell-Independent Antigens Type 2. *Annu Rev Immunol*. 1995;13(1):655–92.
59. Fagarasan S, Honjo T. T-Independent Immune Response: New Aspects of B Cell Biology. *Science*. 2000 Oct 6;290(5489):89–92.
60. Cambier JC, Pleiman CM, Clark MR. Signal Transduction by the B Cell Antigen Receptor and its Coreceptors. *Annu Rev Immunol*. 1994;12(1):457–86.

61. Garside P, Ingulli E, Merica RR, Johnson JG, Noelle RJ, Jenkins MK. Visualization of Specific B and T Lymphocyte Interactions in the Lymph Node. *Science*. 1998 Jul 3;281(5373):96–9.
62. Nishioka Y, Lipsky PE. The role of CD40-CD40 ligand interaction in human T cell-B cell collaboration. *J Immunol*. 1994 Aug 1;153(3):1027–36.
63. Cahalan MD, Parker I. Close encounters of the first and second kind: T–DC and T–B interactions in the lymph node. *Semin Immunol*. 2005 Dec 1;17(6):442–51.
64. Goding JW, Scott DW, Layton JE. Genetics, Cellular Expression and Function of IgD and IgM Receptors. *Immunol Rev*. 1977;37(1):152–80.
65. Blattner FR, Tucker PW. The molecular biology of immunoglobulin D. *Nature*. 1984 Feb;307(5950):417.
66. Abney ER, Cooper MD, Kearney JF, Lawton AR, Parkhouse RME. Sequential Expression of Immunoglobulin on Developing Mouse B Lymphocytes: A Systematic Survey That Suggests a Model for the Generation of Immunoglobulin Isotype Diversity. *J Immunol*. 1978 Jun 1;120(6):2041–9.
67. Xu Z, Zan H, Pone EJ, Mai T, Casali P. Immunoglobulin class-switch DNA recombination: induction, targeting and beyond. *Nat Rev Immunol*. 2012 Jul;12(7):517–31.

68. Ettinger R, Sims GP, Fairhurst A-M, Robbins R, Silva YS da, Spolski R, et al. IL-21 Induces Differentiation of Human Naive and Memory B Cells into Antibody-Secreting Plasma Cells. *J Immunol.* 2005 Dec 15;175(12):7867–79.
69. Kuchen S, Robbins R, Sims GP, Sheng C, Phillips TM, Lipsky PE, et al. Essential Role of IL-21 in B Cell Activation, Expansion, and Plasma Cell Generation during CD4<sup>+</sup> T Cell-B Cell Collaboration. *J Immunol.* 2007 Nov 1;179(9):5886–96.
70. Muramatsu M, Kinoshita K, Fagarasan S, Yamada S, Shinkai Y, Honjo T. Class Switch Recombination and Hypermutation Require Activation-Induced Cytidine Deaminase (AID), a Potential RNA Editing Enzyme. *Cell.* 2000 Sep 1;102(5):553–63.
71. Bransteitter R, Pham P, Scharff MD, Goodman MF. Activation-induced cytidine deaminase deaminates deoxycytidine on single-stranded DNA but requires the action of RNase. *Proc Natl Acad Sci.* 2003 Apr 1;100(7):4102–7.
72. Chaudhuri J, Alt FW. Class-switch recombination: interplay of transcription, DNA deamination and DNA repair. *Nat Rev Immunol.* 2004 Jul;4(7):541–52.
73. Sakano H, Maki R, Kurosawa Y, Roeder W, Tonegawa S. Two types of somatic recombination are necessary for the generation of complete immunoglobulin heavy-chain genes. *Nature.* 1980 Aug;286(5774):676.

74. Shinkura R, Tian M, Smith M, Chua K, Fujiwara Y, Alt FW. The influence of transcriptional orientation on endogenous switch region function. *Nat Immunol*. 2003 May;4(5):435–41.
75. Davies DR, Metzger H. Structural Basis of Antibody Function. *Annu Rev Immunol*. 1983;1(1):87–115.
76. Niles MJ, Matsuuchi L, Koshland ME. Polymer IgM assembly and secretion in lymphoid and nonlymphoid cell lines: evidence that J chain is required for pentamer IgM synthesis. *Proc Natl Acad Sci*. 1995 Mar 28;92(7):2884–8.
77. Nesargikar PN, Spiller B, Chavez R. The complement system: history, pathways, cascade and inhibitors. *Eur J Microbiol Immunol*. 2012 Jun;2(2):103–11.
78. Hadders MA, Beringer DX, Gros P. Structure of C8 $\alpha$ -MACPF Reveals Mechanism of Membrane Attack in Complement Immune Defense. *Science*. 2007 Sep 14;317(5844):1552–4.
79. Tarlinton D, Good-Jacobson K. Diversity Among Memory B Cells: Origin, Consequences, and Utility. *Science*. 2013 Sep 13;341(6151):1205–11.
80. Rubtsova K, Rubtsov AV, Dyk LF van, Kappler JW, Marrack P. T-box transcription factor T-bet, a key player in a unique type of B-cell activation essential for effective viral clearance. *Proc Natl Acad Sci*. 2013 Aug 20;110(34):E3216–24.

81. Barnett BE, Staupe RP, Odorizzi PM, Palko O, Tomov VT, Mahan AE, et al. Cutting Edge: B Cell–Intrinsic T-bet Expression Is Required To Control Chronic Viral Infection. *J Immunol*. 2016 Jul 18;1500368.
82. Branzk N, Lubojemska A, Hardison SE, Wang Q, Gutierrez MG, Brown GD, et al. Neutrophils sense microbe size and selectively release neutrophil extracellular traps in response to large pathogens. *Nat Immunol*. 2014 Nov;15(11):1017–25.
83. Wu LC, Zarrin AA. The production and regulation of IgE by the immune system. *Nat Rev Immunol*. 2014 Apr;14(4):247–59.
84. Sutton BJ, Gould HJ. The human IgE network. *Nature*. 1993 Dec;366(6454):421.
85. Kasugai T, Okada M, Morimoto M, Arizono N, Maeyama K, Yamada M, et al. Infection of *Nippostrongylus brasiliensis* induces normal increase of basophils in mast cell-deficient *Ws/Ws* rats with a small deletion at the kinase domain of *c-kit*. *Blood*. 1993 May 15;81(10):2521–9.
86. Hogan SP, Rosenberg HF, Moqbel R, Phipps S, Foster PS, Lacy P, et al. Eosinophils: Biological Properties and Role in Health and Disease. *Clin Exp Allergy*. 2008;38(5):709–50.
87. Mostov KE. Transepithelial Transport of Immunoglobulins. *Annu Rev Immunol*. 1994;12(1):63–84.

88. Hendrickson BA, Conner DA, Ladd DJ, Kendall D, Casanova JE, Corthesy B, et al. Altered hepatic transport of immunoglobulin A in mice lacking the J chain. *J Exp Med*. 1995 Dec 1;182(6):1905–11.
89. Lamm ME. IV. How epithelial transport of IgA antibodies relates to host defense. *Am J Physiol-Gastrointest Liver Physiol*. 1998 Apr 1;274(4):G614–7.
90. Suzuki K, Meek B, Doi Y, Muramatsu M, Chiba T, Honjo T, et al. Aberrant expansion of segmented filamentous bacteria in IgA-deficient gut. *Proc Natl Acad Sci*. 2004 Feb 17;101(7):1981–6.
91. Corthesy B. Multi-Faceted Functions of Secretory IgA at Mucosal Surfaces. *Front Immunol* [Internet]. 2013 [cited 2019 Apr 20];4. Available from: <https://www.frontiersin.org/articles/10.3389/fimmu.2013.00185/full>
92. Pham P, Bransteitter R, Petruska J, Goodman MF. Processive AID-catalysed cytosine deamination on single-stranded DNA simulates somatic hypermutation. *Nature*. 2003 Jul;424(6944):103–7.
93. Basu U, Chaudhuri J, Alpert C, Dutt S, Ranganath S, Li G, et al. The AID antibody diversification enzyme is regulated by protein kinase A phosphorylation. *Nature*. 2005 Nov;438(7067):508–11.

94. Godoy-Lozano EE, Téllez-Sosa J, Sánchez-González G, Sámano-Sánchez H, Aguilar-Salgado A, Salinas-Rodríguez A, et al. Lower IgG somatic hypermutation rates during acute dengue virus infection is compatible with a germinal center-independent B cell response. *Genome Med.* 2016 Feb 25;8:23.
95. Kitaura K, Yamashita H, Ayabe H, Shini T, Matsutani T, Suzuki R. Different Somatic Hypermutation Levels among Antibody Subclasses Disclosed by a New Next-Generation Sequencing-Based Antibody Repertoire Analysis. *Front Immunol.* 2017;8:389.
96. Gitlin AD, Shulman Z, Nussenzweig MC. Clonal selection in the germinal center by regulated proliferation and hypermutation. *Nature.* 2014 May 29;509(7502):637–40.
97. Silver J, Zuo T, Chaudhary N, Kumari R, Tong P, Giguere S, et al. Stochasticity enables BCR-independent germinal center initiation and antibody affinity maturation. *J Exp Med.* 2017 Dec 15;
98. McKean D, Huppi K, Bell M, Staudt L, Gerhard W, Weigert M. Generation of antibody diversity in the immune response of BALB/c mice to influenza virus hemagglutinin. *Proc Natl Acad Sci.* 1984 May 1;81(10):3180–4.
99. Crotty S. Follicular helper CD4 T cells (TFH). *Annu Rev Immunol.* 2011;29:621–63.

100. Lee SK, Rigby RJ, Zotos D, Tsai LM, Kawamoto S, Marshall JL, et al. B cell priming for extrafollicular antibody responses requires Bcl-6 expression by T cells. *J Exp Med*. 2011 Jul 4;208(7):1377–88.
101. Breitfeld D, Ohi L, Kremmer E, Ellwart J, Sallusto F, Lipp M, et al. Follicular B Helper T Cells Express Cxc Chemokine Receptor 5, Localize to B Cell Follicles, and Support Immunoglobulin Production. *J Exp Med*. 2000 Dec 4;192(11):1545–52.
102. Locci M, Havenar-Daughton C, Landais E, Wu J, Kroenke MA, Arlehamn CL, et al. Human Circulating PD-1+CXCR3–CXCR5+ Memory Tfh Cells Are Highly Functional and Correlate with Broadly Neutralizing HIV Antibody Responses. *Immunity*. 2013 Oct 17;39(4):758–69.
103. Shulman Z, Gitlin AD, Weinstein JS, Lainez B, Esplugues E, Flavell RA, et al. Dynamic signaling by T follicular helper cells during germinal center B cell selection. *Science*. 2014 Aug 29;345(6200):1058–62.
104. Liu D, Xu H, Shih C, Wan Z, Ma X, Ma W, et al. T-B-cell entanglement and ICOSL-driven feed-forward regulation of germinal centre reaction. *Nature*. 2015 Jan 8;517(7533):214–8.
105. Pratama A, Vinuesa CG. Control of TFH cell numbers: why and how? *Immunol Cell Biol*. 2014 Jan;92(1):40–8.
106. Elsner RA, Ernst DN, Baumgarth N. Single and Coexpression of CXCR4 and CXCR5 Identifies CD4 T Helper Cells in Distinct Lymph Node Niches during Influenza Virus Infection. *J Virol*. 2012 Jul 1;86(13):7146–57.

107. Cubas RA, Mudd JC, Savoye A-L, Perreau M, van Grevenynghe J, Metcalf T, et al. Inadequate T follicular cell help impairs B cell immunity during HIV infection. *Nat Med*. 2013 Apr;19(4):494–9.
108. Boswell KL, Paris R, Boritz E, Ambrozak D, Yamamoto T, Darko S, et al. Loss of Circulating CD4 T Cells with B Cell Helper Function during Chronic HIV Infection. *PLoS Pathog*. 2014 Jan 30;10(1):e1003853.
109. Yamamoto T, Lynch RM, Gautam R, Matus-Nicodemos R, Schmidt SD, Boswell KL, et al. Quality and quantity of TFH cells are critical for broad antibody development in SHIVAD8 infection. *Sci Transl Med*. 2015 Jul 29;7(298):298ra120-298ra120.
110. Ma CS, Deenick EK, Batten M, Tangye SG. The origins, function, and regulation of T follicular helper cells. *J Exp Med*. 2012 Jul 2;209(7):1241–53.
111. Shekhar S, Yang X. The darker side of follicular helper T cells: from autoimmunity to immunodeficiency. *Cell Mol Immunol*. 2012 Sep;9(5):380–5.
112. Crotty S. T Follicular Helper Cell Differentiation, Function, and Roles in Disease. *Immunity*. 2014 Oct 16;41(4):529–42.
113. Nurieva RI, Chung Y, Hwang D, Yang XO, Kang HS, Ma L, et al. Generation of T Follicular Helper Cells Is Mediated by Interleukin-21 but Independent of T Helper 1, 2, or 17 Cell Lineages. *Immunity*. 2008 Jul 18;29(1):138–49.

114. Morita R, Schmitt N, Bentebibel S-E, Ranganathan R, Bourdery L, Zurawski G, et al. Human Blood CXCR5+CD4+ T Cells Are Counterparts of T Follicular Cells and Contain Specific Subsets that Differentially Support Antibody Secretion. *Immunity*. 2011 Jan 28;34(1):108–21.
115. Hale JS, Youngblood B, Latner DR, Mohammed AUR, Ye L, Akondy RS, et al. Distinct Memory CD4+ T Cells with Commitment to T Follicular Helper- and T Helper 1-Cell Lineages Are Generated after Acute Viral Infection. *Immunity*. 2013 Apr 18;38(4):805–17.
116. Dullaers M, Li D, Xue Y, Ni L, Gayet I, Morita R, et al. A T Cell-Dependent Mechanism for the Induction of Human Mucosal Homing Immunoglobulin A-Secreting Plasmablasts. *Immunity*. 2009 Jan 16;30(1):120–9.
117. Kemeny DM. The role of the T follicular helper cells in allergic disease. *Cell Mol Immunol*. 2012 Sep;9(5):386–9.
118. de Wit J, Jorritsma T, Makuch M, Remmerswaal EBM, Klaasse Bos H, Souwer Y, et al. Human B cells promote T-cell plasticity to optimize antibody response by inducing coexpression of TH1/TFH signatures. *J Allergy Clin Immunol*. 2015 Apr;135(4):1053–60.
119. Wong MT, Chen J, Narayanan S, Lin W, Anicete R, Kiaang HTK, et al. Mapping the Diversity of Follicular Helper T Cells in Human Blood and Tonsils Using High-Dimensional Mass Cytometry Analysis. *Cell Rep*. 2015 Jun 23;11(11):1822–33.

120. Gigoux M, Shang J, Pak Y, Xu M, Choe J, Mak TW, et al. Inducible costimulator promotes helper T-cell differentiation through phosphoinositide 3-kinase. *Proc Natl Acad Sci*. 2009 Dec 1;106(48):20371–6.
121. Warnatz K, Bossaller L, Salzer U, Skrabl-Baumgartner A, Schwinger W, Burg M van der, et al. Human ICOS deficiency abrogates the germinal center reaction and provides a monogenic model for common variable immunodeficiency. *Blood*. 2006 Apr 15;107(8):3045–52.
122. Choi YS, Kageyama R, Eto D, Escobar TC, Johnston RJ, Monticelli L, et al. ICOS Receptor Instructs T Follicular Helper Cell versus Effector Cell Differentiation via Induction of the Transcriptional Repressor Bcl6. *Immunity*. 2011 Jun 24;34(6):932–46.
123. Good-Jacobson KL, Szumilas CG, Chen L, Sharpe AH, Tomayko MM, Shlomchik MJ. PD-1 regulates germinal center B cell survival and the formation and affinity of long-lived plasma cells. *Nat Immunol*. 2010 Jun;11(6):535–42.
124. Pesu M, Candotti F, Husa M, Hofmann SR, Notarangelo LD, O’Shea JJ. Jak3, severe combined immunodeficiency, and a new class of immunosuppressive drugs. *Immunol Rev*. 2005;203(1):127–42.
125. Johnston RJ, Poholek AC, DiToro D, Yusuf I, Eto D, Barnett B, et al. Bcl6 and Blimp-1 Are Reciprocal and Antagonistic Regulators of T Follicular Helper Cell Differentiation. *Science*. 2009 Aug 21;325(5943):1006–10.

126. Liu X, Chen X, Zhong B, Wang A, Wang X, Chu F, et al. Transcription factor achaete-scute homologue 2 initiates follicular T-helper-cell development. *Nature*. 2014 Mar 27;507(7493):513–8.
127. Xiao N, Eto D, Elly C, Peng G, Crotty S, Liu Y-C. The E3 ubiquitin ligase Itch is required for the differentiation of follicular helper T cells. *Nat Immunol*. 2014 Jul;15(7):657–66.
128. Weber JP, Fuhrmann F, Feist RK, Lahmann A, Baz MSA, Gentz L-J, et al. ICOS maintains the T follicular helper cell phenotype by down-regulating Krüppel-like factor 2. *J Exp Med*. 2015 Feb 9;212(2):217–33.
129. Stone EL, Pepper M, Katayama CD, Kerdiles YM, Lai C-Y, Emslie E, et al. ICOS Coreceptor Signaling Inactivates the Transcription Factor FOXO1 to Promote Tfh Cell Differentiation. *Immunity*. 2015 Feb 17;42(2):239–51.
130. Lee J-Y, Skon CN, Lee YJ, Oh S, Taylor JJ, Malhotra D, et al. The Transcription Factor KLF2 Restrains CD4+ T Follicular Helper Cell Differentiation. *Immunity*. 2015 Feb 17;42(2):252–64.
131. Bentebibel S-E, Lopez S, Obermoser G, Schmitt N, Mueller C, Harrod C, et al. Induction of ICOS+CXCR3+CXCR5+ TH Cells Correlates with Antibody Responses to Influenza Vaccination. *Sci Transl Med*. 2013 Mar 13;5(176):176ra32-176ra32.

132. He J, Tsai LM, Leong YA, Hu X, Ma CS, Chevalier N, et al. Circulating Precursor CCR7<sup>lo</sup>PD-1<sup>hi</sup> CXCR5<sup>+</sup> CD4<sup>+</sup> T Cells Indicate Tfh Cell Activity and Promote Antibody Responses upon Antigen Reexposure. *Immunity*. 2013 Oct 17;39(4):770–81.
133. Herati RS, Reuter MA, Dolfi DV, Mansfield KD, Aung H, Badwan OZ, et al. Circulating CXCR5<sup>+</sup>PD-1<sup>+</sup> Response Predicts Influenza Vaccine Antibody Responses in Young Adults but not Elderly Adults. *J Immunol*. 2014 Oct 1;193(7):3528–37.
134. Schmitt N, Ueno H. Blood Tfh Cells Come with Colors. *Immunity*. 2013 Oct 17;39(4):629–30.
135. Schmitt N, Liu Y, Bentebibel S-E, Munagala I, Bourdery L, Venuprasad K, et al. The cytokine TGF- $\beta$  co-opts signaling via STAT3-STAT4 to promote the differentiation of human T<sub>FH</sub> cells. *Nat Immunol*. 2014 Sep;15(9):856–65.
136. Marshall HD, Ray JP, Laidlaw BJ, Zhang N, Gawande D, Staron MM, et al. The transforming growth factor beta signaling pathway is critical for the formation of CD4 T follicular helper cells and isotype-switched antibody responses in the lung mucosa. *eLife*. 2015 Feb 3;4:e04851.
137. Schmitt N, Ueno H. Regulation of human helper T cell subset differentiation by cytokines. *Curr Opin Immunol*. 2015 Jun;34:130–6.

138. Weisel FJ, Zuccarino-Catania GV, Chikina M, Shlomchik MJ. A Temporal Switch in the Germinal Center Determines Differential Output of Memory B and Plasma Cells. *Immunity*. 2016 Jan 19;44(1):116–30.
139. Suan D, Sundling C, Brink R. Plasma cell and memory B cell differentiation from the germinal center. *Curr Opin Immunol*. 2017 Apr 1;45:97–102.
140. Tangye SG, Tarlinton DM. Memory B cells: Effectors of long-lived immune responses. *Eur J Immunol*. 2009 Aug 1;39(8):2065–75.
141. Wang Z, Karras JG, Howard RG, Rothstein TL. Induction of bcl-x by CD40 engagement rescues slg-induced apoptosis in murine B cells. *J Immunol*. 1995 Oct 15;155(8):3722–5.
142. Deenick EK, Avery DT, Chan A, Berglund LJ, Ives ML, Moens L, et al. Naive and memory human B cells have distinct requirements for STAT3 activation to differentiate into antibody-secreting plasma cells. *J Exp Med*. 2013 Nov 18;210(12):2739–53.
143. Hu C-CA, Dougan SK, McGehee AM, Love JC, Ploegh HL. XBP-1 regulates signal transduction, transcription factors and bone marrow colonization in B cells. *EMBO J*. 2009 Jun 3;28(11):1624–36.
144. Early P, Rogers J, Davis M, Calame K, Bond M, Wall R, et al. Two mRNAs can be produced from a single immunoglobulin  $\mu$  gene by alternative RNA processing pathways. *Cell*. 1980 Jun 1;20(2):313–9.

145. Pinto D, Montani E, Bolli M, Garavaglia G, Sallusto F, Lanzavecchia A, et al. A functional BCR in human IgA and IgM plasma cells. *Blood*. 2013 May 16;121(20):4110–4.
146. Cocco M, Stephenson S, Care MA, Newton D, Barnes NA, Davison A, et al. In Vitro Generation of Long-lived Human Plasma Cells. *J Immunol*. 2012 Dec 15;189(12):5773–85.
147. HORST A, HUNZELMANN N, ARCE S, HERBER M, MANZ RA, RADBRUCH A, et al. Detection and characterization of plasma cells in peripheral blood: correlation of IgE+ plasma cell frequency with IgE serum titre. *Clin Exp Immunol*. 2002 Dec;130(3):370–8.
148. Manz RA, Thiel A, Radbruch A. Lifetime of plasma cells in the bone marrow. *Nature*. 1997 Jul;388(6638):133–4.
149. Slifka MK, Antia R, Whitmire JK, Ahmed R. Humoral Immunity Due to Long-Lived Plasma Cells. *Immunity*. 1998 Mar 1;8(3):363–72.
150. Nguyen DC, Garimalla S, Xiao H, Kyu S, Albizua I, Galipeau J, et al. Factors of the bone marrow microniche that support human plasma cell survival and immunoglobulin secretion. *Nat Commun*. 2018 Sep 12;9(1):3698.
151. Kunkel EJ, Butcher EC. Plasma-cell homing. *Nat Rev Immunol*. 2003 Oct;3(10):822–9.

152. Seong Y, Lazarus NH, Sutherland L, Habtezion A, Abramson T, He X-S, et al. Trafficking receptor signatures define blood plasmablasts responding to tissue-specific immune challenge. *JCI Insight*. 2017 Mar 23;2:6.
153. Quách TD, Rodríguez-Zhurbenko N, Hopkins TJ, Guo X, Hernández AM, Li W, et al. Distinctions among Circulating Antibody-Secreting Cell Populations, Including B-1 Cells, in Human Adult Peripheral Blood. *J Immunol*. 2016 Feb 1;196(3):1060–9.
154. Dullaers M, Bruyne RD, Ramadani F, Gould HJ, Gevaert P, Lambrecht BN. The who, where, and when of IgE in allergic airway disease. *J Allergy Clin Immunol*. 2012 Mar 1;129(3):635–45.
155. Kurosaki T, Kometani K, Ise W. Memory B cells. *Nat Rev Immunol*. 2015 Mar;15(3):149–59.
156. Bulati M, Buffa S, Martorana A, Candore G, Lio D, Caruso C, et al. Trafficking phenotype and production of granzyme B by double negative B cells (IgG+IgD–CD27–) in the elderly. *Exp Gerontol*. 2014 Jun;54:123–9.
157. Karnell JL, Dimasi N, Karnell FG, Fleming R, Kuta E, Wilson M, et al. CD19 and CD32b Differentially Regulate Human B Cell Responsiveness. *J Immunol*. 2014 Feb 15;192(4):1480–90.
158. Hebeis BJ, Klenovsek K, Rohwer P, Ritter U, Schneider A, Mach M, et al. Activation of Virus-specific Memory B Cells in the Absence of T Cell Help. *J Exp Med*. 2004 Feb 16;199(4):593–602.

159. Ehrhardt GRA, Hsu JT, Gartland L, Leu C-M, Zhang S, Davis RS, et al. Expression of the immunoregulatory molecule FcRH4 defines a distinctive tissue-based population of memory B cells. *J Exp Med*. 2005 Sep 19;202(6):783–91.
160. Moir S, Ho J, Malaspina A, Wang W, DiPoto AC, O’Shea MA, et al. Evidence for HIV-associated B cell exhaustion in a dysfunctional memory B cell compartment in HIV-infected viremic individuals. *J Exp Med*. 2008 Aug 4;205(8):1797–805.
161. Peng SL, Szabo SJ, Glimcher LH. T-bet regulates IgG class switching and pathogenic autoantibody production. *Proc Natl Acad Sci*. 2002 Apr 16;99(8):5545–50.
162. Liu N, Ohnishi N, Ni L, Akira S, Bacon KB. CpG directly induces T-bet expression and inhibits IgG1 and IgE switching in B cells. *Nat Immunol*. 2003 Jul;4(7):687–93.
163. Rubtsova K, Rubtsov AV, Thurman JM, Mennona JM, Kappler JW, Marrack P. B cells expressing the transcription factor T-bet drive lupus-like autoimmunity. *J Clin Invest*. 2017 May 12;127(4):1392–404.
164. Frasca D, Diaz A, Romero M, D’Eramo F, Blomberg BB. Aging effects on T-bet expression in human B cell subsets. *Cell Immunol*. 2017 Nov 1;321:68–73.

165. Karnell JL, Kumar V, Wang J, Wang S, Voynova E, Ettinger R. Role of CD11c<sup>+</sup> T-bet<sup>+</sup> B cells in human health and disease. *Cell Immunol.* 2017 Nov 1;321:40–5.
166. Manni M, Gupta S, Ricker E, Chinenov Y, Park SH, Shi M, et al. Regulation of age-associated B cells by IRF5 in systemic autoimmunity. *Nat Immunol.* 2018 Apr;19(4):407–19.
167. Jenks SA, Cashman KS, Zumaquero E, Marigorta UM, Patel AV, Wang X, et al. Distinct Effector B Cells Induced by Unregulated Toll-like Receptor 7 Contribute to Pathogenic Responses in Systemic Lupus Erythematosus. *Immunity.* 2018 Oct 16;49(4):725-739.e6.
168. Knox JJ, Buggert M, Kardava L, Seaton KE, Eller MA, Canaday DH, et al. T-bet<sup>+</sup> B cells are induced by human viral infections and dominate the HIV gp140 response. *JCI Insight.* 2017 Apr 20;2:8.
169. Lau D, Lan LY-L, Andrews SF, Henry C, Rojas KT, Neu KE, et al. Low CD21 expression defines a population of recent germinal center graduates primed for plasma cell differentiation. *Sci Immunol.* 2017 Jan 27;2(7):eaai8153.
170. Sohn HW, Krueger PD, Davis RS, Pierce SK. FcRL4 acts as an adaptive to innate molecular switch dampening BCR signaling and enhancing TLR signaling. *Blood.* 2011 Dec 8;118(24):6332–41.

171. Murphy KM, Reiner SL. Decision making in the immune system: The lineage decisions of helper T cells. *Nat Rev Immunol.* 2002 Dec;2(12):933–44.
172. Szabo SJ, Sullivan BM, Peng SL, Glimcher LH. Molecular Mechanisms Regulating Th1 Immune Responses. *Annu Rev Immunol.* 2003;21(1):713–58.
173. Berberich C, Ramírez-Pineda JR, Hambrecht C, Alber G, Skeiky YAW, Moll H. Dendritic Cell (DC)-Based Protection Against an Intracellular Pathogen Is Dependent Upon DC-Derived IL-12 and Can Be Induced by Molecularly Defined Antigens. *J Immunol.* 2003 Mar 15;170(6):3171–9.
174. Russell JH, Ley TJ. Lymphocyte-Mediated Cytotoxicity. *Annu Rev Immunol.* 2002;20(1):323–70.
175. Szabo SJ, Kim ST, Costa GL, Zhang X, Fathman CG, Glimcher LH. A Novel Transcription Factor, T-bet, Directs Th1 Lineage Commitment. *Cell.* 2000 Mar 17;100(6):655–69.
176. Lazarevic V, Glimcher LH, Lord GM. T-bet: a bridge between innate and adaptive immunity. *Nat Rev Immunol.* 2013 Nov;13(11):777–89.
177. Stein JV, Nombela-Arrieta C. Chemokine control of lymphocyte trafficking: a general overview. *Immunology.* 2005 Sep;116(1):1–12.
178. Kallies A, Good-Jacobson KL. Transcription Factor T-bet Orchestrates Lineage Development and Function in the Immune System. *Trends Immunol.* 2017 Apr 1;38(4):287–97.

179. Lian J, Luster AD. Chemokine-guided cell positioning in the lymph node orchestrates the generation of adaptive immune responses. *Curr Opin Cell Biol.* 2015 Oct;36:1–6.
180. Piovesan D, Tempany J, Di Pietro A, Baas I, Yiannis C, O'Donnell K, et al. c-Myb Regulates the T-Bet-Dependent Differentiation Program in B Cells to Coordinate Antibody Responses. *Cell Rep.* 2017 Apr 18;19(3):461–70.
181. Sallusto F, Lenig D, Förster R, Lipp M, Lanzavecchia A. Two subsets of memory T lymphocytes with distinct homing potentials and effector functions. *Nature.* 1999 Oct;401(6754):708–12.
182. Sallusto F, Geginat J, Lanzavecchia A. Central Memory and Effector Memory T Cell Subsets: Function, Generation, and Maintenance. *Annu Rev Immunol.* 2004;22(1):745–63.
183. Mackay CR, Marston W, Dudler L. Altered patterns of T cell migration through lymph nodes and skin following antigen challenge. *Eur J Immunol.* 1992;22(9):2205–10.
184. Sallusto F, Kremmer E, Palermo B, Hoy A, Ponath P, Qin S, et al. Switch in chemokine receptor expression upon TCR stimulation reveals novel homing potential for recently activated T cells. *Eur J Immunol.* 1999;29(6):2037–45.
185. Schenkel JM, Masopust D. Tissue-Resident Memory T Cells. *Immunity.* 2014 Dec 18;41(6):886–97.

186. Schenkel JM, Fraser KA, Beura LK, Pauken KE, Vezys V, Masopust D. Resident memory CD8 T cells trigger protective innate and adaptive immune responses. *Science*. 2014 Oct 3;346(6205):98–101.
187. Takamura S. Persistence in Temporary Lung Niches: A Survival Strategy of Lung-Resident Memory CD8+ T Cells. *Viral Immunol*. 2017 Apr 18;30(6):438–50.
188. Lanzavecchia A, Sallusto F. Understanding the generation and function of memory T cell subsets. *Curr Opin Immunol*. 2005 Jun 1;17(3):326–32.
189. Schiött Å, Lindstedt M, Johansson-Lindbom B, Roggen E, Borrebaeck CAK. CD27– CD4+ memory T cells define a differentiated memory population at both the functional and transcriptional levels. *Immunology*. 2004 Nov 1;113(3):363–70.
190. Saule P, Trauet J, Dutriez V, Lekeux V, Dessaint J-P, Labalette M. Accumulation of memory T cells from childhood to old age: Central and effector memory cells in CD4+ versus effector memory and terminally differentiated memory cells in CD8+ compartment. *Mech Ageing Dev*. 2006 Mar 1;127(3):274–81.
191. Flather D, Semler BL. Picornaviruses and nuclear functions: targeting a cellular compartment distinct from the replication site of a positive-strand RNA virus. *Virology*. 2015;6:594.

192. Hadfield AT, Lee W, Zhao R, Oliveira MA, Minor I, Rueckert RR, et al. The refined structure of human rhinovirus 16 at 2.15 Å resolution: implications for the viral life cycle. *Structure*. 1997 Mar 15;5(3):427–41.
193. Palmenberg AC, Spiro D, Kuzmickas R, Wang S, Djikeng A, Rathe JA, et al. Sequencing and Analyses of All Known Human Rhinovirus Genomes Reveal Structure and Evolution. *Science*. 2009 Apr 3;324(5923):55–9.
194. Bochkov YA, Watters K, Ashraf S, Griggs TF, Devries MK, Jackson DJ, et al. Cadherin-related family member 3, a childhood asthma susceptibility gene product, mediates rhinovirus C binding and replication. *Proc Natl Acad Sci*. 2015 Apr 28;112(17):5485–90.
195. Fuchs R, Blaas D. Uncoating of human rhinoviruses. *Rev Med Virol*. 2010 Sep 1;20(5):281–97.
196. Newcomb DC, Sajjan U, Nanua S, Jia Y, Goldsmith AM, Bentley JK, et al. Phosphatidylinositol 3-Kinase Is Required for Rhinovirus-induced Airway Epithelial Cell Interleukin-8 Expression. *J Biol Chem*. 2005 Nov 4;280(44):36952–61.
197. Jackson DJ, Makrinioti H, Rana BMJ, Shamji BWH, Trujillo-Torralbo M-B, Footitt J, et al. IL-33–Dependent Type 2 Inflammation during Rhinovirus-induced Asthma Exacerbations In Vivo. *Am J Respir Crit Care Med*. 2014 Dec 15;190(12):1373–82.

198. Gielen V, Sykes A, Zhu J, Chan B, Macintyre J, Regamey N, et al. Increased nuclear suppressor of cytokine signaling 1 in asthmatic bronchial epithelium suppresses rhinovirus induction of innate interferons. *J Allergy Clin Immunol*. 2015 Jul;136(1):177-188.e11.
199. Fleet WF, Couch RB, Cate TR, Knight V. Homologous and Heterologous Resistance to Rhinovirus Common Cold. *Am J Epidemiol*. 1965 Sep 1;82(2):185–96.
200. Parry DE, Busse WW, Sukow KA, Dick CR, Swenson C, Gern JE. Rhinovirus-induced PBMC responses and outcome of experimental infection in allergic subjects. *J Allergy Clin Immunol*. 2000 Apr;105(4):692–8.
201. Barclay WS, al-Nakib W, Higgins PG, Tyrrell DA. The time course of the humoral immune response to rhinovirus infection. *Epidemiol Infect*. 1989 Dec;103(3):659–69.
202. Edlmayr J, Niespodziana K, Popow-Kraupp T, Krzyzanek V, Focke-Tejkl M, Blaas D, et al. Antibodies induced with recombinant VP1 from human rhinovirus exhibit cross-neutralisation. *Eur Respir J*. 2011 Jan 1;37(1):44–52.
203. Gern JE, Dick EC, Kelly EAB, Vrtis R, Klein B. Rhinovirus-Specific T Cells Recognize both Shared and Serotype-Restricted Viral Epitopes. *J Infect Dis*. 1997 May 1;175(5):1108–14.

204. Kwong PD, Mascola JR, Nabel GJ. Broadly neutralizing antibodies and the search for an HIV-1 vaccine: the end of the beginning. *Nat Rev Immunol*. 2013 Sep;13(9):693–701.
205. Fera D, Schmidt AG, Haynes BF, Gao F, Liao H-X, Kepler TB, et al. Affinity maturation in an HIV broadly neutralizing B-cell lineage through reorientation of variable domains. *Proc Natl Acad Sci*. 2014 Jul 15;111(28):10275–80.
206. Pappas L, Foglierini M, Piccoli L, Kallewaard NL, Turrini F, Silacci C, et al. Rapid development of broadly influenza neutralizing antibodies through redundant mutations. *Nature*. 2014 Dec 18;516(7531):418–22.
207. Smith SA, Derdeyn CA. A pathway to HIV-1 neutralization breadth. *Nat Med*. 2015 Nov;21(11):1246–7.
208. Wang Y, Keck Z, Saha A, Xia J, Conrad F, Lou J, et al. Affinity Maturation to Improve Human Monoclonal Antibody Neutralization Potency and Breadth against Hepatitis C Virus. *J Biol Chem*. 2011 Dec 23;286(51):44218–33.
209. O’Ryan M, Vidal R, Canto F del, Salazar JC, Montero D. Vaccines for viral and bacterial pathogens causing acute gastroenteritis: Part I: Overview, vaccines for enteric viruses and *Vibrio cholerae*. *Hum Vaccines Immunother*. 2015 Mar 4;11(3):584–600.

210. O’Ryan M, Vidal R, Canto F del, Salazar JC, Montero D. Vaccines for viral and bacterial pathogens causing acute gastroenteritis: Part II: Vaccines for Shigella, Salmonella, enterotoxigenic E. coli (ETEC) enterohemorrhagic E. coli (EHEC) and Campylobacter jejuni. *Hum Vaccines Immunother.* 2015 Mar 4;11(3):601–19.
211. Zhang W, Sack DA. Current Progress in Developing Subunit Vaccines against Enterotoxigenic Escherichia coli-Associated Diarrhea. *Clin Vaccine Immunol.* 2015 Sep 1;22(9):983–91.
212. Staneková Z, Varečková E. Conserved epitopes of influenza A virus inducing protective immunity and their prospects for universal vaccine development. *Virology.* 2010;7:351.
213. Zhao Q, Li S, Yu H, Xia N, Modis Y. Virus-like particle-based human vaccines: quality assessment based on structural and functional properties. *Trends Biotechnol.* 2013 Nov;31(11):654–63.
214. Wang K, Goodman KN, Li DY, Raffeld M, Chavez M, Cohen JI. An Herpes Simplex Virus 2 (HSV-2) gD Mutant Impaired for Neural Tropism is Superior to HSV-2 gD Subunit Vaccine to Protect Animals from Challenge with HSV-2. *J Virol.* 2015 Nov 11;JVI.01845-15.
215. Niespodziana K, Napora K, Cabauatan C, Focke-Tejkl M, Keller W, Niederberger V, et al. Misdirected antibody responses against an N-terminal epitope on human rhinovirus VP1 as explanation for recurrent RV infections. *FASEB J.* 2012 Mar 1;26(3):1001–8.

216. Niespodziana K, Cabauatan CR, Jackson DJ, Gallerano D, Trujillo-Torralbo B, del Rosario A, et al. Rhinovirus-induced VP1-specific Antibodies are Group-specific and Associated With Severity of Respiratory Symptoms. *EBioMedicine*. 2014 Nov 18;2(1):64–70.
217. Pan K. Understanding Original Antigenic Sin in Influenza with a Dynamical System. *PLoS ONE*. 2011 Aug 29;6(8):e23910.
218. St.Groth SF de, Webster RG. Disquisitions on Original Antigenic Sin: I. Evidence in Man. *J Exp Med*. 1966 Sep 1;124(3):331–45.
219. Yu JZ, Wilson JE, Wood SM, Kandolf R, Klingel K, Yang D, et al. Secondary Heterotypic Versus Homotypic Infection by Coxsackie B Group Viruses: Impact on Early and Late Histopathological Lesions and Virus Genome Prominence. *Cardiovasc Pathol*. 1999 Mar;8(2):93–102.
220. Fridman WH. Regulation of B-cell activation and antigen presentation by Fc receptors. *Curr Opin Immunol*. 1993 Jun 1;5(3):355–60.
221. Mackay M, Stanevsky A, Wang T, Aranow C, Li M, Koenig S, et al. Selective dysregulation of the FcγIIb receptor on memory B cells in SLE. *J Exp Med*. 2006 Sep 4;203(9):2157–64.
222. Kim JH, Skountzou I, Compans R, Jacob J. Original Antigenic Sin Responses to Influenza Viruses. *J Immunol*. 2009 Sep 1;183(5):3294–301.
223. Adalja AA, Henderson DA. Original Antigenic Sin and Pandemic (H1N1) 2009. *Emerg Infect Dis*. 2010 Jun;16(6):1028–9.

224. Tsai W-Y, Durbin A, Tsai J-J, Hsieh S-C, Whitehead S, Wang W-K. Complexity of neutralization antibodies against multiple dengue viral serotypes after heterotypic immunization and secondary infection revealed by in-depth analysis of cross-reactive antibodies. *J Virol*. 2015 May 13;JVI.00273-15.
225. Hartmann FJ, Simonds EF, Bendall SC. A Universal Live Cell Barcoding-Platform for Multiplexed Human Single Cell Analysis. *Sci Rep*. 2018 Jul 17;8(1):10770.
226. Balcerzak M. Noble Metals, Analytical Chemistry of. *Encycl Anal Chem*. 2015;1–29.
227. Turner R b., Woodfolk J a., Borish L, Steinke J w., Patrie J t., Muehling L m., et al. Effect of probiotic on innate inflammatory response and viral shedding in experimental rhinovirus infection – a randomised controlled trial. *Benef Microbes*. 2017 Mar 27;8(2):207–15.
228. Muehling LM, Mai DT, Kwok WW, Heymann PW, Pomés A, Woodfolk JA. Circulating Memory CD4+ T Cells Target Conserved Epitopes of Rhinovirus Capsid Proteins and Respond Rapidly to Experimental Infection in Humans. *J Immunol*. 2016 Oct 15;197(8):3214–24.
229. Muehling LM, Turner RB, Brown KB, Wright PW, Patrie JT, Lahtinen SJ, et al. Single-Cell Tracking Reveals a Role for Pre-Existing CCR5+ Memory Th1 Cells in the Control of Rhinovirus-A39 After Experimental Challenge in Humans. *J Infect Dis*. 2018 Jan 17;217(3):381–92.

230. Gwaltney J, Colonno R, Hamparian V, Turner R. Rhinovirus. In: Schmidt N, Emmons R, editors. *Diagnostic Procedures for Viral, Rickettsial, and Chlamydial Infections*. 6th ed. Washington, DC: American Public Health Association; 1989. p. 579–614.
231. Turner RB, Weingand KW, Yeh C-H, Leedy DW. Association between Interleukin-8 Concentration in Nasal Secretions and Severity of Symptoms of Experimental Rhinovirus Colds. *Clin Infect Dis*. 1998;26(4):840–6.
232. Lee W-M, Chen Y, Wang W, Mosser A. Growth of Human Rhinovirus in H1-HeLa Cell Suspension Culture and Purification of Virions. Jans DA, Ghildyal R, editors. *Rhinoviruses Methods Protoc*. 2015;1221:49–61.
233. Mei HE, Leipold MD, Maecker HT. Platinum-conjugated antibodies for application in mass cytometry. *Cytometry A*. 2016;89(3):292–300.
234. Zunder ER, Finck R, Behbehani GK, Amir ED, Krishnaswamy S, Gonzalez VD, et al. Palladium-based mass tag cell barcoding with a doublet-filtering scheme and single-cell deconvolution algorithm. *Nat Protoc*. 2015 Feb;10(2):316–33.
235. Mei HE, Leipold MD, Schulz AR, Chester C, Maecker HT. Barcoding of Live Human Peripheral Blood Mononuclear Cells for Multiplexed Mass Cytometry. *J Immunol*. 2015 Feb 15;194(4):2022–31.
236. Maaten L van der, Hinton G. Visualizing Data using t-SNE. *J Mach Learn Res*. 2008;9(Nov):2579–605.

237. Nowicka M, Krieg C, Weber LM, Hartmann FJ, Guglietta S, Becher B, et al. CyTOF workflow: differential discovery in high-throughput high-dimensional cytometry datasets. *F1000Research*. 2017 May 26;6:748.
238. Gassen SV, Callebaut B, Helden MJV, Lambrecht BN, Demeester P, Dhaene T, et al. FlowSOM: Using self-organizing maps for visualization and interpretation of cytometry data. *Cytometry A*. 2015 Jul 1;87(7):636–45.
239. Wilkerson MD, Hayes DN. ConsensusClusterPlus: a class discovery tool with confidence assessments and item tracking. *Bioinformatics*. 2010 Jun 15;26(12):1572–3.
240. Weber LM, Robinson MD. Comparison of clustering methods for high-dimensional single-cell flow and mass cytometry data. *Cytometry A*. 2016;89(12):1084–96.
241. Karahan GE, Eikmans M, Anholts JDH, Claas FHJ, Heidt S. Polyclonal B cell activation for accurate analysis of pre-existing antigen-specific memory B cells. *Clin Exp Immunol*. 2014 Jul;177(1):333–40.
242. Wang S, Wang J, Kumar V, Karnell JL, Naiman B, Gross PS, et al. IL-21 drives expansion and plasma cell differentiation of autoreactive CD11c<sup>hi</sup> T-bet<sup>+</sup> B cells in SLE. *Nat Commun*. 2018 May 1;9(1):1758.
243. Li H, Borrego F, Nagata S, Tolnay M. Fc Receptor-like 5 Expression Distinguishes Two Distinct Subsets of Human Circulating Tissue-like Memory B Cells. *J Immunol*. 2016 May 15;196(10):4064–74.

244. Megremis S, Niespodziana K, Cabauatan C, Xepapadaki P, Kowalski ML, Jartti T, et al. Rhinovirus Species–Specific Antibodies Differentially Reflect Clinical Outcomes in Health and Asthma. *Am J Respir Crit Care Med*. 2018 Aug 22;198(12):1490–9.
245. Doi H, Tanoue S, Kaplan DE. Peripheral CD27–CD21– B-cells represent an exhausted lymphocyte population in hepatitis C cirrhosis. *Clin Immunol*. 2014 Feb 1;150(2):184–91.
246. Lanzavecchia A, Parodi B, Celada F. Activation of human B lymphocytes: frequency of antigen-specific B cells triggered by alloreactive or by antigen-specific T cell clones. *Eur J Immunol*. 1983 Jan 1;13(9):733–8.
247. Doria-Rose NA, Klein RM, Manion MM, O’Dell S, Phogat A, Chakrabarti B, et al. Frequency and Phenotype of Human Immunodeficiency Virus Envelope-Specific B Cells from Patients with Broadly Cross-Neutralizing Antibodies. *J Virol*. 2009 Jan 1;83(1):188–99.
248. Franz B, May KF, Dranoff G, Wucherpfennig K. Ex vivo characterization and isolation of rare memory B cells with antigen tetramers. *Blood*. 2011 Jul 14;118(2):348–57.
249. Rouers A, Klingler J, Su B, Samri A, Laumond G, Even S, et al. HIV-Specific B Cell Frequency Correlates with Neutralization Breadth in Patients Naturally Controlling HIV-Infection. *EBioMedicine*. 2017 Jul 1;21:158–69.

250. Kardava L, Moir S, Wang W, Ho J, Buckner CM, Posada JG, et al. Attenuation of HIV-associated human B cell exhaustion by siRNA downregulation of inhibitory receptors. *J Clin Invest*. 2011 Jul 1;121(7):2614–24.
251. Tedder TF, Poe JC, Haas KM. CD22: A Multifunctional Receptor That Regulates B Lymphocyte Survival and Signal Transduction. *Adv Immunol*. 2005 Jan 1;88:1–50.
252. Walker JA, Smith KGC. CD22: an inhibitory enigma. *Immunology*. 2008;123(3):314–25.
253. Kawasaki N, Rademacher C, Paulson JC. CD22 Regulates Adaptive and Innate Immune Responses of B Cells. *J Innate Immun*. 2011;3(4):411–9.
254. Sanz I, Wei C, Lee FE-H, Anolik J. Phenotypic and functional heterogeneity of human memory B cells. *Semin Immunol*. 2008 Feb;20(1):67–82.
255. Anolik JH, Looney RJ, Lund FE, Randall TD, Sanz I. Insights into the heterogeneity of human B cells: diverse functions, roles in autoimmunity, and use as therapeutic targets. *Immunol Res*. 2009 Apr 7;45(2):144.
256. Mohr E, Cunningham AF, Toellner K-M, Bobat S, Coughlan RE, Bird RA, et al. IFN- $\gamma$  produced by CD8 T cells induces T-bet-dependent and – independent class switching in B cells in responses to alum-precipitated protein vaccine. *Proc Natl Acad Sci*. 2010 Oct 5;107(40):17292–7.

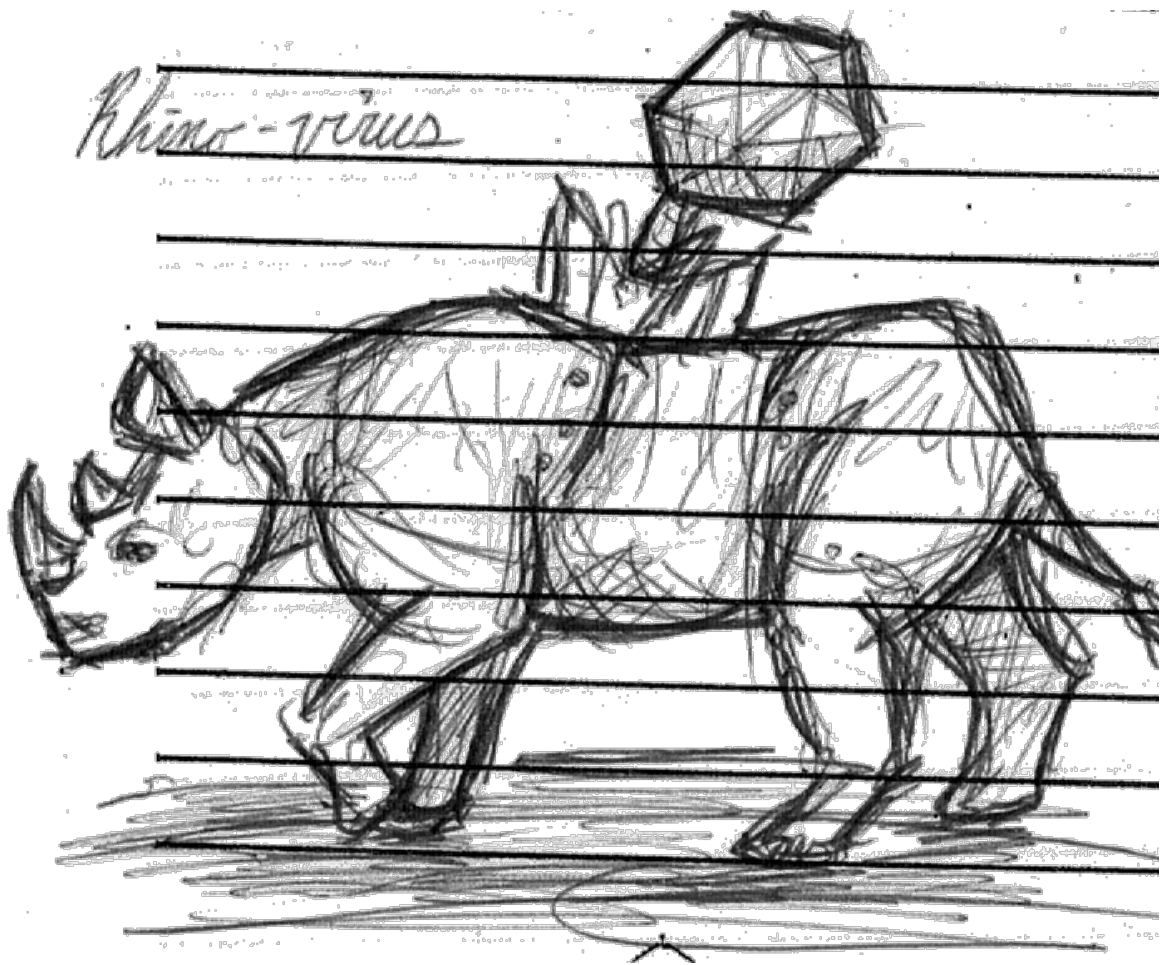
257. Kainulainen L, Vuorinen T, Rantakokko-Jalava K, Österback R, Ruuskanen O. Recurrent and persistent respiratory tract viral infections in patients with primary hypogammaglobulinemia. *J Allergy Clin Immunol.* 2010 Jul 1;126(1):120–6.
258. Taylor HP, Dimmock NJ. Mechanism of neutralization of influenza virus by secretory IgA is different from that of monomeric IgA or IgG. *J Exp Med.* 1985 Jan 1;161(1):198–209.
259. Muramatsu M, Yoshida R, Yokoyama A, Miyamoto H, Kajihara M, Maruyama J, et al. Comparison of Antiviral Activity between IgA and IgG Specific to Influenza Virus Hemagglutinin: Increased Potential of IgA for Heterosubtypic Immunity. *PLOS ONE.* 2014 Jan 17;9(1):e85582.
260. Gould VMW, Francis JN, Anderson KJ, Georges B, Cope AV, Tregoning JS. Nasal IgA Provides Protection against Human Influenza Challenge in Volunteers with Low Serum Influenza Antibody Titre. *Front Microbiol.* 2017;8:900.
261. Renegar KB, Small PA, Boykins LG, Wright PF. Role of IgA versus IgG in the Control of Influenza Viral Infection in the Murine Respiratory Tract. *J Immunol.* 2004 Aug 1;173(3):1978–86.
262. Cate TR, Rossen RD, Douglas RG, Butler WT, Couch RB. The role of nasal secretion and serum antibody in the rhinovirus common cold. *Am J Epidemiol.* 1966 Sep 1;84(2):352–63.

263. Bartlett NW, Walton RP, Edwards MR, Aniscenko J, Caramori G, Zhu J, et al. Mouse models of rhinovirus-induced disease and exacerbation of allergic airway inflammation. *Nat Med*. 2008 Feb;14(2):199–204.
264. Ellebedy AH, Jackson KJL, Kissick HT, Nakaya HI, Davis CW, Roskin KM, et al. Defining antigen-specific plasmablast and memory B cell subsets in human blood after viral infection or vaccination. *Nat Immunol*. 2016 Oct;17(10):1226–34.
265. Adachi Y, Onodera T, Yamada Y, Daio R, Tsuiji M, Inoue T, et al. Distinct germinal center selection at local sites shapes memory B cell response to viral escape. *J Exp Med*. 2015 Sep 21;212(10):1709–23.
266. Spensieri F, Borgogni E, Zedda L, Bardelli M, Buricchi F, Volpini G, et al. Human circulating influenza-CD4<sup>+</sup> ICOS1<sup>+</sup>IL-21<sup>+</sup> T cells expand after vaccination, exert helper function, and predict antibody responses. *Proc Natl Acad Sci*. 2013 Aug 27;110(35):14330–5.
267. Brewer JM, Conacher M, Hunter CA, Mohrs M, Brombacher F, Alexander J. Aluminium Hydroxide Adjuvant Initiates Strong Antigen-Specific Th2 Responses in the Absence of IL-4- or IL-13-Mediated Signaling. *J Immunol*. 1999 Dec 15;163(12):6448–54.
268. Awate S, Babiuk LA, Mutwiri G. Mechanisms of Action of Adjuvants. *Front Immunol*. 2013 May 16;4:114.

269. Wong KJ, Timbrell V, Xi Y, Upham JW, Collins AM, Davies JM. IgE<sup>+</sup> B cells are scarce, but allergen-specific B cells with a memory phenotype circulate in patients with allergic rhinitis. *Allergy*. 2015;n/a-n/a.
270. Laffleur B, Duchez S, Tarte K, Denis-Lagache N, Péron S, Carrion C, et al. Self-Restrained B Cells Arise following Membrane IgE Expression. *Cell Rep*. 2015 Feb 17;10(6):900–9.
271. Wiesner M, Zentz C, Mayr C, Wimmer R, Hammerschmidt W, Zeidler R, et al. Conditional Immortalization of Human B Cells by CD40 Ligation. *PLOS ONE*. 2008 Jan 23;3(1):e1464.
272. Nojima T, Haniuda K, Moutai T, Matsudaira M, Mizokawa S, Shiratori I, et al. In-vitro derived germinal centre B cells differentially generate memory B or plasma cells in vivo. *Nat Commun*. 2011 Sep 6;2:465.
273. Néron S, Roy A, Dumont N. Large-Scale In Vitro Expansion of Polyclonal Human Switched-Memory B Lymphocytes. *PLOS ONE*. 2012 Dec 17;7(12):e51946.
274. Pepper M, Jenkins MK. Origins of CD4<sup>+</sup> effector and central memory T cells. *Nat Immunol*. 2011 Jun;12(6):467–71.
275. Brown MN, Fintushel SR, Lee MH, Jennrich S, Geherin SA, Hay JB, et al. Chemoattractant Receptors and Lymphocyte Egress from Extralymphoid Tissue: Changing Requirements during the Course of Inflammation. *J Immunol*. 2010 Oct 15;185(8):4873–82.

276. Förster R, Braun A, Worbs T. Lymph node homing of T cells and dendritic cells via afferent lymphatics. *Trends Immunol.* 2012 Jun 1;33(6):271–80.
277. Girard J-P, Moussion C, Förster R. HEVs, lymphatics and homeostatic immune cell trafficking in lymph nodes. *Nat Rev Immunol.* 2012 Nov;12(11):762–73.
278. Carlsen HS, Bækkevold ES, Morton HC, Haraldsen G, Brandtzaeg P. Monocyte-like and mature macrophages produce CXCL13 (B cell-attracting chemokine 1) in inflammatory lesions with lymphoid neogenesis. *Blood.* 2004 Nov 15;104(10):3021–7.
279. Rao DA, Gurish MF, Marshall JL, Slowikowski K, Fonseka CY, Liu Y, et al. Pathologically expanded peripheral T helper cell subset drives B cells in rheumatoid arthritis. *Nature.* 2017 Feb 2;542(7639):110–4.
280. Hansen SG, Jr MP, Ventura AB, Hughes CM, Gilbride RM, Ford JC, et al. Immune clearance of highly pathogenic SIV infection. *Nature.* 2013 Oct;502(7469):100–4.
281. Gao W, Xiong Y, Li Q, Yang H. Inhibition of Toll-Like Receptor Signaling as a Promising Therapy for Inflammatory Diseases: A Journey from Molecular to Nano Therapeutics. *Front Physiol.* 2017 Jul 19;8:508.
282. Iwasaki J, Smith W-A, Stone SR, Thomas WR, Hales BJ. Species-Specific and Cross-Reactive IgG1 Antibody Binding to Viral Capsid Protein 1 (VP1) Antigens of Human Rhinovirus Species A, B and C. *PLoS ONE.* 2013 Aug 7;8(8):e70552.

283. Takahashi Y, Dutta PR, Cerasoli DM, Kelsoe G. In Situ Studies of the Primary Immune Response to (4-Hydroxy-3-Nitrophenyl)Acetyl. V. Affinity Maturation Develops in Two Stages of Clonal Selection. *J Exp Med*. 1998 Mar 16;187(6):885–95.
284. Oracki SA, Walker JA, Hibbs ML, Corcoran LM, Tarlinton DM. Plasma cell development and survival. *Immunol Rev*. 2010;237(1):140–59.
285. Good-Jacobson KL, Shlomchik MJ. Plasticity and Heterogeneity in the Generation of Memory B Cells and Long-Lived Plasma Cells: The Influence of Germinal Center Interactions and Dynamics. *J Immunol*. 2010 Sep 15;185(6):3117–25.
286. Chan TD, Brink R. Affinity-based selection and the germinal center response. *Immunol Rev*. 2012;247(1):11–23.
287. Takeda K, Sakakibara S, Yamashita K, Motooka D, Nakamura S, Hussien MAE, et al. Allergic conversion of protective mucosal immunity against nasal bacteria in patients with chronic rhinosinusitis with nasal polyposis. *J Allergy Clin Immunol*. 2019 Mar 1;143(3):1163-1175.e15.



Artist's Rendering of RV

Jocelyn Ray

UVA MSTP